Supporting Information

Pt(II) Decorated Covalent Organic Framework for Photocatalytic Difluoroalkylation and Oxidative Cyclization Reactions

Zainab Almansaf,[†○] Jiyun Hu,[†○] Federica Zanca,[‡] Hamid R. Shahsavari[▽,*⁋†] Benjamin Kampmeyer,[†] Miu Tsuji,[†] Kartik Maity,[†] Valerie Lomonte,[†] Yumi Ha,[†] Piero Mastrorilli,[§] Stefano Todisco,[§] Mourad Benamara,[‖] Rama Oktavian,[‡] Arsalan Mirjafari,[⊥] Peyman Z. Moghadam,[*‡] Ahmad R. Khosropour[▽,*Δ†] Hudson Beyzavi[*†]

[†] Department of Chemistry and Biochemistry, University of Arkansas, Fayetteville, Arkansas, 72701, United States. *E-mail: beyzavi@uark.edu*; Website: https://beyzavigroup.uark.edu/
[‡] Department of Chemical and Biological Engineering, The University of Sheffield, Sheffield, S1 3JD, United Kingdom. (P. Z. Moghadam is the corresponding author of computational section). *E-mail: p.moghadam@sheffield.ac.uk*
[⁋] Department of Chemistry, Institute for Advanced Studies in Basic Sciences (IASBS), Zanjan, 45137-66731, Iran. *E-mail: shahsavari@iasbs.ac.ir*
[§] DICATECh, Politecnico di Bari, I-70125, Bari, Italy.
[‖] Institute for Nano Science and Engineering, University of Arkansas, Fayetteville, Arkansas, 72701, United States.
[⊥] Department of Chemistry and Physics, Florida Gulf Coast University, Fort Myers, Florida, 33965, United States.
[Δ] Department of Chemistry, University of Isfahan, Isfahan, 81746-73441, Iran. *E-mail: khosropour@chem.ui.ac.ir*
[○] Authors contributed equally.
[▽] On sabbatical leave from IASBS, (H. R. Shahsavari) and University of Isfahan, (A. R. Khosropour).

Table of Contents

1. Materials and Methods S3

2. Synthesis and Experimental Procedures S4

2.1. Synthesis of COF linkers S4

2.1.1. Synthesis of 1,3,6,8-tetrakis(4-aminophenyl)pyrene (L1) S4

2.1.2. Synthesis of 2-(4-formylphenyl)-5-formylpyridine (L2) S5

2.2. Synthesis of COFs S6

2.2.1. Synthesis of COF-UARK-49 ..... S6

2.2.2. Synthesis of COF-UARK-49-Pt S6

2.2.3. Synthesis of Py-2P COF S6

2.2.4. Synthesis of Py-2P-Pt COF S6

3. Structure Simulation S7

4. Photocatalysis S8

4.1. General Procedure for Difluoroalkylation Reaction S8

4.2. Difluoroalkylation reaction with TEMPO S8

4.3. General Reaction Procedure for the Oxidative Cyclization Reaction S9

5. Supporting Figures S10

6. Spectroscopic Data of the Products S18

7. NMR Spectra S26

8. Reference S72

1. Materials and Methods

NMR spectra were recorded on a 400 MHz NMR spectrometer. Chemical shifts δ are reported in ppm, and the abbreviations s, d, t, q, m and *J* are used for singlet, doublet, triplet, quartet, multiplet, and coupling constant, respectively. Infrared spectra were recorded on a Shimadzu IRAffinity-1S spectrophotometer. Solid-state NMR runs were operated on a Bruker UltrashieldTM 400 MHz NMR spectrometer. The ^{13}C cross-polarization magic-angle spinning (CP/MAS) NMR spectra were recorded with a 4-mm triple-resonance MAS probe and a sample spinning rate of 10.0 kHz; a contact time of 3 ms (ramp 100) and pulse delay of 2 s were applied. The sample was packed in a zirconia rotor.

Powder X-ray diffraction (PXRD) data was gathered with a Rigaku MiniFlex II desktop X-Ray diffractometer operated at 30 kV and 15 mA. Scanning electron microscopy (SEM) observations were performed on a FEI Nova 200 Nano Lab microscope. Transmission electron microscopy (TEM) images were obtained with a FEI Titan 80-300 transmission electron microscope. Gas adsorption isotherms were obtained by a volumetric method using a Quantachrome Autosorb iQ-MP/XR gas sorption analyzer. Surface area was calculated from the adsorption data using Brunauer-Emmett-Teller (BET) method. The pore-size-distribution curve was obtained from the adsorption branches using nonlocal density functional theory (NLDFT) method.

2. Synthesis and Experimental Procedures

2.1. Synthesis of COF linkers

2.1.1. Synthesis of 1,3,6,8-tetrakis(4-aminophenyl)pyrene (L1)[1]

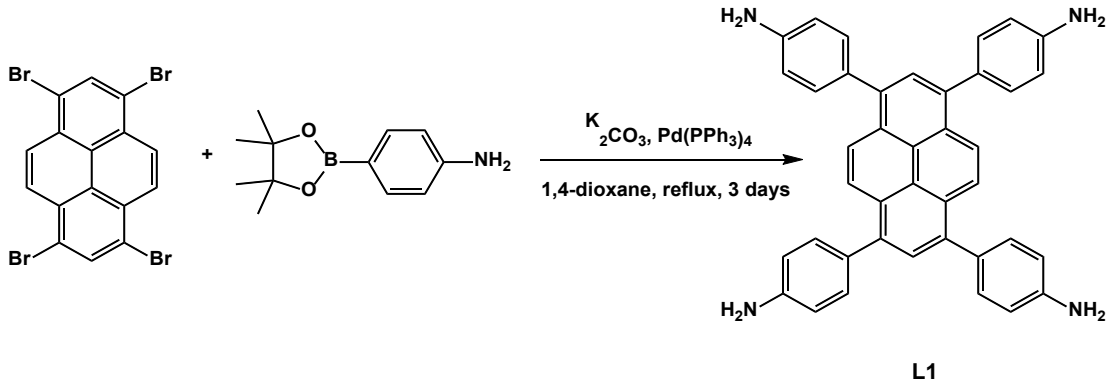

Scheme S1. Synthetic route for lignad **L1**.

1,3,6,8-Tetrabromopyrene (1.5 g, 2.9 mmol), 4-aminophenylboronic acid pinacol ester (3.0 g, 13.7 mmol), K_2CO_3 (2.2 g, 15.7 mmol), and $Pd(PPh_3)_4$ (330 mg, 0.29 mmol) in were added to degassed dioxane:water (4:1, 40 mL). The mixture was heated at 115 °C for 3 days. Then it was cooled down to room temperature, and water (50 mL) was added leading to a precipitate which was collected by filtration and rinsed with water (50 mL) and MeOH (100 mL). The title compound was recrystallized from dioxane, and then was dried under high vacuum yielding the product, as a bright yellow powder (1.45 g, 89%).

^{1}H NMR (400 MHz, DMSO-d_6) δ 8.14 (s, 4H), 7.80 (s, 2H), 7.36 (d, J = 8.4 Hz, 8H), 6.78 (d, J = 8.4 Hz, 8H), 5.31 (s, 8H).

^{13}C NMR (101 MHz, DMSO-d_6) δ 148.6, 137.6, 131.5, 129.5, 128.0, 127.2, 126.6, 124.9, 114.4.

2.1.2. Synthesis of 2-(4-formylphenyl)-5-formylpyridine (L2)[2]

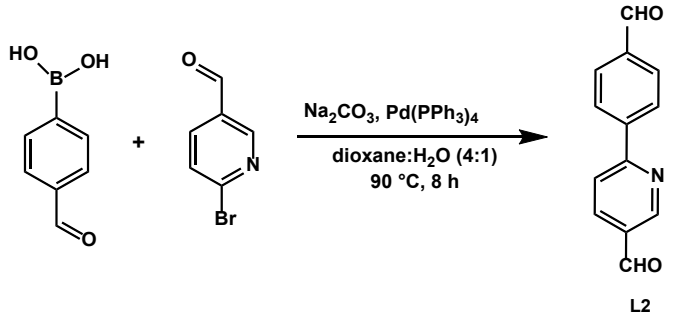

Scheme S2. Synthetic route for lignad **L2**.

4-Formylphenylboronic acid (1.0 g, 6.7 mmol), 6-bromo-3-pyridinecarboxaldehyde (1.2 g, 6.45 mmol), sodium carbonate (1.9 g, 17.9 mmol), and tetrakis(triphenylphosphine)-palladium (0.30 g, 0.26 mmol) were dissolved in a degassed mixture of dioxane:water (4:1, 30 mL). The mixture was heated at 90 °C under N_2 for 8 h. The resulting reaction mixture was cooled down to room temperature and the product was extracted with CH_2Cl_2. Using saturated sodium hydrogen carbonate solution and brine, the organic phase was washed, followed by drying with $MgSO_4$. Then the organic solvent was evaporated, and the crude compound was recrystallized from $CHCl_3$/hexane to give the pure product as an off-white solid (1.1 g, 81 %).

^{1}H NMR (400 MHz, $CDCl_3$) δ 10.18 (s, 1H), 10.11 (s, 1H), 9.18 (s, 1H), 8.28 (dd, J = 12.2, 5.2 Hz, 3H), 8.01 (dd, J = 16.2, 8.3 Hz, 3H).

^{13}C NMR (101 MHz, DMSO-d_6) δ 193.3, 192.5, 159.4, 152.0, 143.0, 137.9, 137.4, 130.9, 130.4, 128.4, 122.2.

2.2. Synthesis of COFs

2.2.1. Synthesis of COF-UARK-49

2-(4-Formylphenyl)-5-formylpyridine (8.4 mg, 0.04 mmol) and 1,3,6,8-tetrakis(4-aminophenyl)-pyrene (11.3 mg, 0.02 mmol) were placed in a glass ampule vessel (20 mL), followed by adding a solution of mesitylene:dioxane:acetic acid (3 M) (0.5:0.5:0.1 mL). The resulting mixture was sonicated for 5 min followed by flash freezing in liquid N_2. The glass ampule vessel was evacuated to an inner pressure of ~20 Pa, followed by flame-sealing, and heating for 3 days at 120 °C. The resultant solid was rinsed in sequence with DMF (× 3) and acetone (× 3) leading to a powder, which was dried under vacuum for 12 h at 120 °C to yield COF-UARK-49 (11.6 mg, 64%).

2.2.2. Synthesis of COF-UARK-49-Pt

COF-UARK-49 COF (70 mg), *cis*-[$PtCl_2(DMSO)_2$] (30 mg, 0.071mmol), and NaOAc (7.2 mg, 0.088 mmol) were mixed in 4 mL toluene and the mixture was heated at 50 °C overnight. The resulting suspension was filtered and rinsed in sequence with DMF (× 3) and acetone (× 3) to yield a brown powder, followed by drying for 12 h under vacuum to furnish Pt loaded COF (83 mg). The Pt loading was determined to be 9.1% by ICP-MS.

2.2.3. Synthesis of Py-2P COF

4,4'-Biphenyldicarboxaldehyde (12.6 mg, 59.93 μmol) and 1,3,6,8-tetrakis(4-aminophenyl)-pyrene (21 mg, 0.02 mmol) were added into a reaction tube, and then mesitylene (1 mL), 1,4-dioxane (0.5 mL), and 6 M acetic acid (0.15 mL) were added. Then, the tube was sealed, and the reaction mixture was heated for 3 d at 120 °C. Then, the mixture was cooled to room temperature, and the resulting solid was collected via filtration, furnishing an orange powder. This framework was found to lose its crystallinity upon evaporation of the solvent.

2.2.4. Synthesis of Py-2P-Pt COF

Py-2P COF (20 mg) and *cis*-[$PtCl_2(DMSO)_2$] (10 mg, 0.024mmol) were mixed in 2 mL toluene and the mixture was heated at 50 °C overnight. The resulting suspension was filtered and rinsed in sequence with DMF (× 3) and acetone (× 3) to yield a brown powder, followed by drying for 12 h under vacuum to furnish Pt loaded COF. The Pt loading was determined to be 12.5% by ICP-MS.

3. Structure Simulation

N_2 adsorption isotherms were calculated using grand canonical Monte Carlo (GCMC) simulations performed with the multi-purpose simulation package RASPA.[3] The atoms of framework were kept fixed at the crystallographic positions for both COFs. We applied the standard Lennard-Jones (LJ) potential to model the interactions between fluid/fluid and fluid/framework atoms. The LJ parameters for the framework atoms were obtained from the Dreiding force field.[4] N_2 was modeled using the TraPPE[5] potential with charges placed on each atom and at the center of mass. The Lorentz-Berthelot mixing rules were employed to calculate fluid/solid LJ parameters, and LJ interactions beyond 12.8 Å were neglected. The Ewald sum method was applied to compute the electrostatic interactions. 10^4 Monte Carlo cycles were performed, the first 50% of cycles were applied for equilibration, and the remaining cycles were applied to calculate the ensemble averages.

4. Photocatalysis

4.1. General Procedure for Difluoroalkylation Reaction

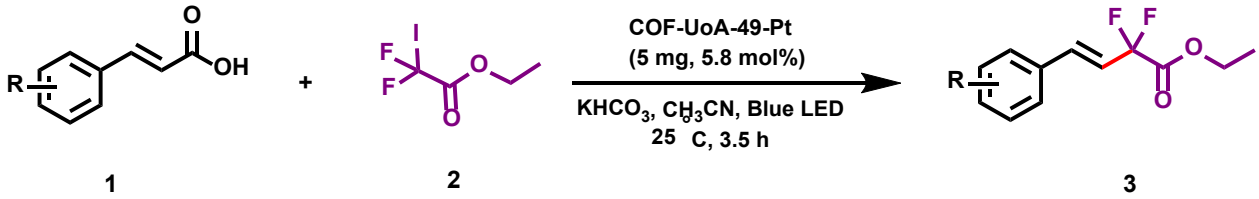

Scheme S3. General method for the difluoroalkylation.

The cinnamic acid derivatives (0.04 mmol), ethyldifluoroiodoacetate (0.044 mmol), potassium dicarbonate (0.044 mmol) and COF-UARK-49-Pt (5 mg, 5.8 mol%) were dissolved in 1 mL CH_3CN in a 4 mL reaction tube supplied with magnetic stir bar. Then, the reaction tube was deaerated with N_2 for 15 min and then sealed. Then the reaction mixture was irradiated with a blue LED light for 3.5 h. After reaction, the product was isolated by TLC plate chromatography of silica gel using *n*-hexane:ethyl acetate (10:1) as the eluent.

4.2. Difluoroalkylation reaction with TEMPO

The cinnamic acid derivatives (0.04 mmol), ethyldifluoroiodoacetate (0.044 mmol), TEMPO (0.044 mmol), potassium dicarbonate (0.044 mmol), and COF-UARK-49-Pt (5 mg, 5.8 mol%) were mixed in 1 mL CH_3CN in a 4 mL reaction tube supplied with magnetic stir bar. The mixture was deaerated with N_2 for 15 min before the reaction tube was sealed. The mixture was irradiated with a blue LED light for 3.5 h. The product was confirmed by ESI-MS. **HRMS** (ESI) (m/z): $[M+H]^+$calcd. for $C_{13}H_{24}F_2NO_3$: 280.1646, found:280.1718.

4.3. General Reaction Procedure for the Oxidative Cyclization Reaction

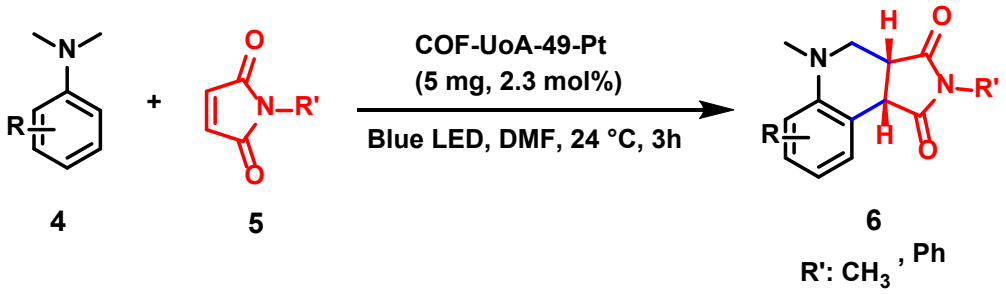

Scheme S4. General method for the oxidative cyclization.

N,*N*-dimethylaniline derivatives (0.2 mmol), *N*-phenylmaleimide (0.1 mmol), and COF-UARK-49-Pt catalyst (5 mg, 2.3 mol%) were mixed in 1 mL DMF in a 4 mL glass vial supplied with a magnetic stir bar. Then, the vial was capped and irradiated with a blue LED light for 3 h.

5. Supporting Figures

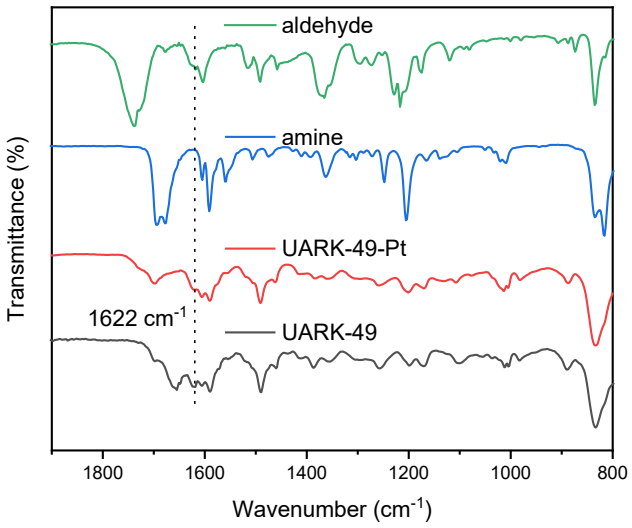

Figure S1. FT-IR spectra of COF-UARK-49-Pt (red), COF-UARK-49 (grey), aldehyde linker (green), and amine linker (blue).

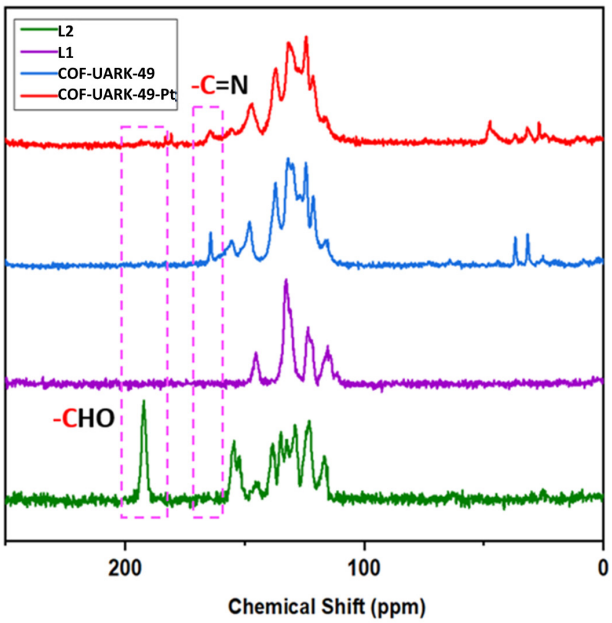

Figure S2. ^{13}C CP/MAS spectra of L1, L2, COF-UARK-49, and COF-UARK-49-Pt.

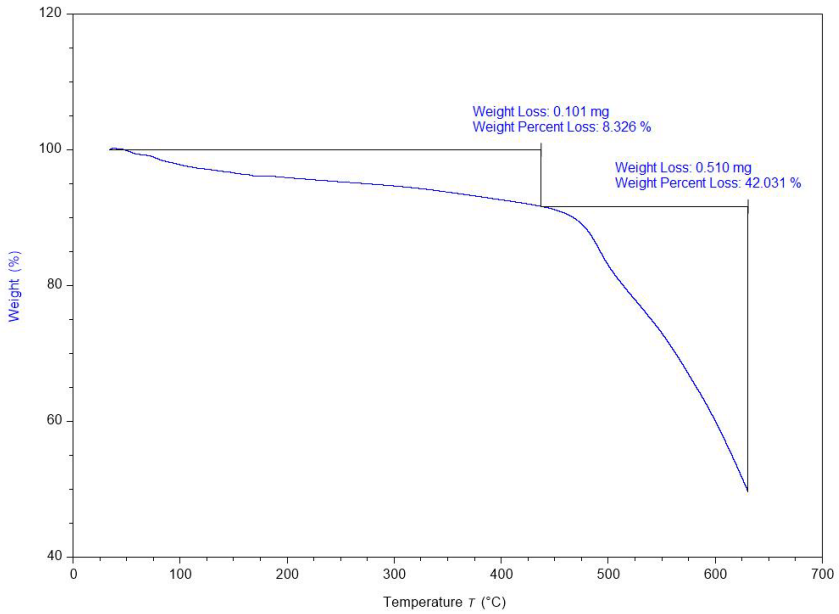

Figure S3. TGA trace of COF-UARK-49 under N_2 atmosphere.

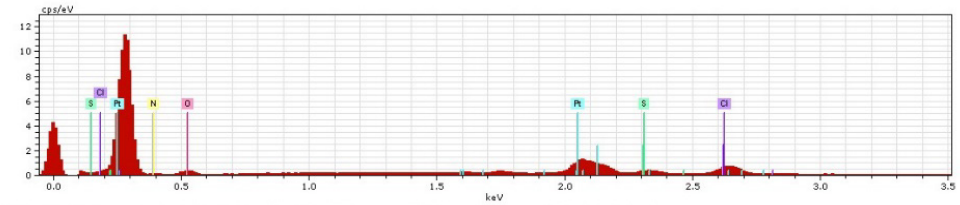

Acquisition Date:7/6/2020 6:26:33 PM HV:15.0kV Puls th.:1.97kcps

El	AN	Series	unn. C [wt.%]	norm. C [wt.%]	Atom. C [at.%]	Error (1 Sigma) [wt.%]
N	7	K-series	5.28	16.64	36.64	1.31
O	8	K-series	6.34	19.98	38.51	1.25
S	16	K-series	1.66	5.22	5.02	0.10
Cl	17	K-series	4.74	14.94	13.00	0.20
Pt	78	M-series	13.71	43.22	6.83	0.57
		Total:	31.73	100.00	100.00	

Figure S4. EDX spectrum of COF-UARK-49-Pt.

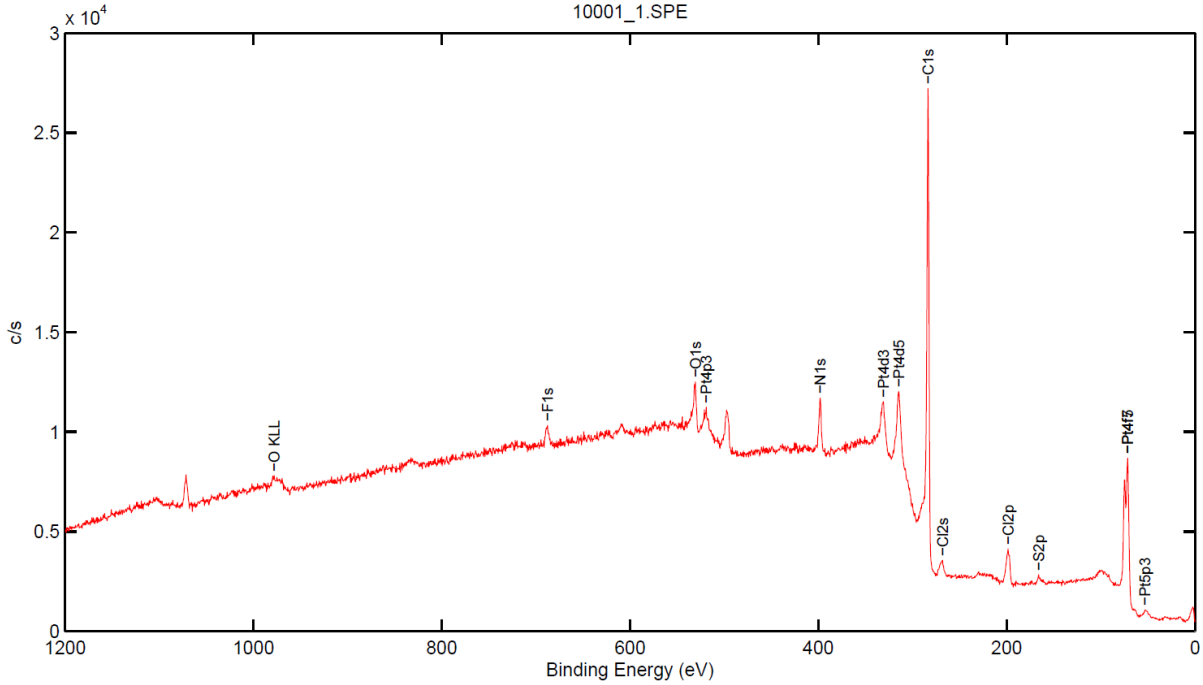

Figure S5. XPS Survey spectrum of COF-UARK-49-Pt.

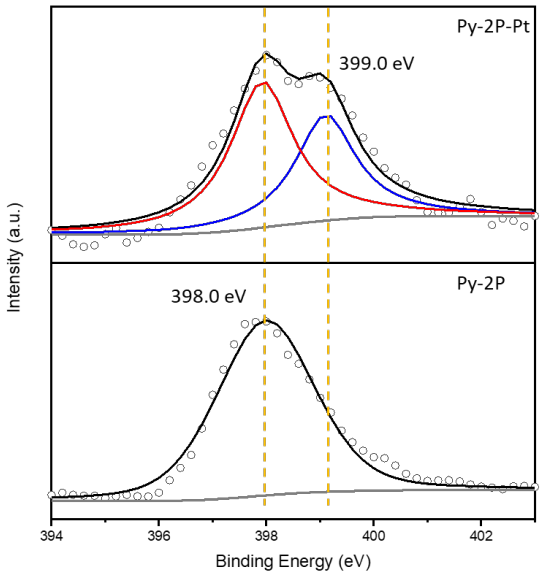

Figure S6. N 1s XPS spectra of Py-2P and Py-2P-Pt.

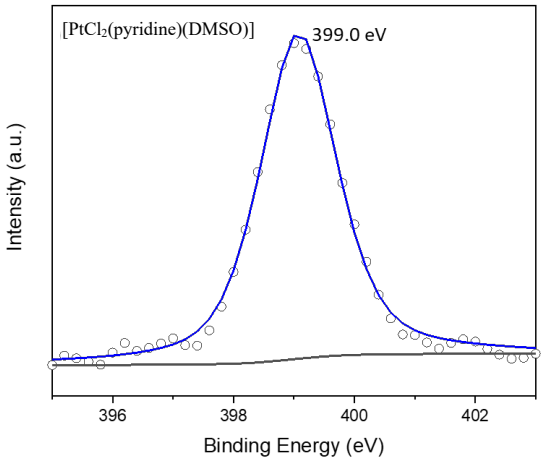

Figure S7. N 1s XPS spectra of [$PtCl_2$(pyridine)(DMSO)] (*cis* and *trans* 1:1 mixture).

Table S1. DFT calculated structure of different N coordinated Pt complex based on the model imine compound. [a]

Coordination mode	Optimized structure	Gibbs free energy / Hartrees	Relative energy to pyridine coordinated structure / kcal mol^{-1}
Pyridine N	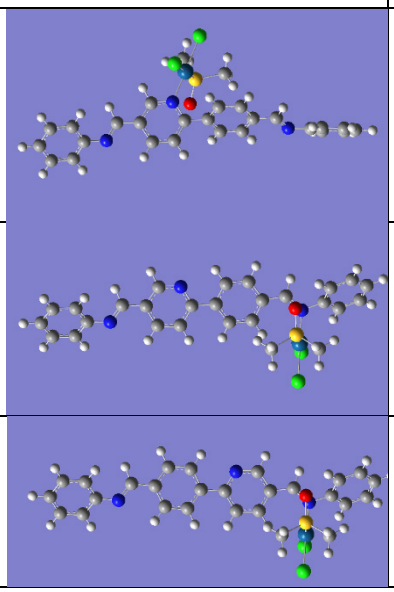	-2720.395809	0
Imine N		-2720.396953	-0.72
Imine N		-2720.395518	0.90

[a] The geometry optimization was carried out by B3LYP hybrid functional with 6-31G(d,p) basis set for the main group atoms and the effective core potentials (ECPs) of Hay and Wadt with the LanL2DZ double-valence basis set for Pt.

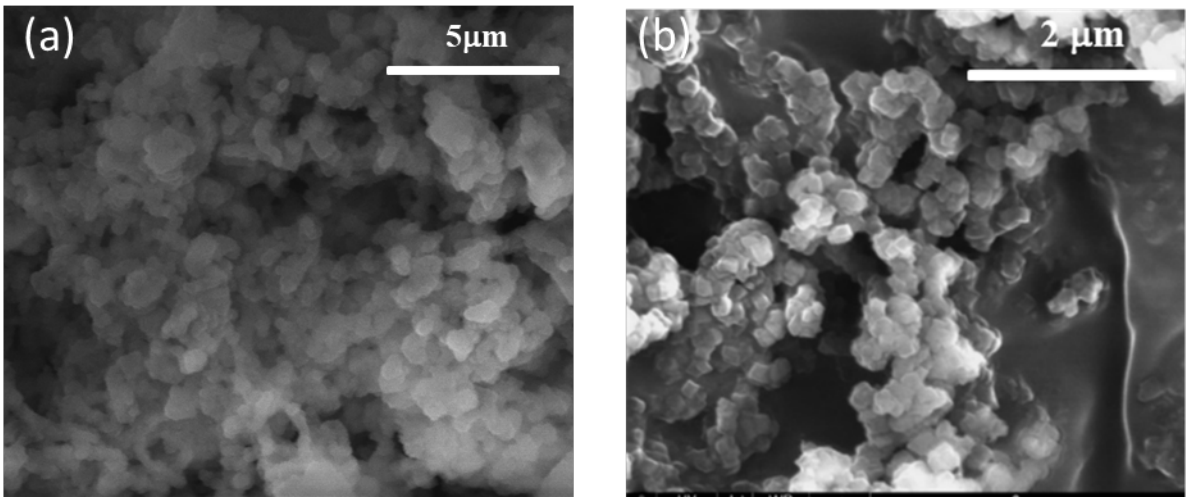

Figure S8. SEM images of (a) COF-UARK-49 and (b) COF-UARK-49-Pt.

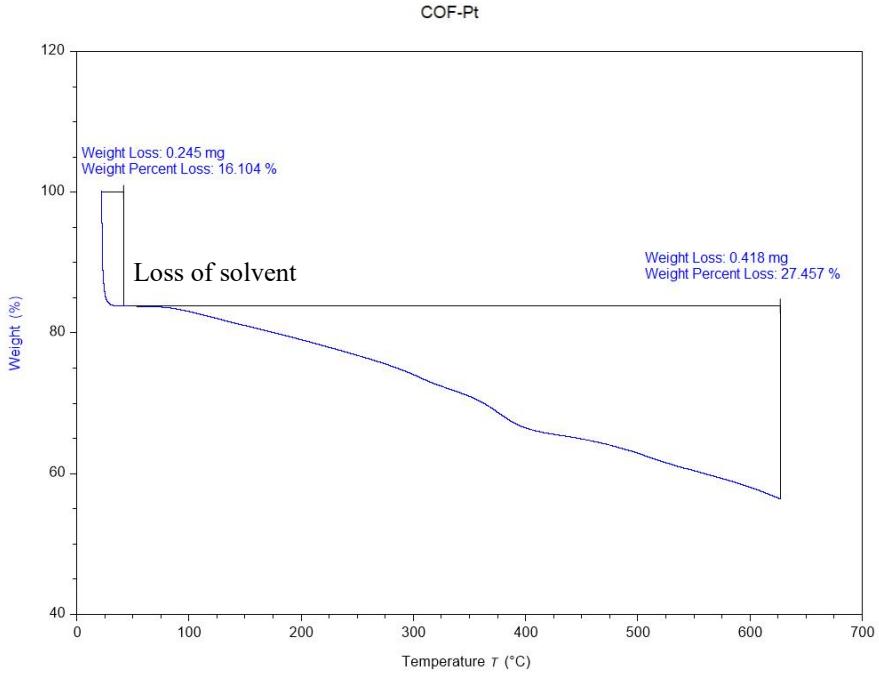

Figure S9. TGA trace of COF-UARK-49-Pt under N_2 atmosphere.

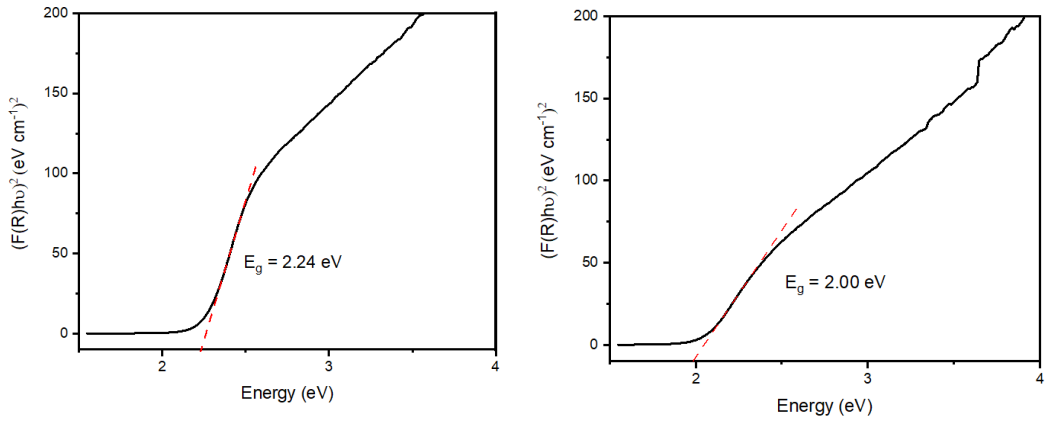

Figure S10. Plot of Kubelka-Munk function used for band gap extraction of COF-UARK-49 (left) and COF-UARK-49-Pt (right).

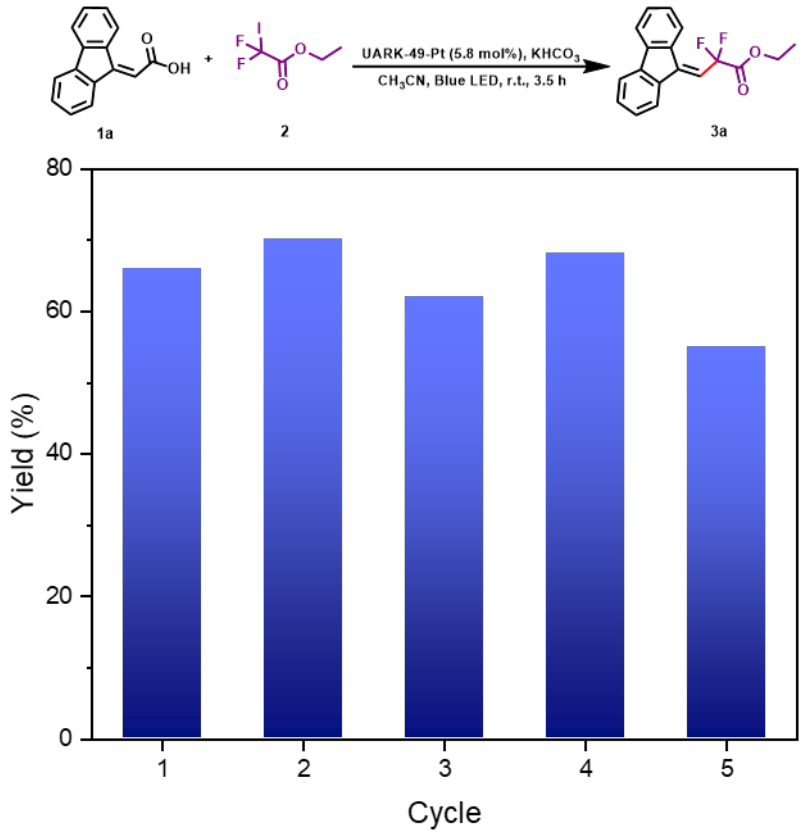

Figure S11. Recyclability test of COF-UARK-49-Pt in decarboxylation-difluoroalkylation reaction.

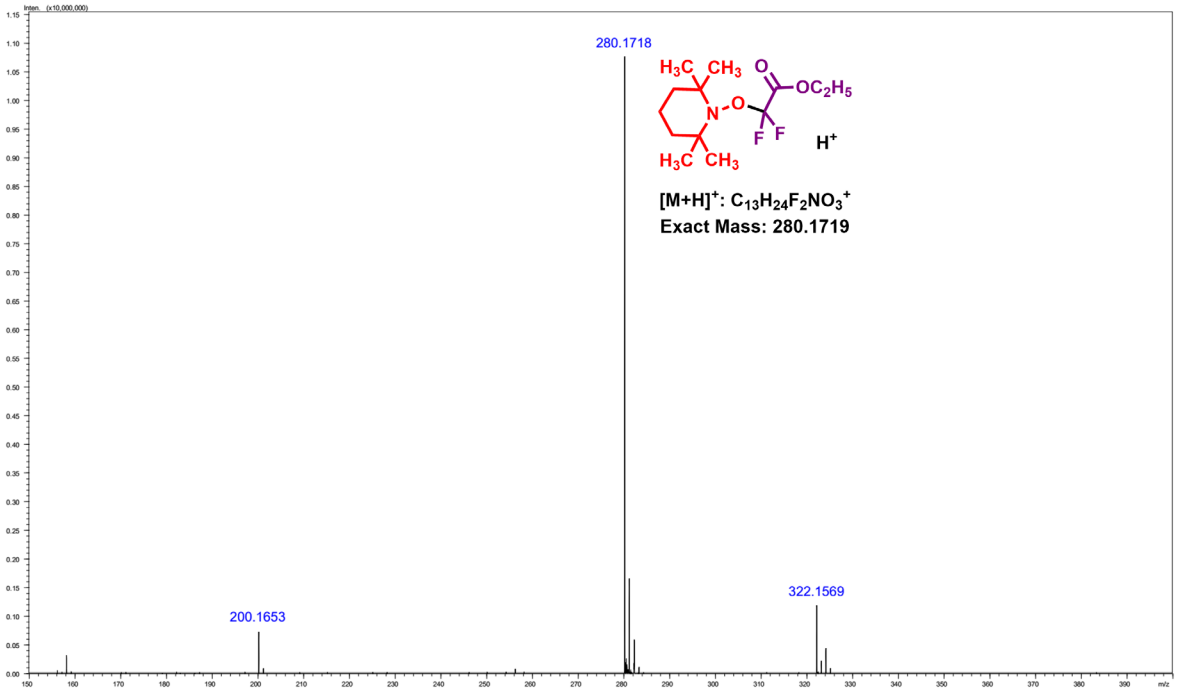

Figure S12. HR ESI-MS of the adduct of TEMPO and difluoro radical.

Table S2. Optimization Reaction Conditions for the Photocatalytic Oxidative Cyclization Reaction. [a]

Entry	Difference from the Standard Condition	Yield (%)[b]
1	None	66
2	Without light	No reaction
3	Without catalyst	<4
4	COF-UARK-49 instead of COF-UARK-49-Pt	23
5	In the presence of 0.1 mmol $AgNO_3$	25
6	In the presence of 0.1 mmol KI	trace
7	In the presence of 0.1 mmol 1,4-benzoquinone	trace
8	Under N_2 atmosphere	7
9	$PtCl_2$(DMSO)(pyridine) instead of COF-UARK-49-Pt	46

[a]A mixture of **4a** (0.2 mol) and **5a** (0.1 mol) in 1 mL DMF in the presence of 5 mg (2.3 mol%) of the catalyst. [b]HPLC yield.

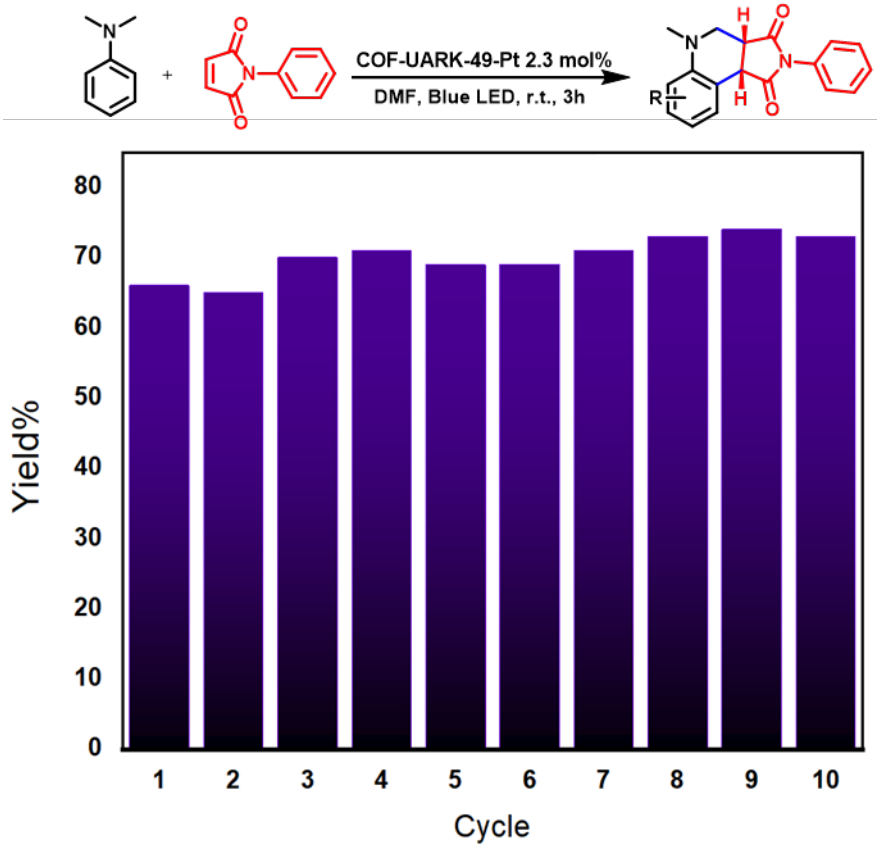

Figure S13. Recyclability test of COF-UARK-49-Pt in oxidative cyclization reaction.

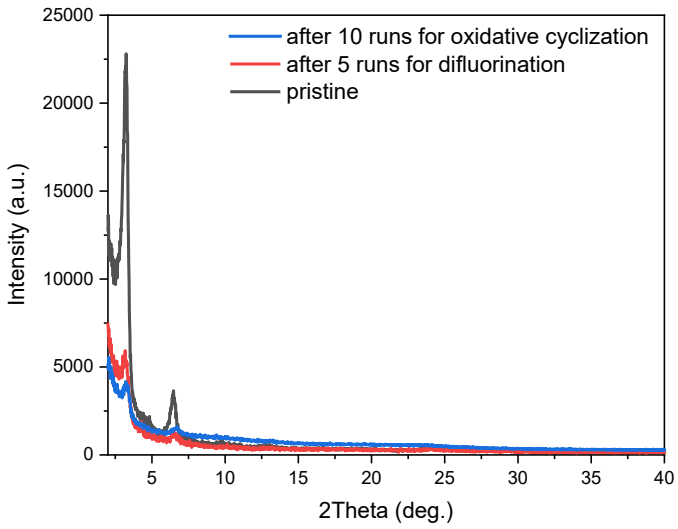

Figure S14. PXRD spectra of recovered COF-UARK-49-Pt.

6. Spectroscopic Data of the Products

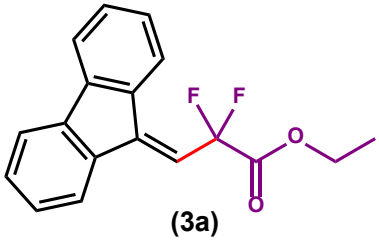

(3a)

Scheme S5. The chemical structure of **3a**.

Ethyl 3-(9H-fluoren-9-ylidene)-2,2-difluoropropanoate (lit.[6]) (3a)

^{1}H NMR (400 MHz, $CDCl_3$) δ 8.11 (d, *J* = 7.8 Hz, 1H), 7.65 (t, *J* = 6.5 Hz, 3H), 7.48 – 7.35 (m, 2H), 7.35 – 7.24 (m, 2H), 6.65 (t, *J* = 15.8 Hz, 1H), 4.36 (q, *J* = 7.1 Hz, 2H), 1.32 (t, *J* = 7.1 Hz, 3H).

^{13}C NMR (101 MHz, $CDCl_3$) δ 163.5 (t, *J* = 34.8 Hz), 143.8 (t, *J* = 7.6 Hz), 142.2, 140.1, 138.1, 134.0 (t, *J* = 1.8 Hz), 130.4, 130.1, 127.7, 127.4, 127.2 (t, *J* = 7.5 Hz), 121.0, 119.8, 119.7 (d, *J* = 2.2 Hz), 115.1 (t, *J* = 29.4 Hz), 112.8 (t, 248.0 Hz), 63.4, 13.9.

^{19}F NMR (376 MHz, $CDCl_3$) δ -96.04 (2F).

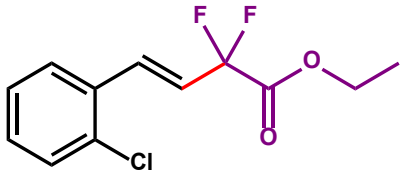

(3b)

Scheme S6. The chemical structure of **3b**.

Ethyl (*E*)-4-(2-chlorophenyl)-2,2-difluorobut-3-enoate (lit.[6]) (3b)

^{1}H NMR (400 MHz, $CDCl_3$) δ 7.60 – 7.54 (m, 1H), 7.51 (dt, *J* = 16.2, 2.6 Hz, 1H), 7.45 – 7.37 (m, 1H), 7.39-7.21 (m, 2H), 6.33 (dt, *J* = 16.2, 11.1 Hz, 1H), 4.38 (q, *J* = 7.1 Hz, 2H), 1.39 (t, *J* = 7.1 Hz, 3H).

^{13}C NMR (101 MHz, $CDCl_3$) δ 163.7, 134.3, 133.2 (t, *J* = 9.8 Hz), 132.4, 130.5, 130.0, 127.3, 127.0, 121.5 (t, *J* = 25.3 Hz), 112.4 (t, *J* =245 Hz), 63.2, 13.9.

^{19}F NMR (376 MHz, $CDCl_3$) δ -103.15 (2F).

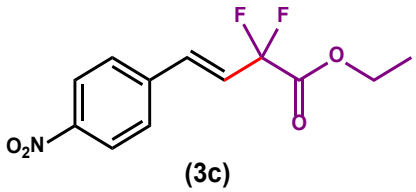

(3c)

Scheme S7. The chemical structure of **3c**.

Ethyl (*E*)-2,2-difluoro-4-(4-nitrophenyl)but-3-enoate ((lit.[6]) (3c)

^{1}H NMR (400 MHz, $CDCl_3$) δ 8.27 (d, *J* = 8.7 Hz, 2H), 7.64 (d, *J* = 8.7 Hz, 2H), 7.17 (d, *J* = 14.1 Hz, 1H), 6.49 (dt, *J* = 16.2, 11.1 Hz, 1H), 4.40 (q, *J* = 7.1 Hz, 2H), 1.40 (t, *J* = 7.2 Hz, 3H).

^{13}C NMR (101 MHz, $CDCl_3$) δ 163.3 (t, *J* = 39.5 Hz), 148.2, 140.2, 134.5 (t, *J* = 9.2 Hz), 128.1, 124.1, 123.3 (t, *J* = 25.0 Hz), 112.0 (t, *J* = 249.6 Hz), 63.4, 13.9.

^{19}F NMR (376 MHz, $CDCl_3$) δ = -103.96 (2F).

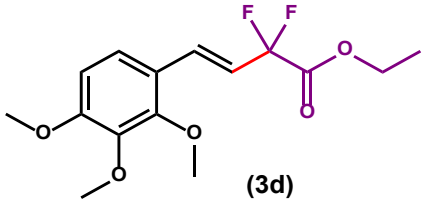

(3d)

Scheme S8. The chemical structure of **3d**.

Ethyl (*E*)-2,2-difluoro-4-(2,3,4-trimethoxyphenyl)but-3-enoate(3d)

^{1}H NMR (400 MHz, $CDCl_3$) δ 7.23 (m,1H), 7.17 (d, *J* = 8.8 Hz, 1H), 6.68 (d, *J* = 8.8 Hz, 1H), 6.29 (dt, *J* = 16.3, 11.5 Hz, 1H), 4.35 (q, *J* = 7.1 Hz, 2H), 3.88 (d, *J* = 6.9 Hz, 9H), 1.36 (t, *J* = 7.2 Hz, 3H).

^{13}C NMR (101 MHz, $CDCl_3$) δ 164.5 – 163.7 (m), 154.9, 152.6, 142.3, 131.6 (t, *J* = 9.9 Hz), 122.4, 121.1, 117.8 (t, *J* = 24.9 Hz), 113.0 (t, *J* = 248.1 Hz), 62.9, 61.2, 60.8, 56.0, 13.9.

^{19}F NMR (376 MHz, CDCl3) δ = -102.90 (2F).

HRMS (ESI) (m/z): $[M+H]^+$ calcd. for $C_{15}H_{19}F_2O_5$: 317.11, found: 317.109

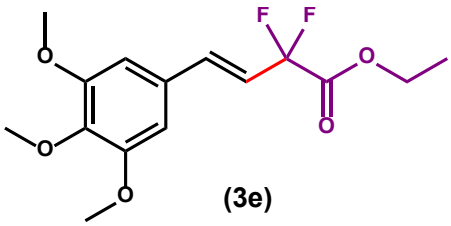

(3e)

Scheme S9. The chemical structure of **3e**.

Ethyl (*E*)-2,2-difluoro-4-(3,4,5-trimethoxyphenyl)but-3-enoate(lit.[6]) (3e)

^{1}H NMR (400 MHz, $CDCl_3$) δ 7.01 (dt, *J* = 16.1, 2.3 Hz, 1H), 6.68 (s, 2H), 6.21 (dt, *J* = 16.1, 11.4 Hz, 1H), 4.37 (q, *J* = 7.1 Hz, 2H), 3.89 (d, *J* = 8.7 Hz, 9H), 1.38 (t, *J* = 7.1 Hz, 3H).

^{13}C NMR (101 MHz, $CDCl_3$) δ 163.9 (t, *J* = 34.9 Hz), 153.4, 139.5, 136.8 (t, *J* = 9.5 Hz), 129.6 (d, *J* = 1.3 Hz), 118.1 (t, *J* = 25.0 Hz), 112.7 (t, *J* = 248.8 Hz), 104.6, 63.1, 60.9, 56.1, 13.9.

^{19}F NMR (376 MHz, CDCl3) δ = -103.25(2F).

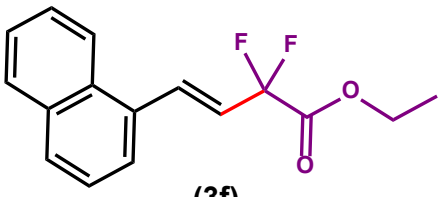

(3f)

Scheme S10. The chemical structure of **3f**.

Ethyl (*E*)-2,2-difluoro-4-(naphthalen-1-yl)but-3-enoate (lit.[6]) (3f)

^{1}H NMR (400 MHz, $CDCl_3$) δ 8.09 (d, *J* = 8.3 Hz, 1H), 7.95 – 7.83 (m, 3H), 7.66 (d, *J* = 7.2 Hz, 1H), 7.54 (ddd, *J* = 19.3, 15.8, 7.3 Hz, 3H), 6.39 (dt, *J* = 15.9, 11.4 Hz, 1H), 4.40 (q, *J* = 7.1 Hz, 2H), 1.40 (t, *J* = 7.1 Hz, 3H).

^{13}C NMR (101 MHz, $CDCl_3$) δ 163.9 (t, *J* = 34.7 Hz), 134.3 (t, *J* = 9.3 Hz), 133.5, 131.7, 131.1, 129.8, 128.7, 126.7, 126.2, 125.4, 124.7 (t, *J* = 1.7 Hz), 123.3, 121.8 (t, *J* = 24.8 Hz), 112.6 (t, *J* = 248.7 Hz), 63.1, 14.0.

^{19}F NMR (376 MHz, $CDCl_3$) δ = -103.09 (2F).

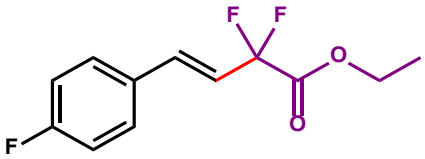

(3g)

Scheme S11. The chemical structure of **3g**.

Ethyl (*E*)-2,2-difluoro-4-(4-fluorophenyl)but-3-enoate (lit.[6]) (3g)

^{1}H NMR (400 MHz, $CDCl_3$) δ 7.44 (dd, *J* = 8.4, 5.4 Hz, 2H), 7.14 – 6.99 (m, 3H), 6.24 (dt, *J* = 16.2, 11.3 Hz, 1H), 4.37 (q, *J* = 7.1 Hz, 2H), 1.38 (t, *J* = 7.1 Hz, 3H).

^{13}C NMR (101 MHz, $CDCl_3$) δ 164.8, 162.3, 136.3 (t, *J* = 9.5 Hz), 130.1, 129.3 (d, *J* = 8.4 Hz), , 117.9 (t, *J* = 24.9 Hz), 116.0 (d, *J* = 21.9 Hz), 112.4 (t, *J* = 248.7 Hz), 63.1, 13.9.

^{19}F NMR (377 MHz, $CDCl_3$) δ -103.46 (2F), -111.16 (1F).

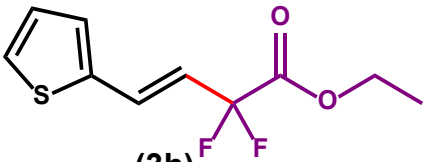

(3h)

Scheme S12. The chemical structure of **3h**.

Ethyl (*E*)-2,2-difluoro-4-(thiophen-2-yl)but-3-enoate (lit.[7]) (3h)

^{1}H NMR (400 MHz, $CDCl_3$) δ 7.33 (d, *J* = 5.0 Hz, 1H), 7.24 – 7.14 (m, 2H), 7.03 (dd, *J* = 5.0, 3.7 Hz, 1H), 6.12 (dt, *J* = 15.9, 11.5 Hz, 1H), 4.36 (q, *J* = 7.1 Hz, 2H), 1.38 (t, *J* = 7.1 Hz, 3H).

^{13}C NMR (101 MHz, $CDCl_3$) δ 163.8 (t, *J* = 35.0 Hz), 138.9 (t, *J* = 1.5 Hz), 129.7 (t, *J* = 10.1 Hz), 129.3 (t, *J* = 1.4 Hz), 127.8, 127.2 (d, *J* = 0.9 Hz), 117.5 (t, *J* = 25.3 Hz), 112.4, 63.1, 13.9.

^{19}F NMR (376 MHz, $CDCl_3$) δ -102.97 (2F).

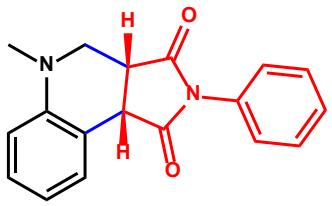

(6a)

Scheme S13. The chemical structure of **6a**.

(3a*R,9b*S**)-5-Methyl-2-phenyl-3a,4,5,9b-tetrahydro-1H-pyrrolo[3,4-c]quinoline-1,3(2H)-dione (lit.[8]) (6a)**

^{1}H NMR (400 MHz, $CDCl_3$) δ 7.54 (d, *J* = 7.5 Hz, 1H), 7.44 (t, *J* = 7.5 Hz, 2H), 7.36 (t, *J* = 7.4 Hz, 1H), 7.26 (dd, *J* = 16.8, 8.0 Hz, 3H), 6.92 (t, *J* = 7.4 Hz, 1H), 6.76 (d, *J* = 8.2 Hz, 1H), 4.18 (d, *J* = 9.6 Hz, 1H), 3.63 (dd, *J* = 11.4, 2.7 Hz, 1H), 3.55 (ddd, *J* = 9.6, 4.2, 2.8 Hz, 1H), 3.14 (dd, *J* = 11.4, 4.4 Hz, 1H), 2.85 (s, 3H).

^{13}C NMR (101 MHz, $CDCl_3$) δ 177.6, 175.7, 148.4, 132.0, 130.3, 129.0, 128.7, 128.5, 126.3, 119.7, 118.5, 112.5, 50.6, 43.5, 42.1, 39.4.

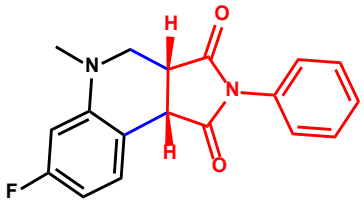

(6b-1)

Scheme S14. The chemical structure of **6b-1**.

(3a*R,9b*S**)-7-Fluoro-5-methyl-2-phenyl-3a,4,5,9b-tetrahydro-1H-pyrrolo[3,4-c]quinoline-1,3(2H)-dione (6b-1):**

^{1}H NMR (400 MHz, $CDCl_3$) δ 7.53 – 7.41 (m, 3H), 7.37 (t, *J* = 7.4 Hz, 1H), 7.27 (dd, *J* = 6.1, 2.4 Hz, 2H), 6.60 (td, *J* = 8.3, 2.4 Hz, 1H), 6.50 – 6.38 (m, 1H), 4.14 (d, *J* = 9.6 Hz, 1H), 3.68 – 3.60 (m, 1H), 3.55 (ddd, *J* = 9.6, 4.3, 2.9 Hz, 1H), 3.16 (d, *J* = 15.9 Hz, 1H), 2.84 (s, 3H).

^{13}C NMR (101 MHz, $CDCl_3$) δ 177.3, 175.6 (d, *J* = 1.5 Hz), 164.6, 162.1, 149.9, 149.8, 131.8, 131.5 (d, *J* = 10.0 Hz), 129.0, 128.6, 126.3, 113.8 (d, *J* = 2.9 Hz), 106.1 (d, *J* = 21.9 Hz), 100.1 (d, *J* = 26.1 Hz), 50.1, 43.1, 41.4, 39.4.

^{19}F NMR (376 MHz, $CDCl_3$) δ -112.62 (1F).

HRMS (ESI) (m/z): $[M+H]^+$ calcd. for $C_{18}H_{16}FN_2O_2$: 311.1118, found: 311.1192.

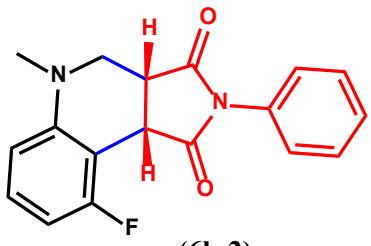

(6b-2)

Scheme S15. The chemical structure of **6b-2**.

(3a*R,9b*S**)-9-Fluoro-5-methyl-2-phenyl-3a,4,5,9b-tetrahydro-1H-pyrrolo[3,4-c]quinoline-1,3(2H)-dione (6b-2)**

^{1}H NMR (400 MHz, $CDCl_3$) δ 7.45 (t, *J* = 7.5 Hz, 2H), 7.37 (t, *J* = 7.4 Hz, 1H), 7.34 – 7.27 (m, 2H), 7.19 (dd, *J* = 14.7, 8.2 Hz, 1H), 6.70 (t, *J* = 8.6 Hz, 1H), 6.55 (d, *J* = 8.3 Hz, 1H), 4.60 (d, *J* = 9.7 Hz, 1H), 3.67 – 3.60 (m, 1H), 3.55 (ddd, *J* = 9.8, 4.6, 2.0 Hz, 1H), 3.11 – 3.02 (m, 1H), 2.84 (s, 3H).

^{13}C NMR (101 MHz, $CDCl_3$) δ 177.6, 174.4, 163.1, 160.7, 150.8, 131.9, 129.3 (d, *J* = 10.3 Hz), 129.0, 128.5, 126.3, 108.3 (d, *J* = 2.8 Hz), 107.0, 106.8, 51.7, 43.4, 39.7, 36.5.

^{19}F NMR (376 MHz, $CDCl_3$) δ -116.78 (1F).

HRMS (ESI) (m/z): $[M+H]^+$calcd. for $C_{18}H_{16}FN_2O_2$: 311.1118, found: 311.1192.

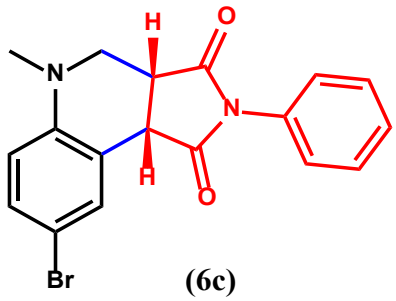

(6c)

Scheme S16. The chemical structure of **6c**.

(3a*R,9b*S**)-8-Bromo-5-methyl-2-phenyl-3a,4,5,9b-tetrahydro-1H-pyrrolo[3,4-c]quinoline-1,3(2H)-dione (lit.[8]) (6c)**

^{1}H NMR (400 MHz, $CDCl_3$) δ 7.67 (d, *J* = 2.0 Hz, 1H), 7.46 (t, *J* = 7.5 Hz, 2H), 7.43 – 7.25 (m, 4H), 6.63 (d, *J* = 8.8 Hz, 1H), 4.13 (d, *J* = 9.6 Hz, 1H), 3.63 (dd, *J* = 11.5, 2.7 Hz, 1H), 3.56 (ddd, *J* = 9.5, 4.2, 2.9 Hz, 1H), 3.13 (dd, *J* = 11.5, 4.4 Hz, 1H), 2.84 (s, 3H).

^{13}C NMR (101 MHz, $CDCl_3$) δ 177.1, 175.1, 147.4, 132.7,131.8, 131.4, 129.1, 128.6, 126.1, 120.3, 114.2, 111.7, 50.3, 43.3, 41.8, 39.4.

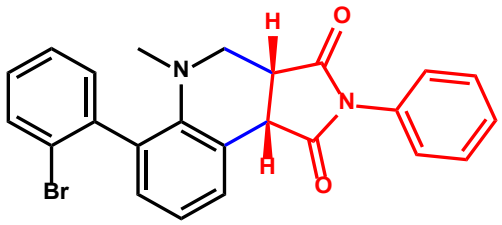

(6d)

Scheme S17. The chemical structure of **6d**.

(3a*R,9b*S**)-6-(2-Bromophenyl)-5-methyl-2-phenyl-3a,4,5,9b-tetrahydro-1H-pyrrolo[3,4-c]quinoline -1,3(2H)-dione (6d)**

^{1}H NMR (400 MHz, $CDCl_3$) δ 7.84 – 7.63 (m, 2H), 7.54 – 7.45 (m, 2H), 7.45 – 7.27 (m, 5H), 7.27 – 7.08 (m, 3H), 4.25 (t, *J* = 9.4 Hz, 1H), 3.56 (tdd, *J* = 17.5, 12.8, 5.0 Hz, 2H), 3.49 – 3.38 (m, 1H), 2.43 (s, 3H).

^{13}C NMR (101 MHz, $CDCl_3$) δ 177.8, 175.8, 146.1, 141.4, 134.9, 134.2, 132.6, 132.0, 131.6, 131.1, 130.8, 130.5, 129.1, 128.6, 127.2, 126.2, 124.2, 122.8,122.6, 122.4, 50.8, 42.2, 41.0, 39.4.

HRMS (ESI) (m/z): $[M+H]^+$ calcd. for $C_{24}H_{20}BrN_2O_2$: 447.0630, found: 447.0705.

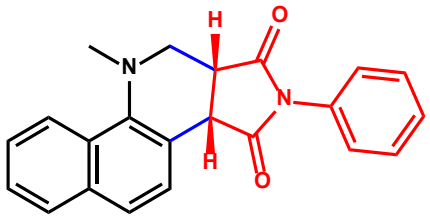

(6e)

Scheme S18. The chemical structure of **6e**.

(3a*R,9b*S**)-10-methyl-2-phenyl-3a,10,11,11a-tetrahydro-1H-benzo[h]pyrrolo[3,4-c]quinoline-1,3(2H)-dione (6e)**

^{1}H NMR (400 MHz, $CDCl_3$) δ 8.19 (d, *J* = 8.3 Hz, 1H), 7.84 (dd, *J* = 8.0, 4.1 Hz, 2H), 7.65 (d, *J* = 8.6 Hz, 1H), 7.57 – 7.44 (m, 5H), 7.40 (t, *J* = 7.4 Hz, 1H), 7.29 (s, 1H), 4.32 (d, *J* = 8.5 Hz, 1H), 3.73 – 3.62 (m, 3H), 3.58 – 3.49 (m, 1H), 3.01 (s, 3H).

^{13}C NMR (101 MHz, $CDCl_3$) δ 177.6, 175.5, 144.5, 133.9, 131.9, 129.1, 128.6, 128.5, 128.3, 127.5, 126.3,126.2, 125.9, 124.2, 123.6, 119.3, 51.1, 43.9, 41.7, 38.3.

HRMS (ESI) (m/z): $[M+H]^+$ calcd. for $C_{22}H_{19}N_2O_2$: 343.1368, found: 343.1443.

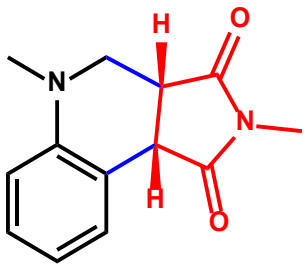

(6f)

Scheme S19. The chemical structure of **6f**.

(3a*R,9b*S**)-2,5-Dimethyl-3a,4,5,9b-tetrahydro-1H-pyrrolo[3,4-c]quinoline-1,3(2H)-dione (lit.[8]) (6f)**

^{1}H NMR (400 MHz, $CDCl_3$) δ 7.49 (d, *J* = 7.5 Hz, 1H), 7.22 (t, *J* = 7.8 Hz, 1H), 6.90 (t, *J* = 7.2 Hz, 1H), 6.71 (d, *J* = 8.2 Hz, 1H), 4.01 (d, *J* = 9.5 Hz, 1H), 3.54 (dd, *J* = 11.5, 2.4 Hz, 1H), 3.37 (ddd, *J* = 9.4, 4.3, 2.4 Hz, 1H), 3.05 (dd, *J* = 11.5, 4.5 Hz, 1H), 3.00 (s, 3H), 2.80 (s, 3H).

^{13}C NMR (101 MHz, $CDCl_3$) δ 178.7, 176.8, 148.4, 130.1, 128.5, 119.6, 118.7, 112.4, 50.4, 43.6, 42.0, 39.4, 25.3.

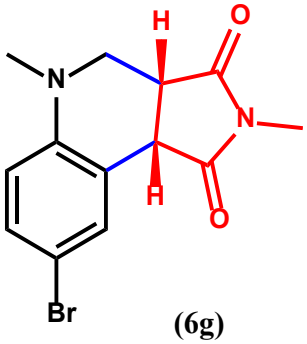

(6g)

Scheme S20. The chemical structure of **6g**.

(3a*R,9b*S**)-8-bromo-2,5-dimethyl-3a,4,5,9b-tetrahydro-1H-pyrrolo[3,4-c]quinoline-1,3(2H)-dione (lit.[8]) (6g)**

^{1}H NMR (400 MHz, $CDCl_3$) δ 7.60 (d, *J* = 2.1 Hz, 1H), 7.29 (dd, *J* = 8.7, 2.3 Hz, 1H), 6.57 (d, *J* = 8.8 Hz, 1H), 3.95 (d, *J* = 9.5 Hz, 1H), 3.53 (dd, *J* = 11.5, 2.5 Hz, 1H), 3.37 (ddd, *J* = 9.3, 4.2, 2.6 Hz, 1H), 3.04 (d, *J* = 4.5 Hz, 1H), 3.00 (s, 3H), 2.78 (s, 3H).

^{13}C NMR (101 MHz, $CDCl_3$) δ 178.2, 176.1, 147.4, 132.6, 131.3, 120.5, 114.1, 111.6, 50.2, 43.3, 41.7, 39.4, 25.4.

7. NMR Spectra

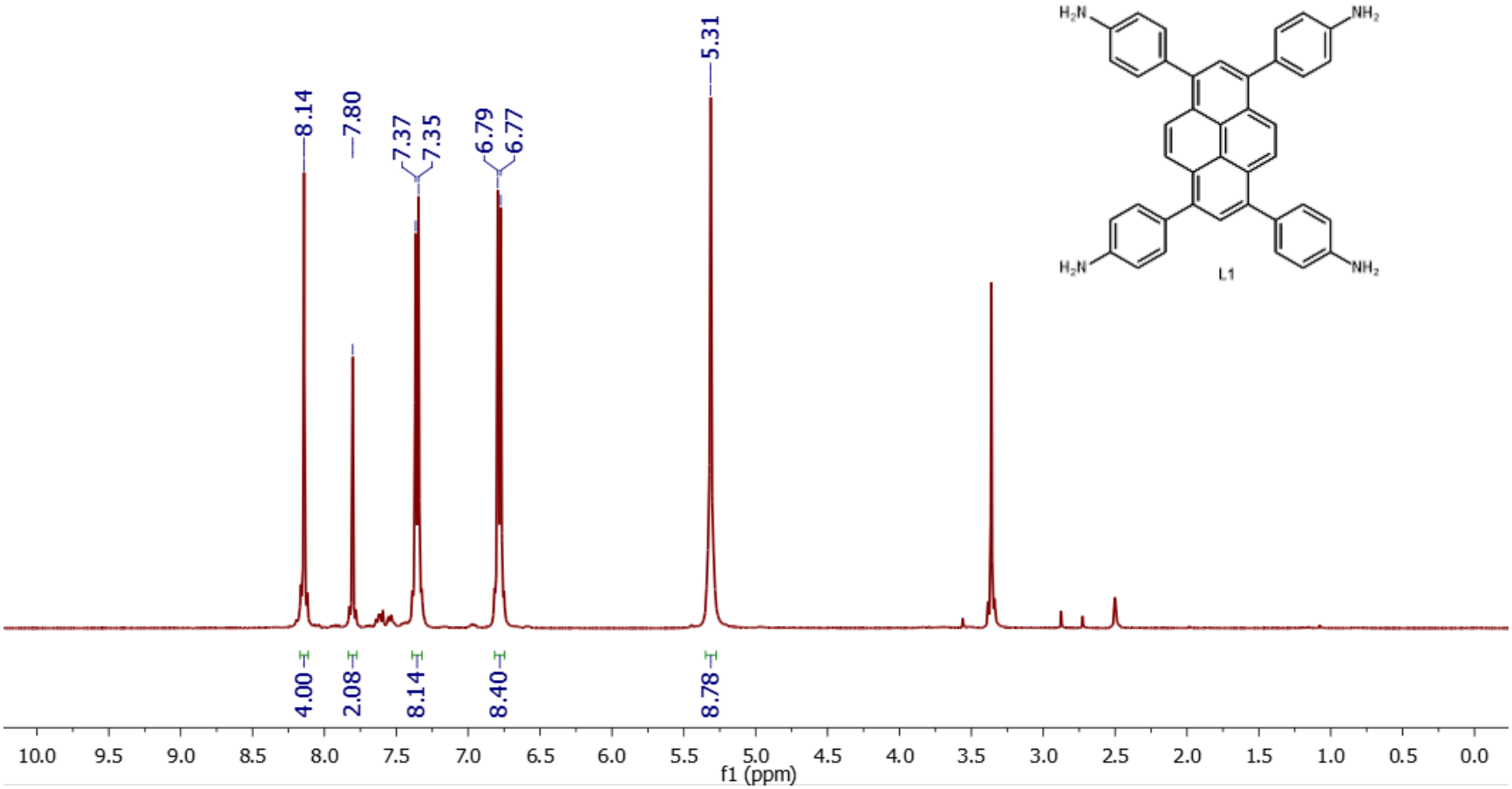

Figure S15. ^{1}H NMR (400 MHz) of **L1** in DMSO-*d*$_6$.

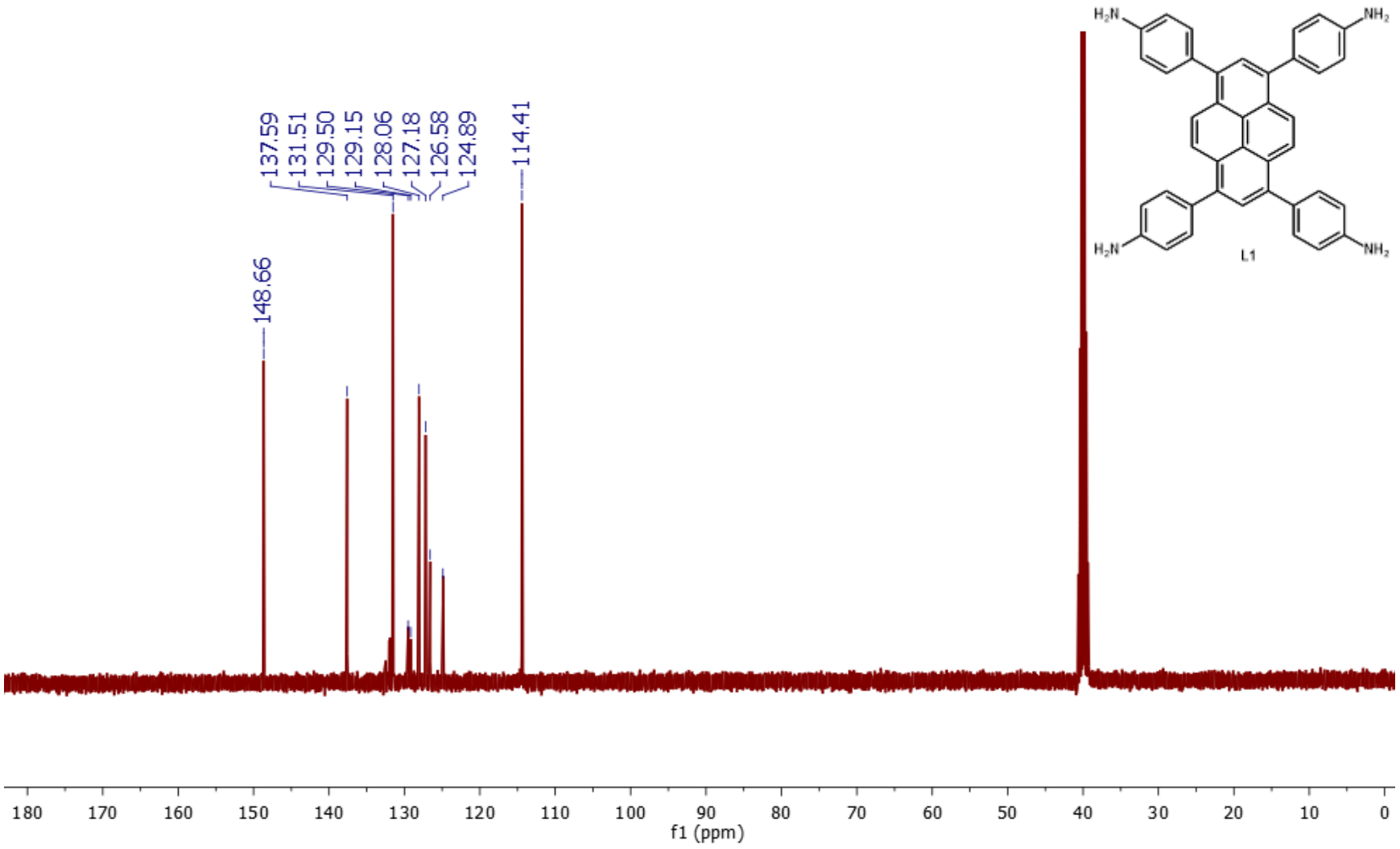

Figure S16. ^{13}C NMR (101 MHz) of **L1** in DMSO-*d*$_6$.

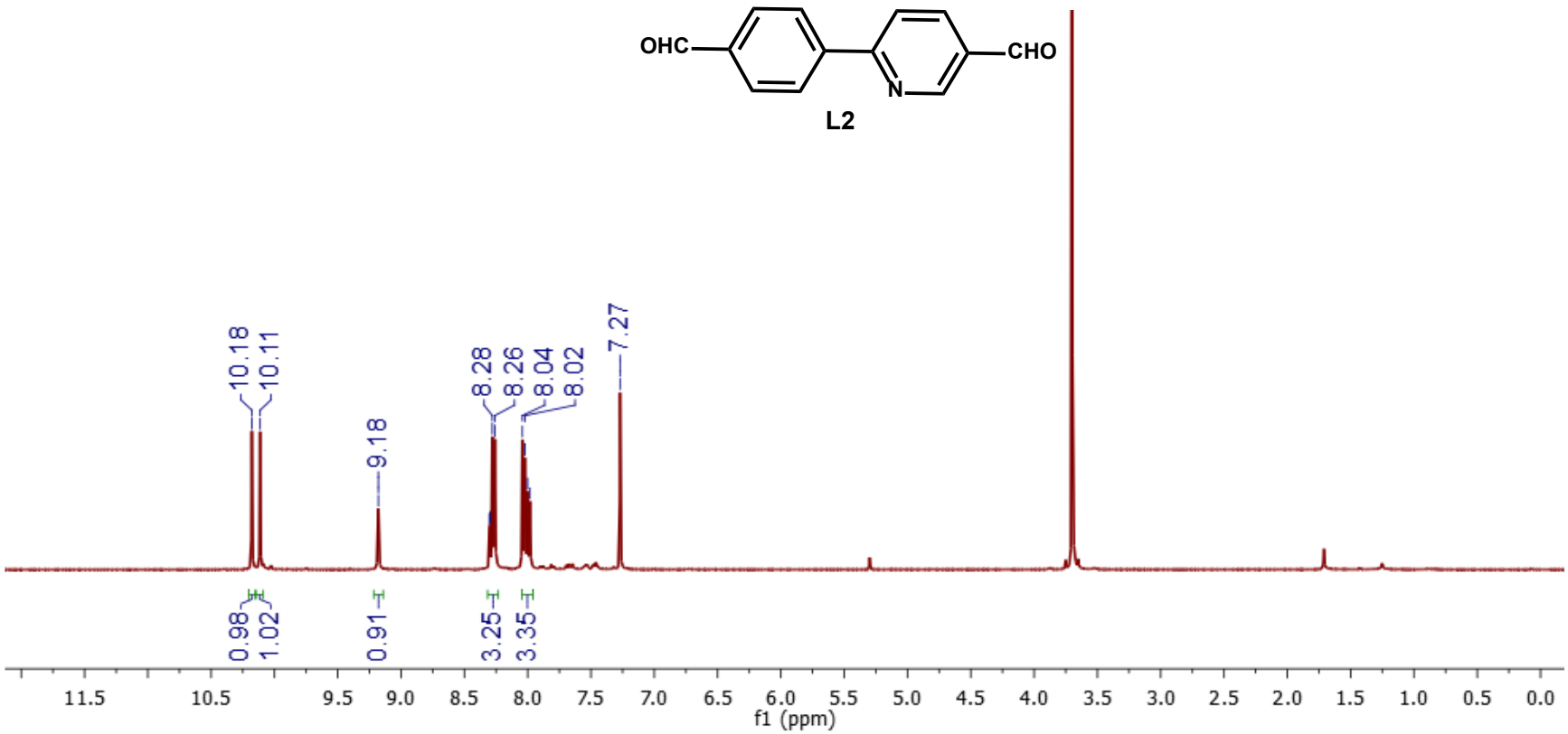

Figure S17. ^{1}H NMR (400 MHz) of **L2** in $CDCl_3$.

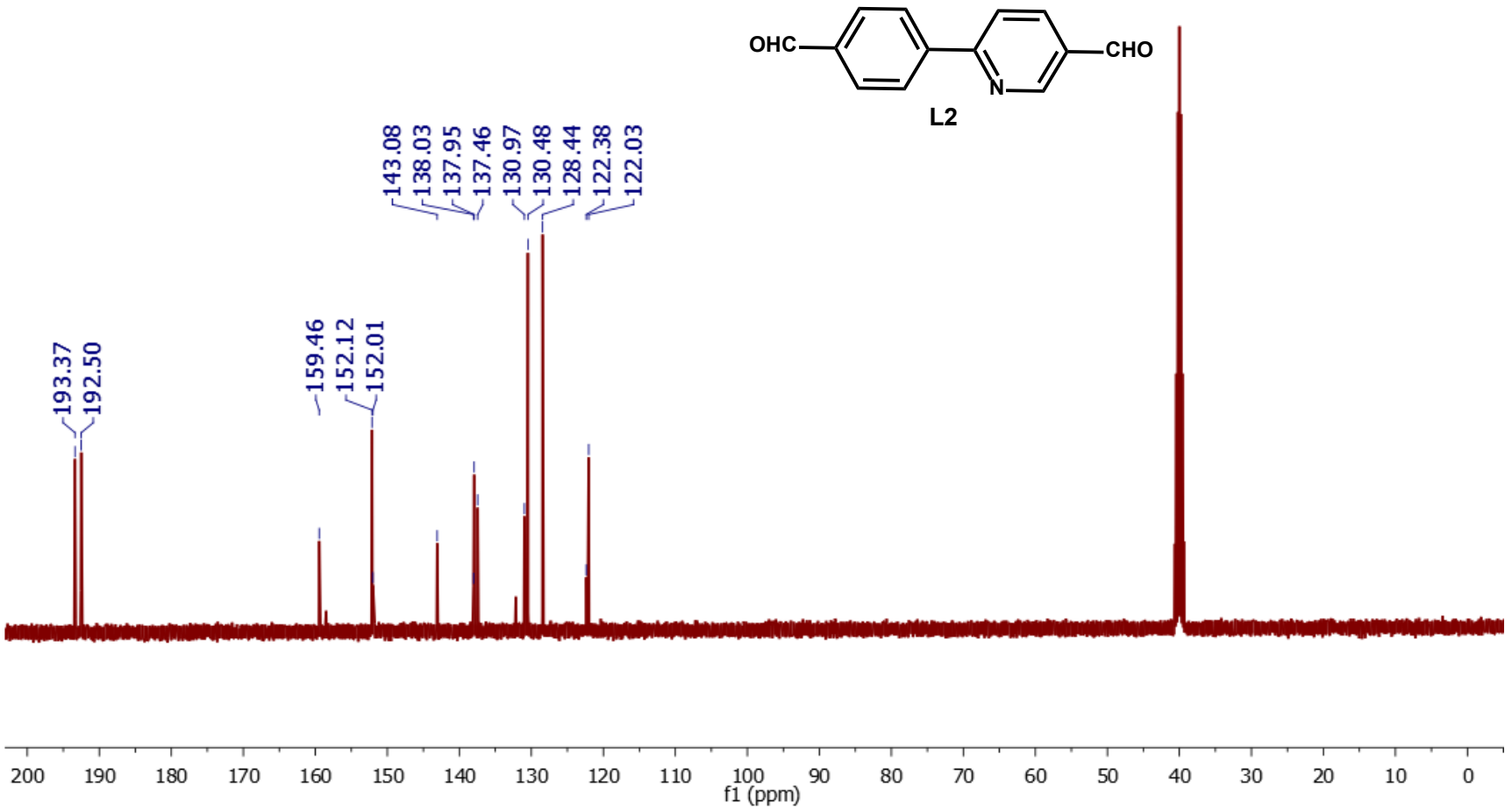

Figure S18. ^{13}C NMR (101 MHz) of **L2** in DMSO-*d*$_6$.

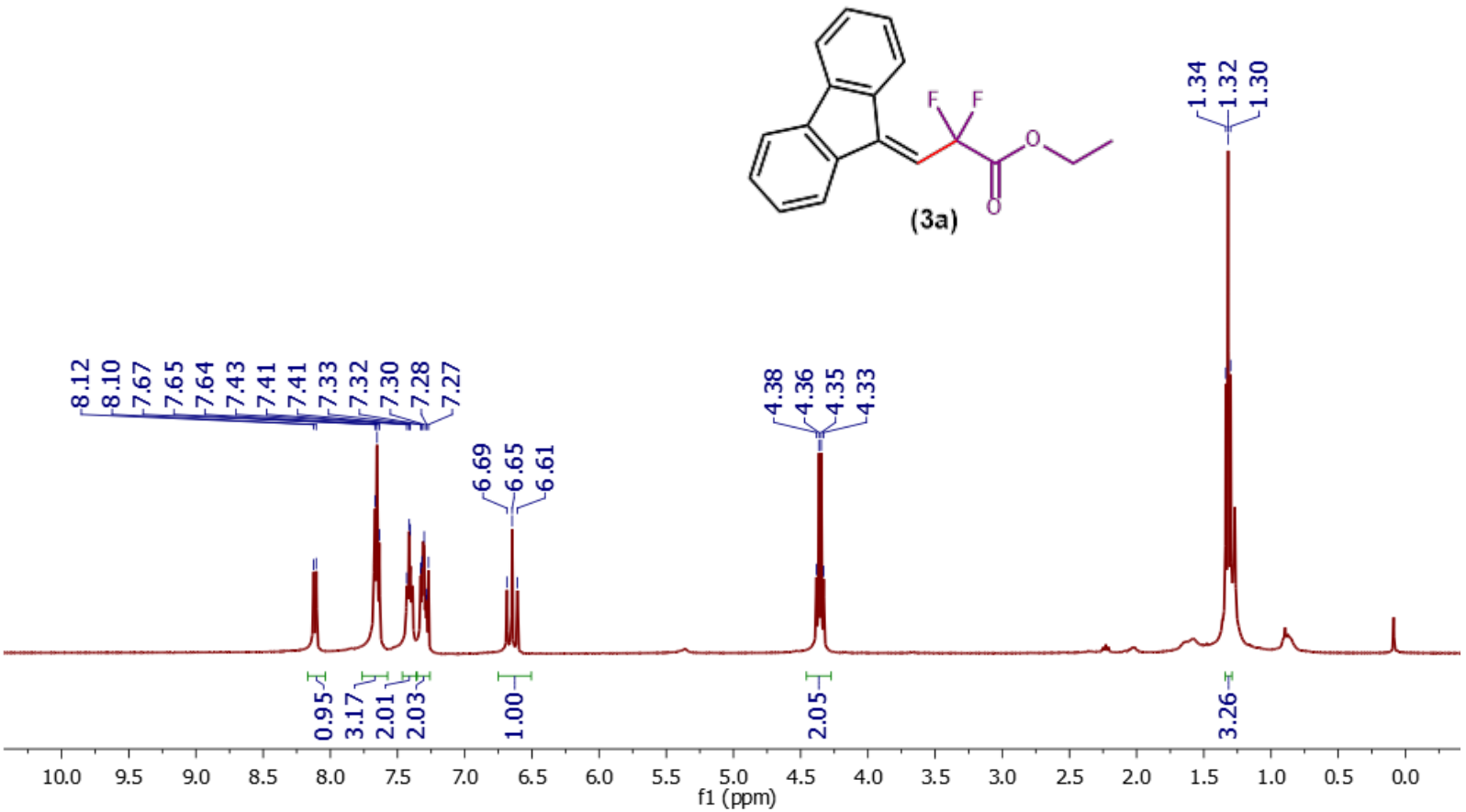

Figure S19. ^{1}H NMR (400 MHz) of **3a** in $CDCl_3$.

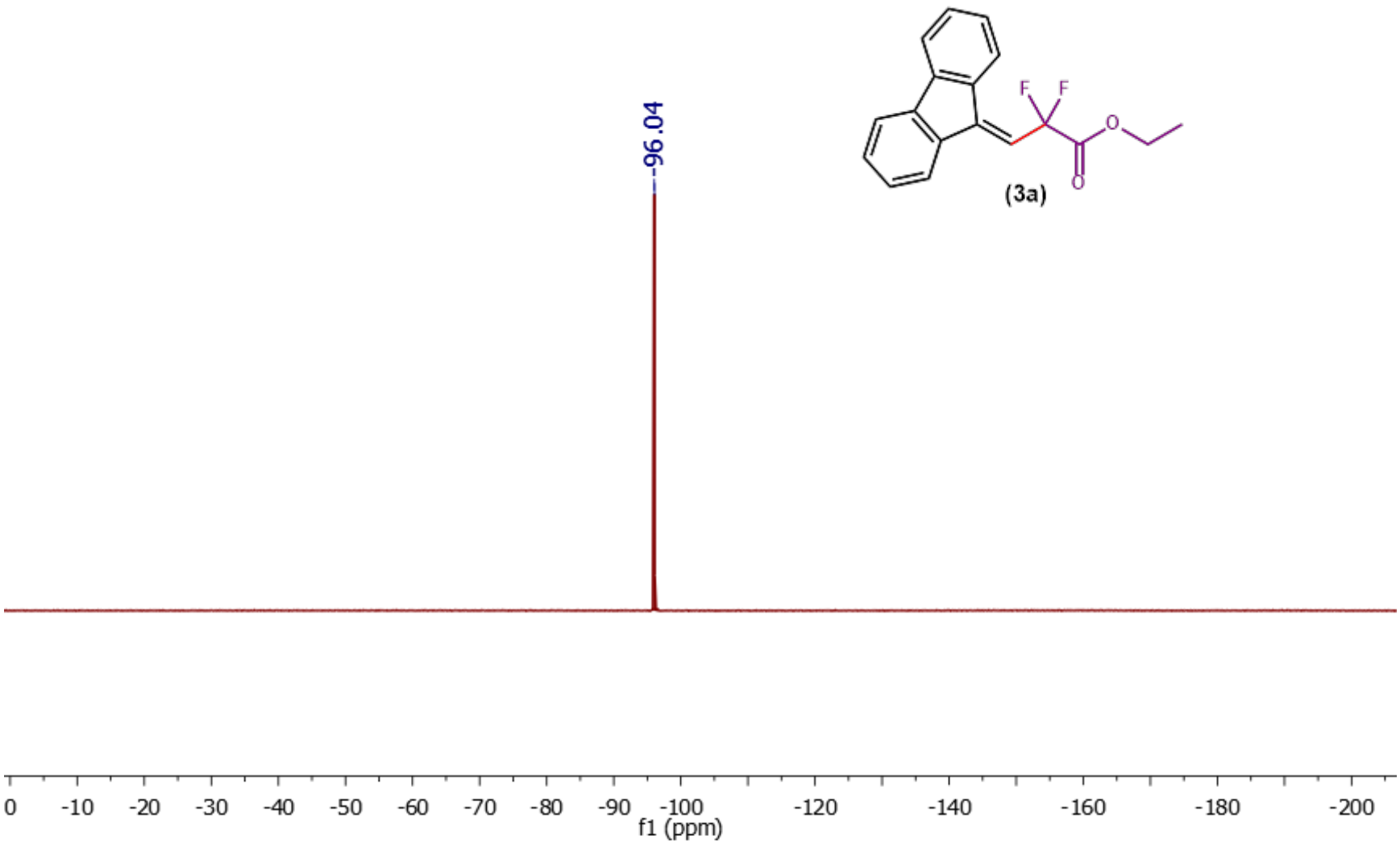

Figure S20. ^{19}F NMR (376 MHz) of **3a** in $CDCl_3$.

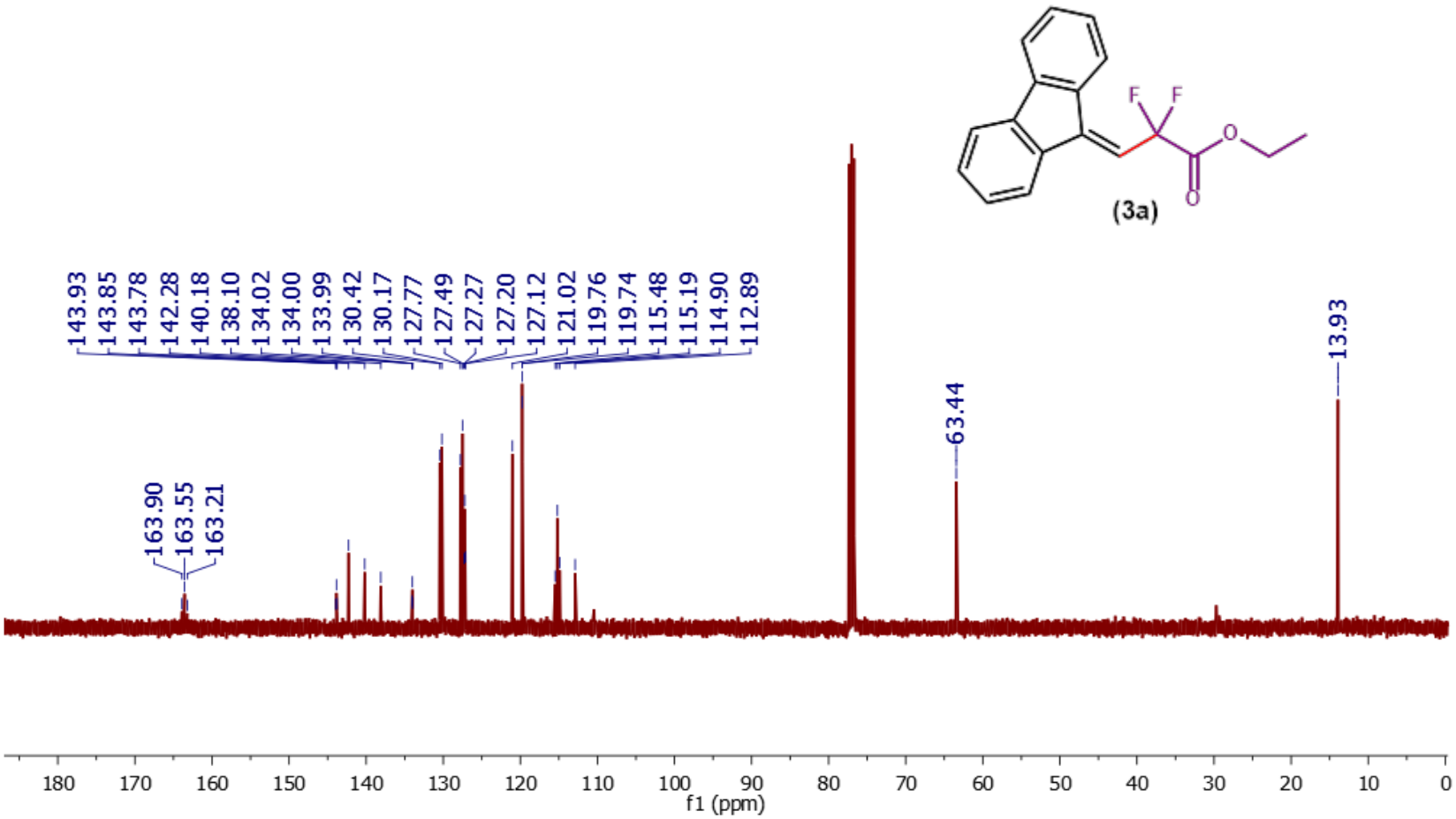

Figure S21. ^{13}C NMR (101 MHz) of **3a** in $CDCl_3$.

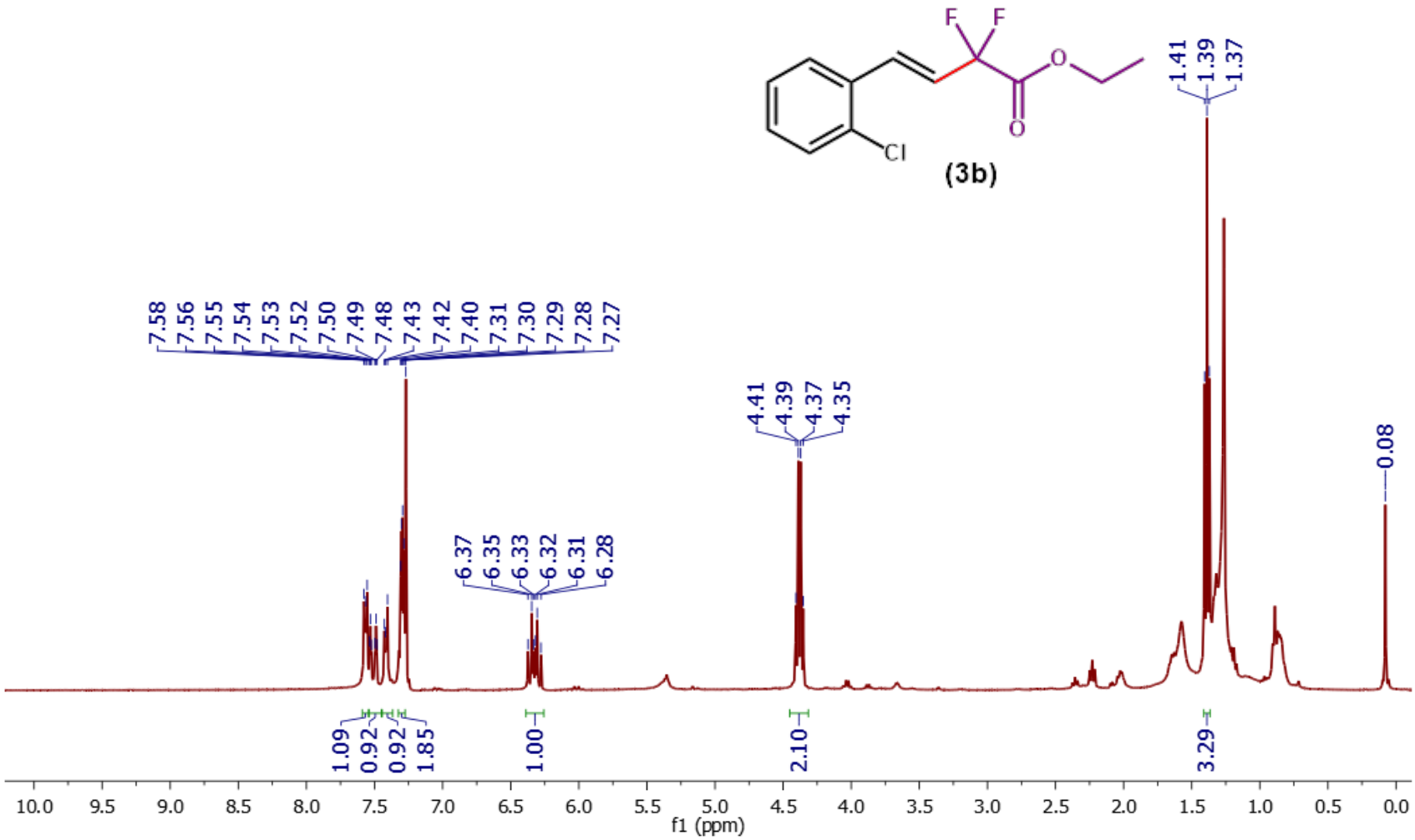

Figure S22. ^{1}H NMR (400 MHz) of **3b** in $CDCl_3$.

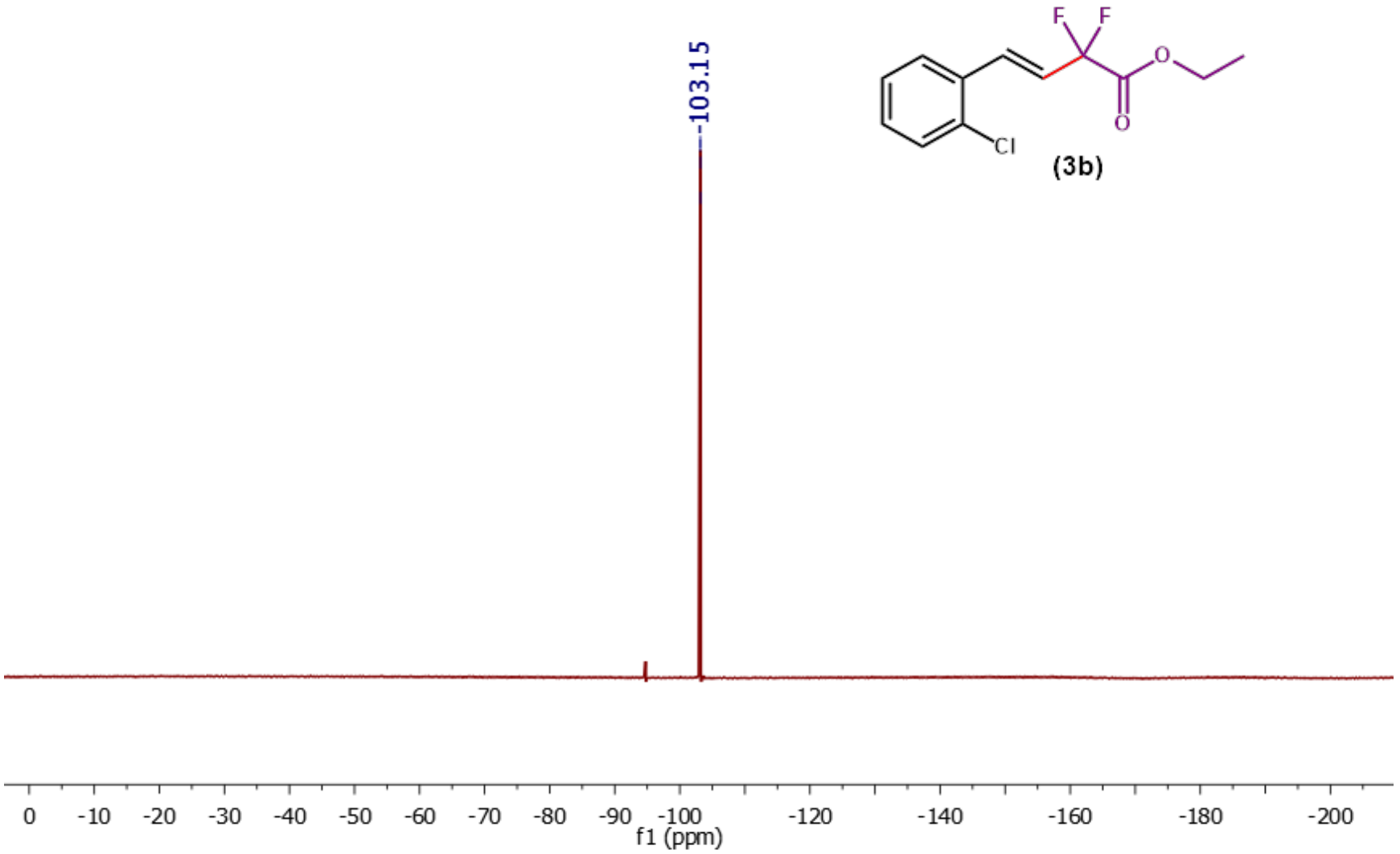

Figure S23. ^{19}F NMR (376 MHz) of **3b** in $CDCl_3$.

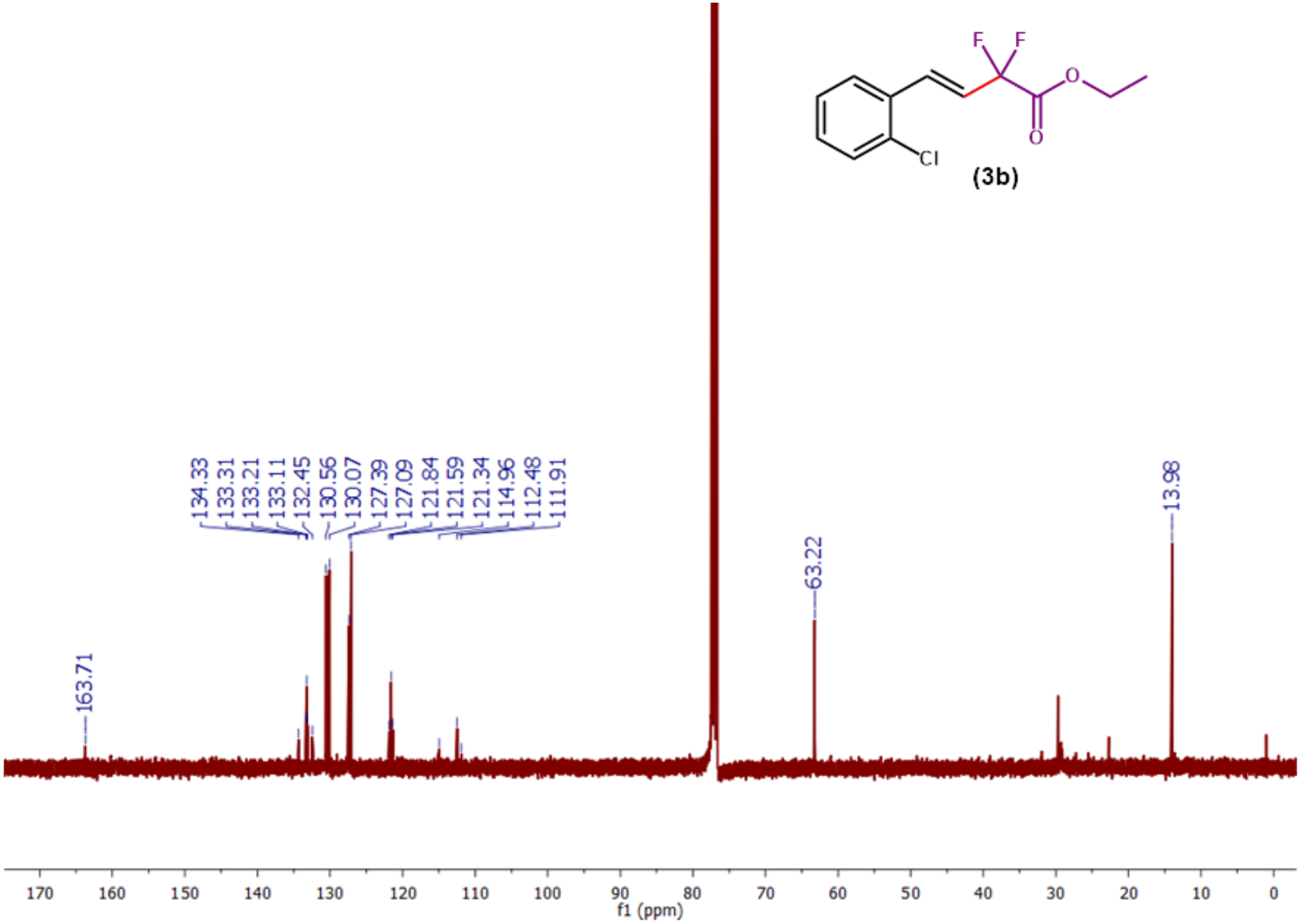

Figure S24. ^{13}C NMR (101 MHz) of **3b** in $CDCl_3$.

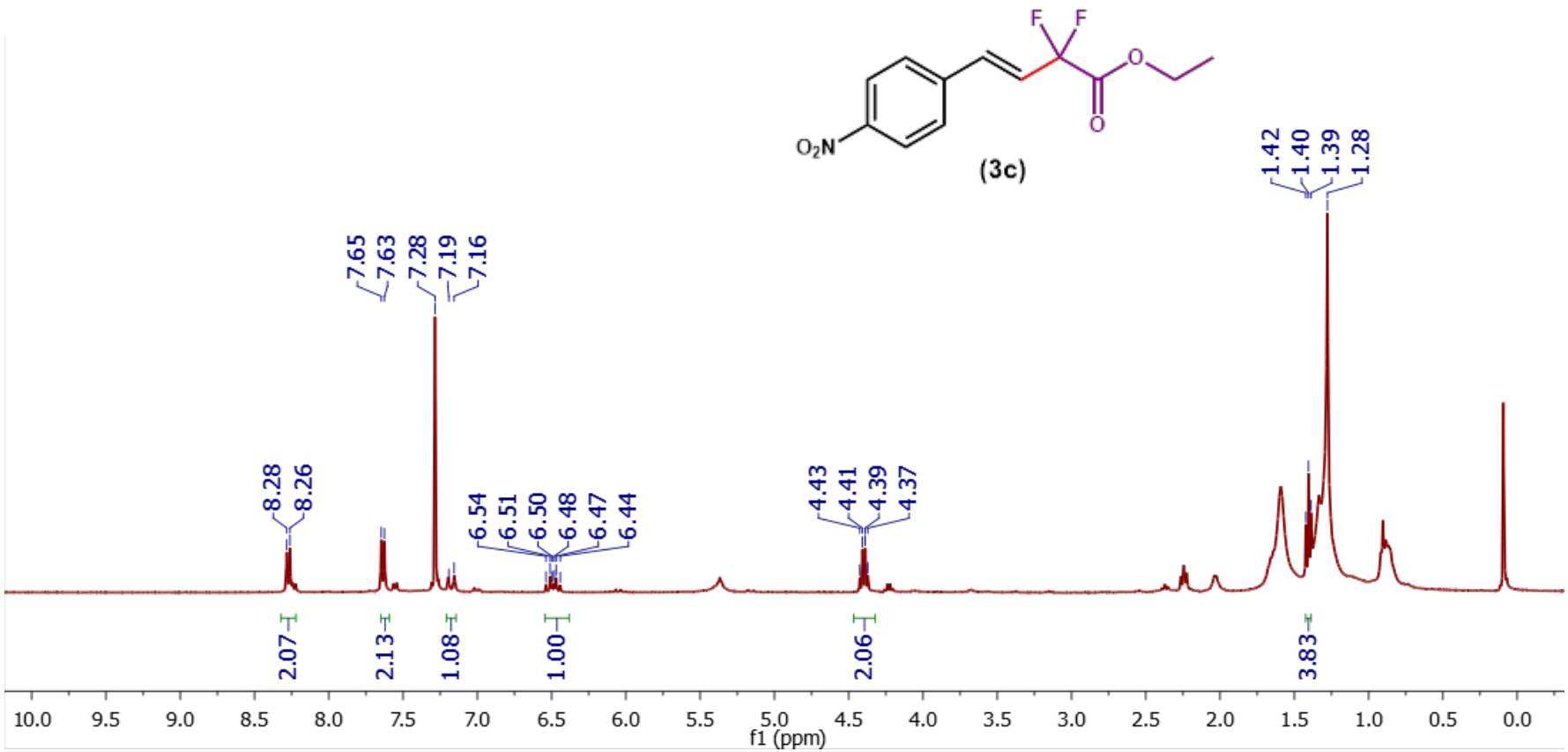

Figure S25. ^{1}H NMR (400 MHz) of **3c** in $CDCl_3$.

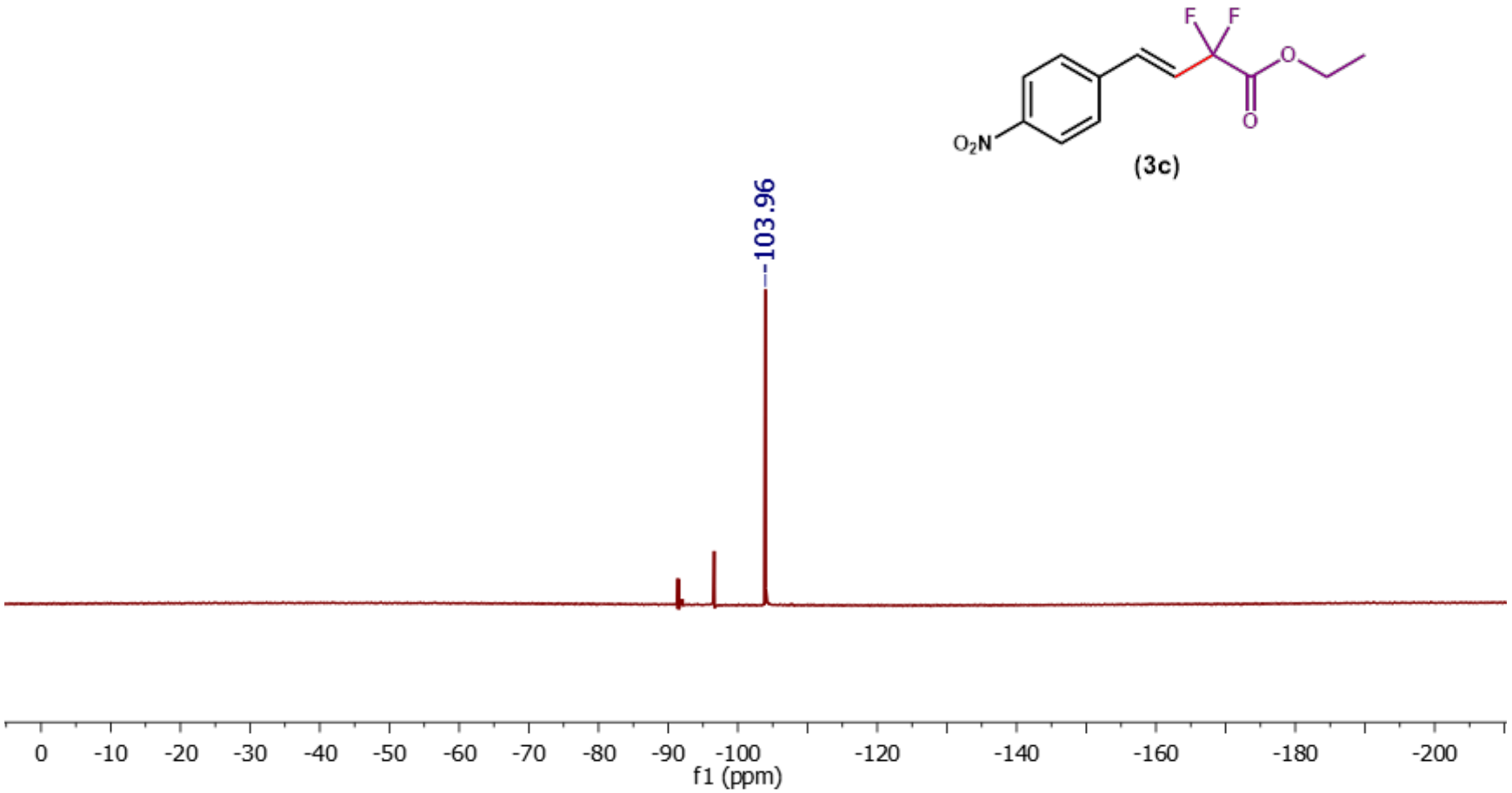

Figure S26. ^{19}F NMR (376 MHz) of **3c** in $CDCl_3$.

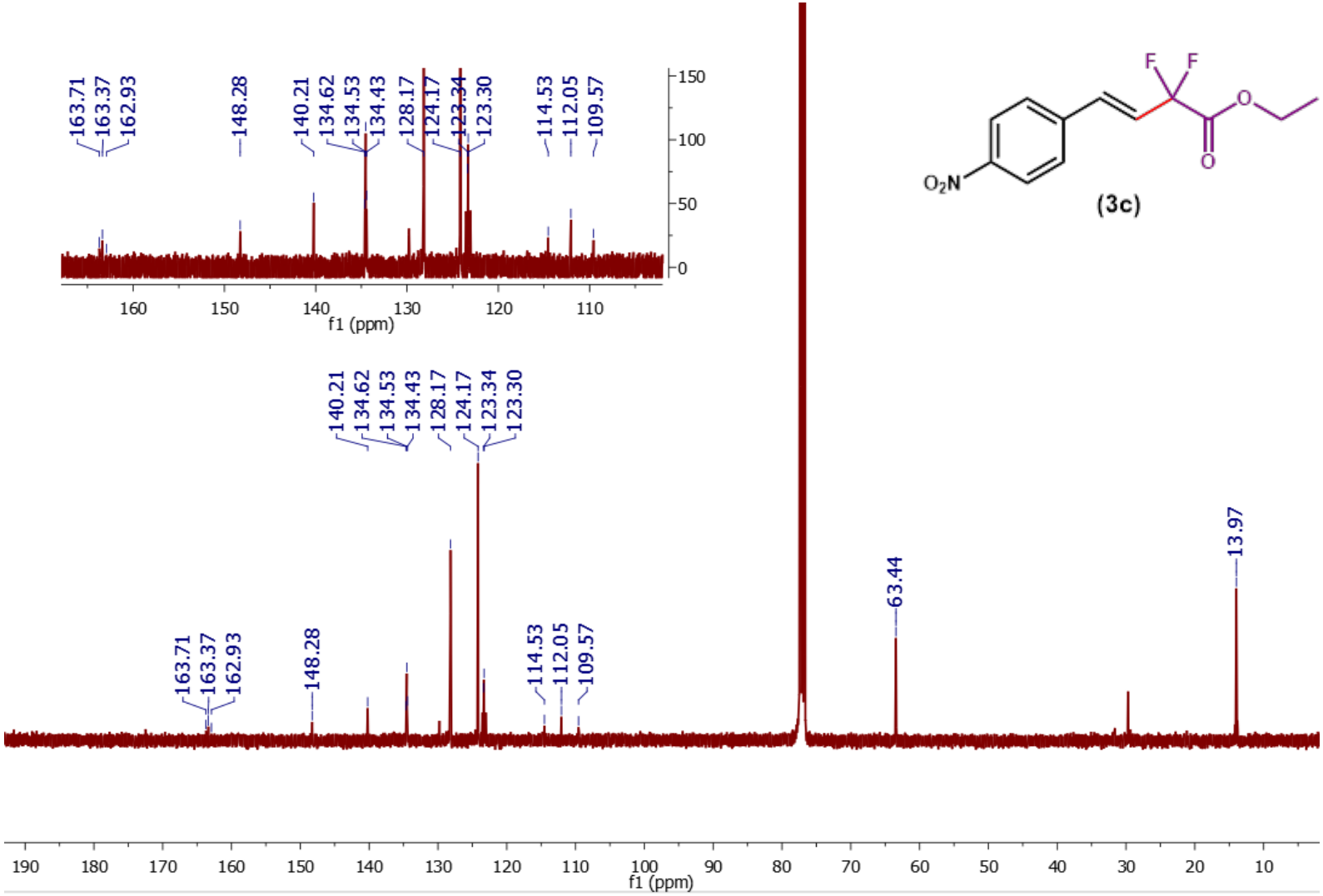

Figure S27. ^{13}C NMR (101 MHz) of **3c** in $CDCl_3$.

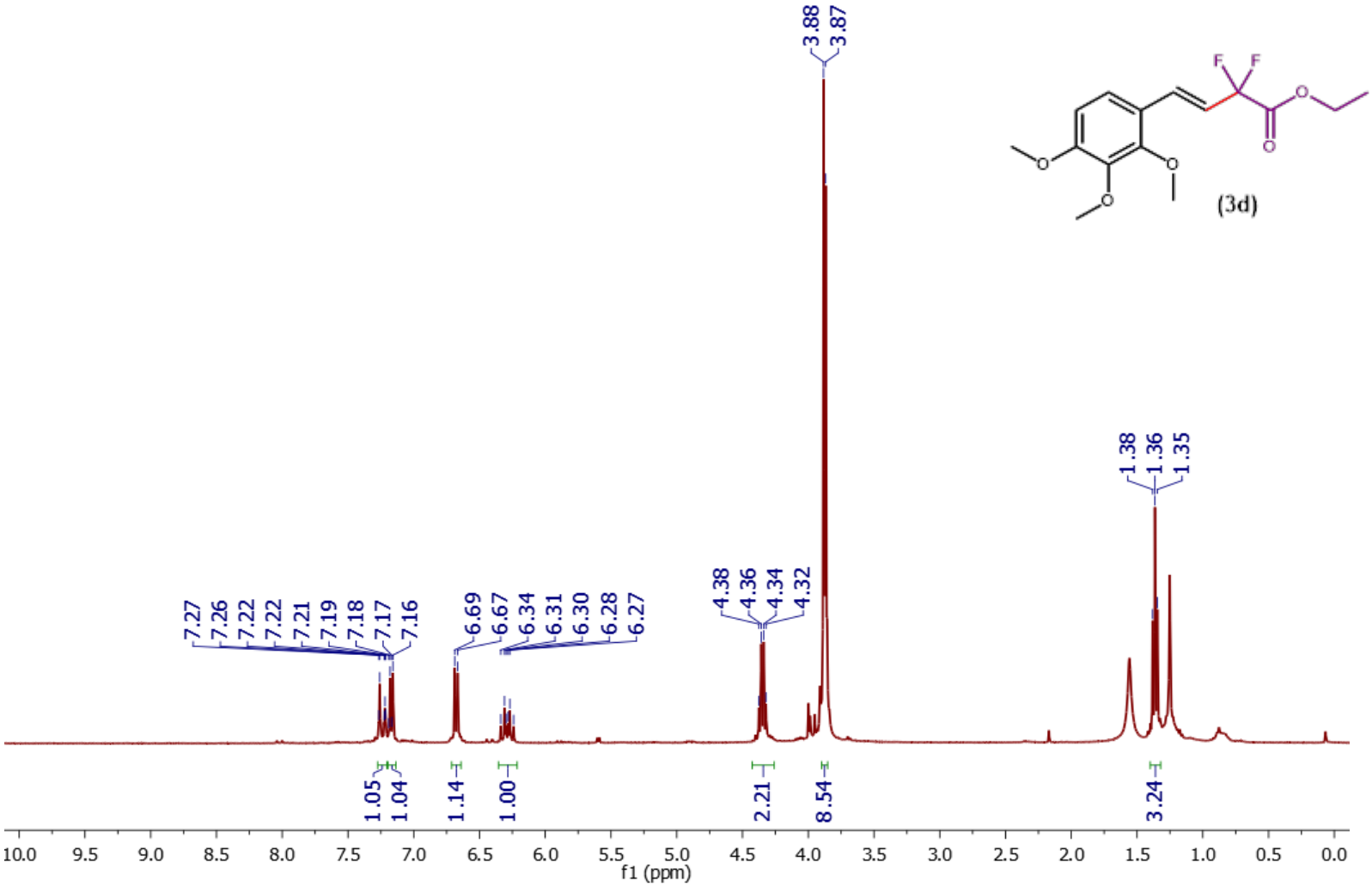

Figure S28. ^{1}H NMR (400 MHz) of **3d** in $CDCl_3$.

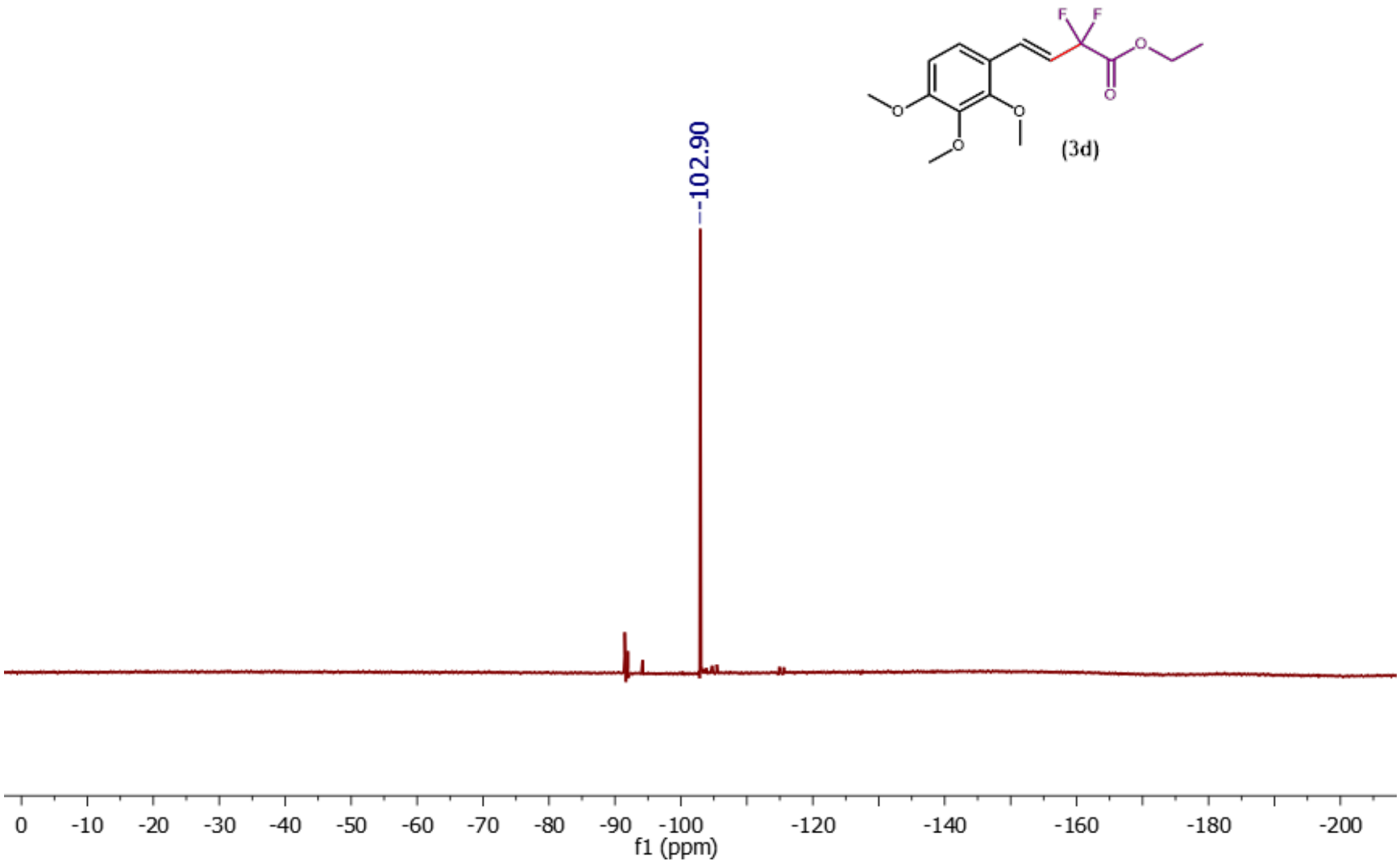

Figure S29. ^{19}F NMR (376 MHz) of **3d** in $CDCl_3$.

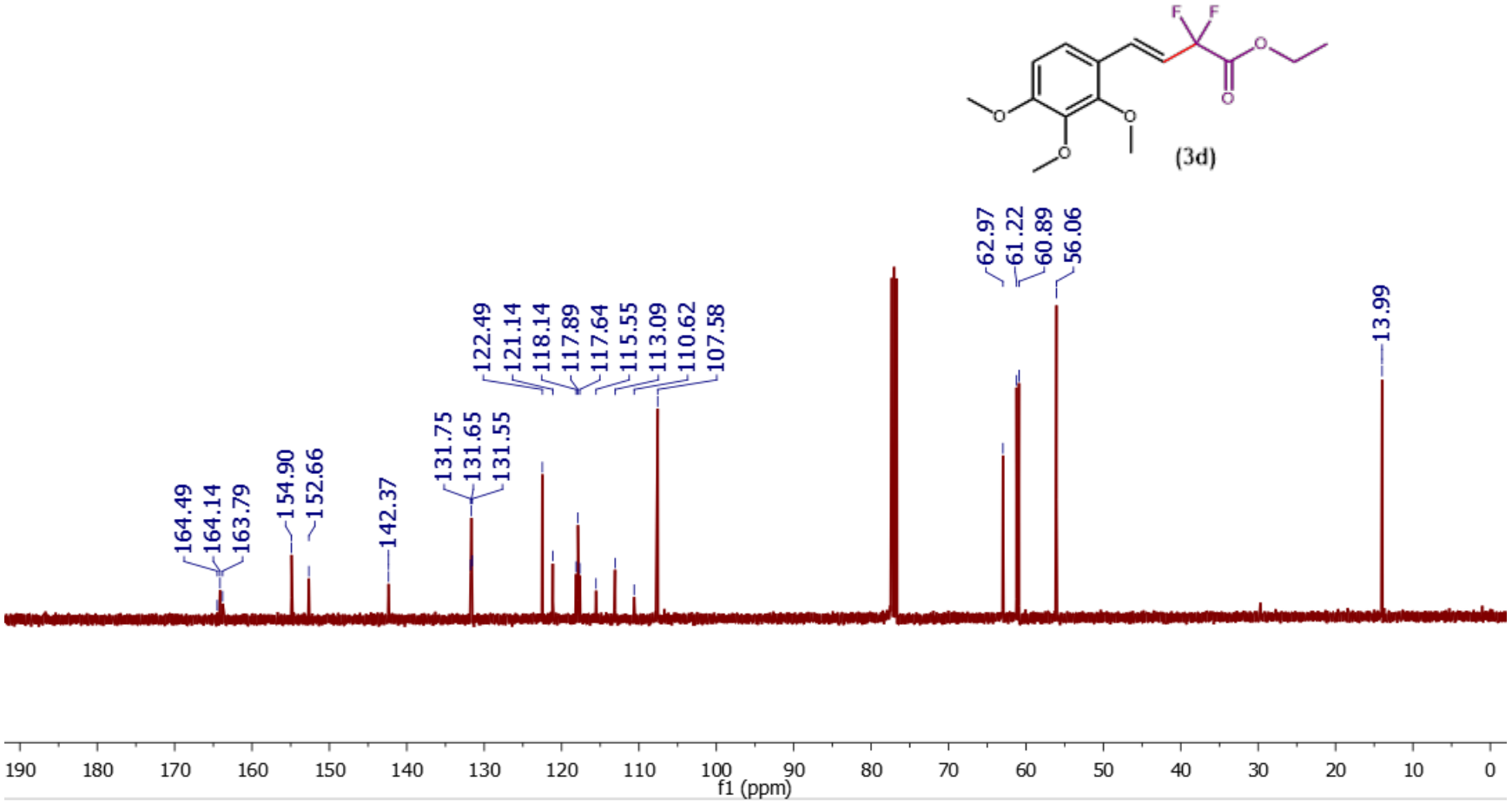

Figure S30. ^{13}C NMR (101 MHz) of **3d** in $CDCl_3$.

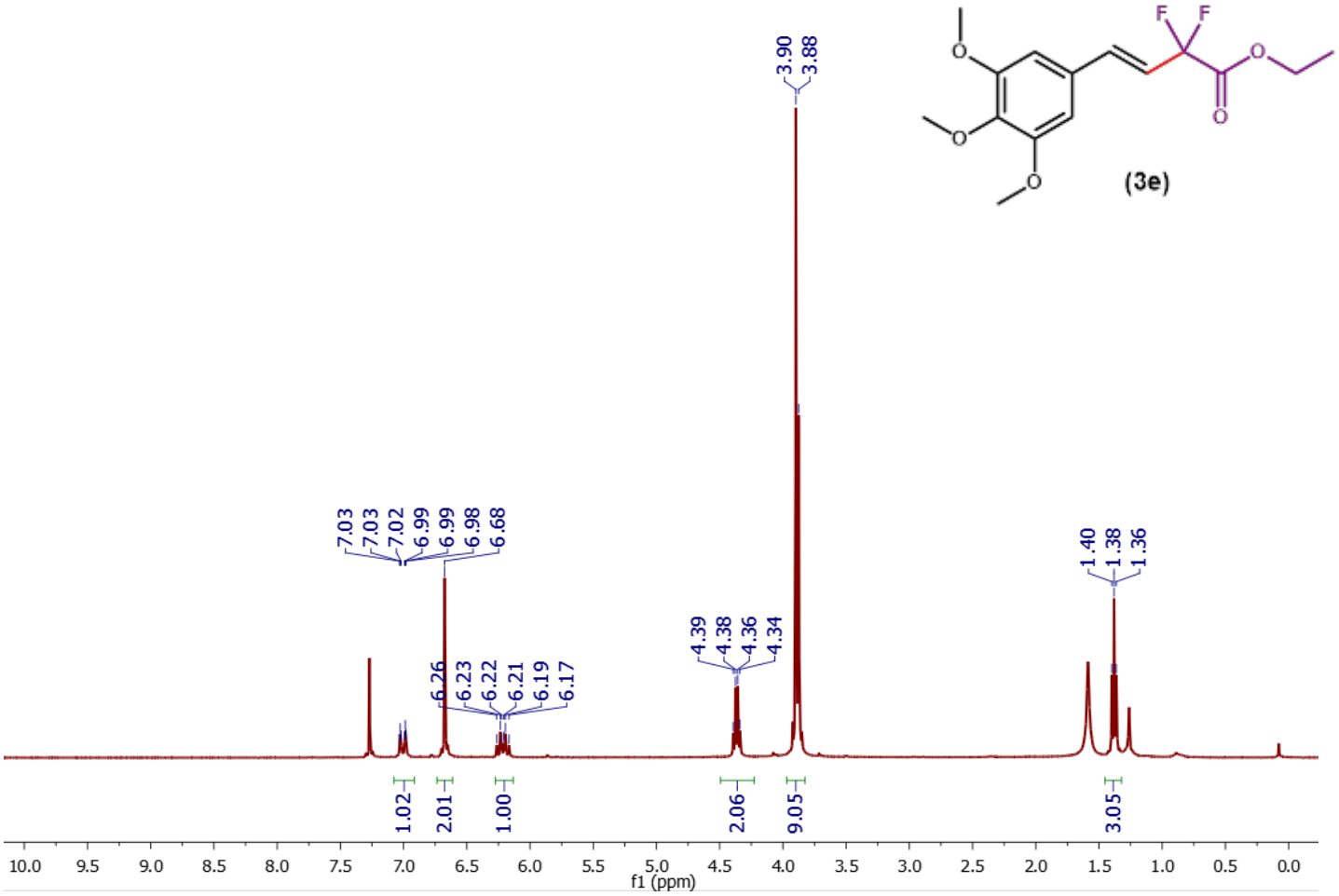

Figure S31. ^{1}H NMR (400 MHz) of **3e** in $CDCl_3$.

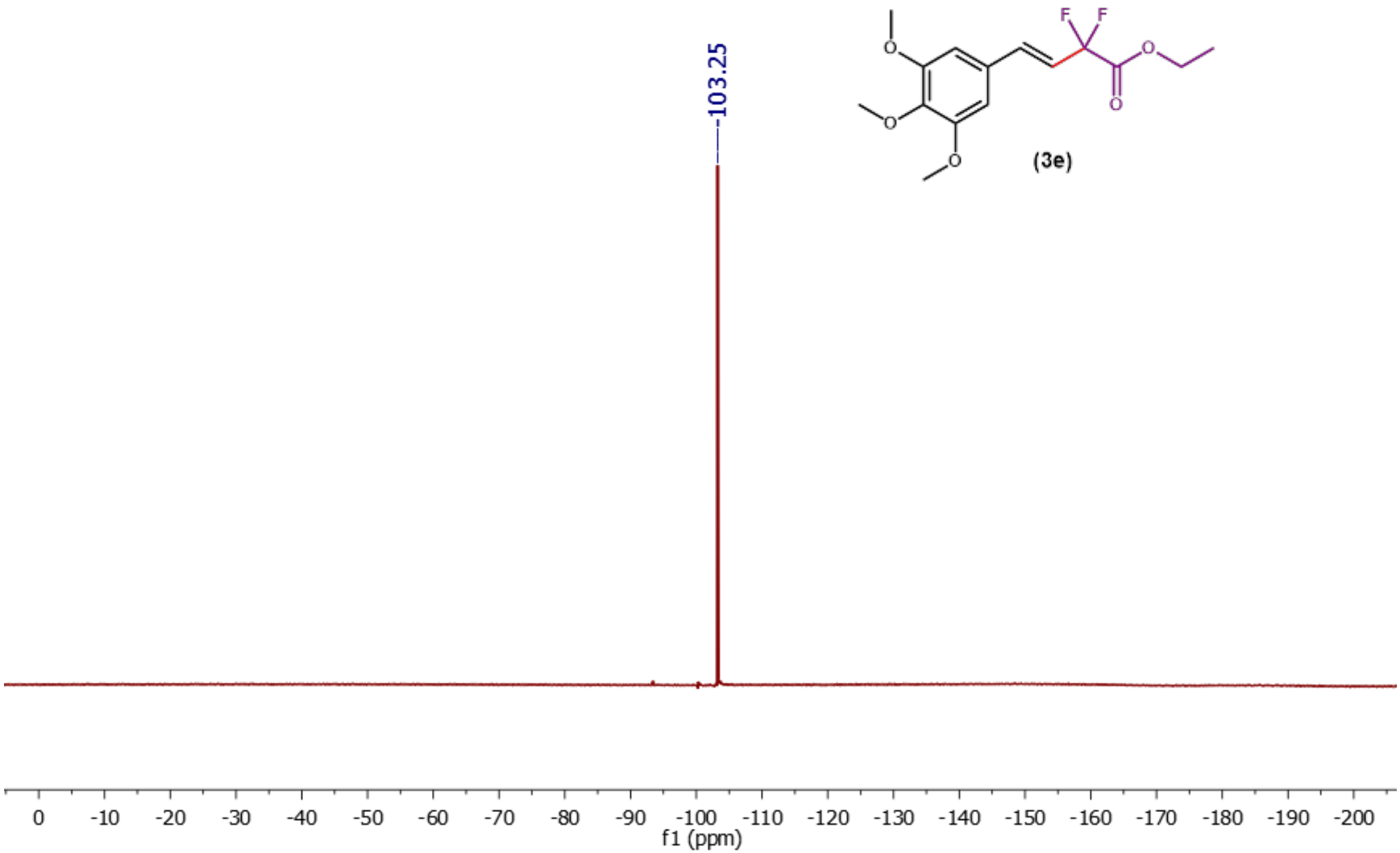

Figure S32. ^{19}F NMR (376 MHz) of **3e** in $CDCl_3$.

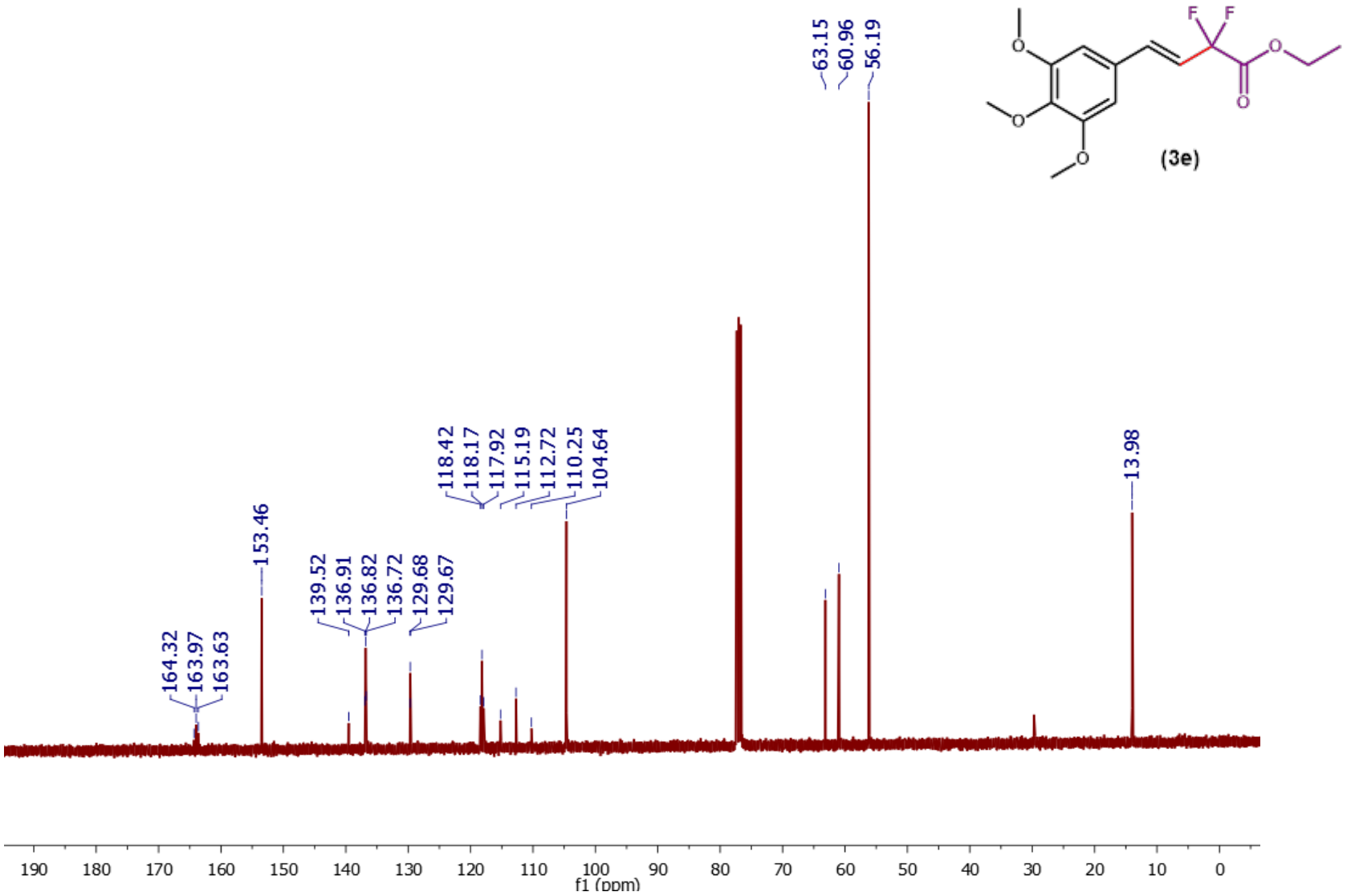

Figure S33. ^{13}C NMR (101 MHz) of **3e** in $CDCl_3$.

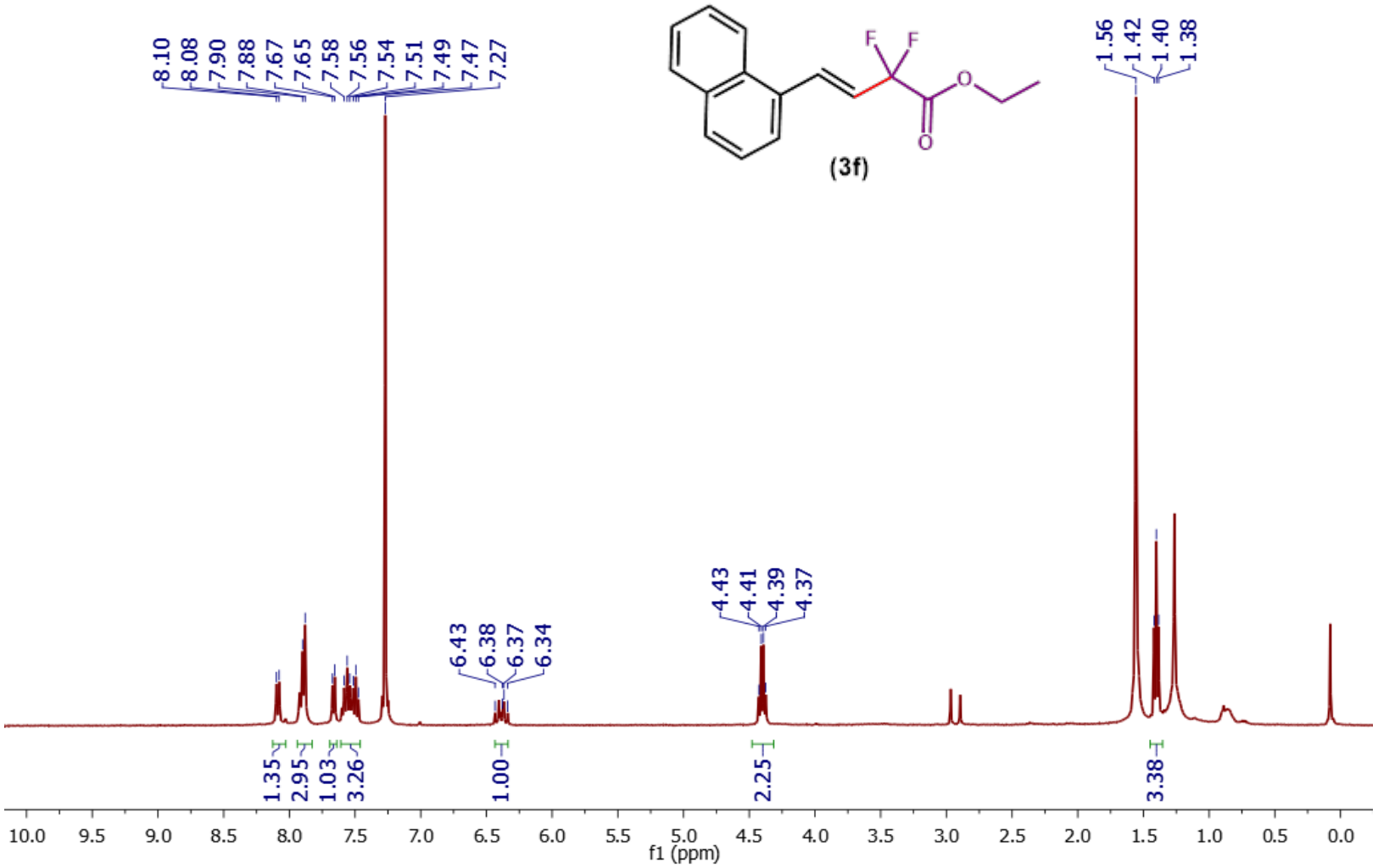

Figure S34. ^{1}H NMR (400 MHz) of **3f** in $CDCl_3$.

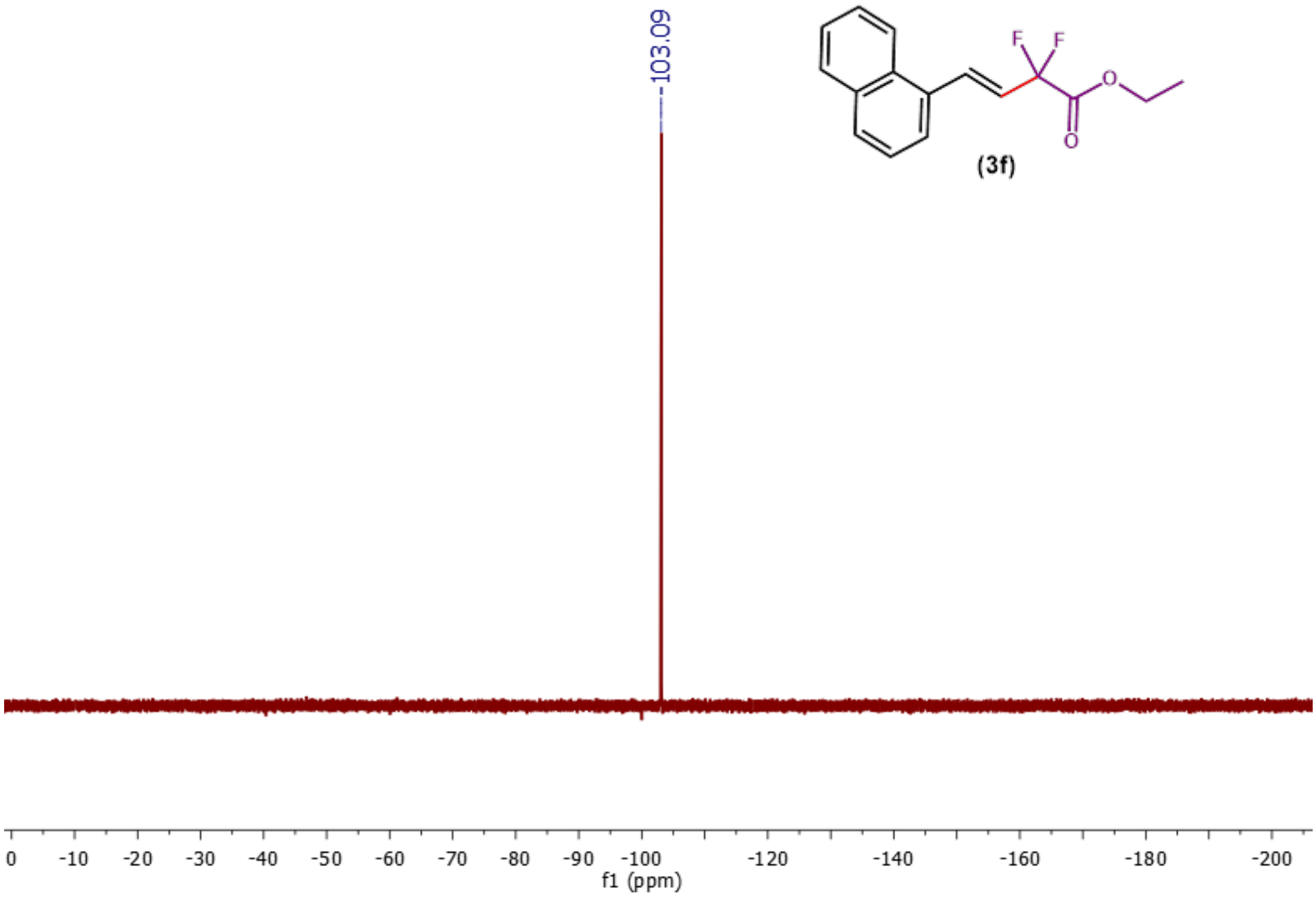

Figure S35. ^{19}F NMR (376 MHz) of **3f** in $CDCl_3$.

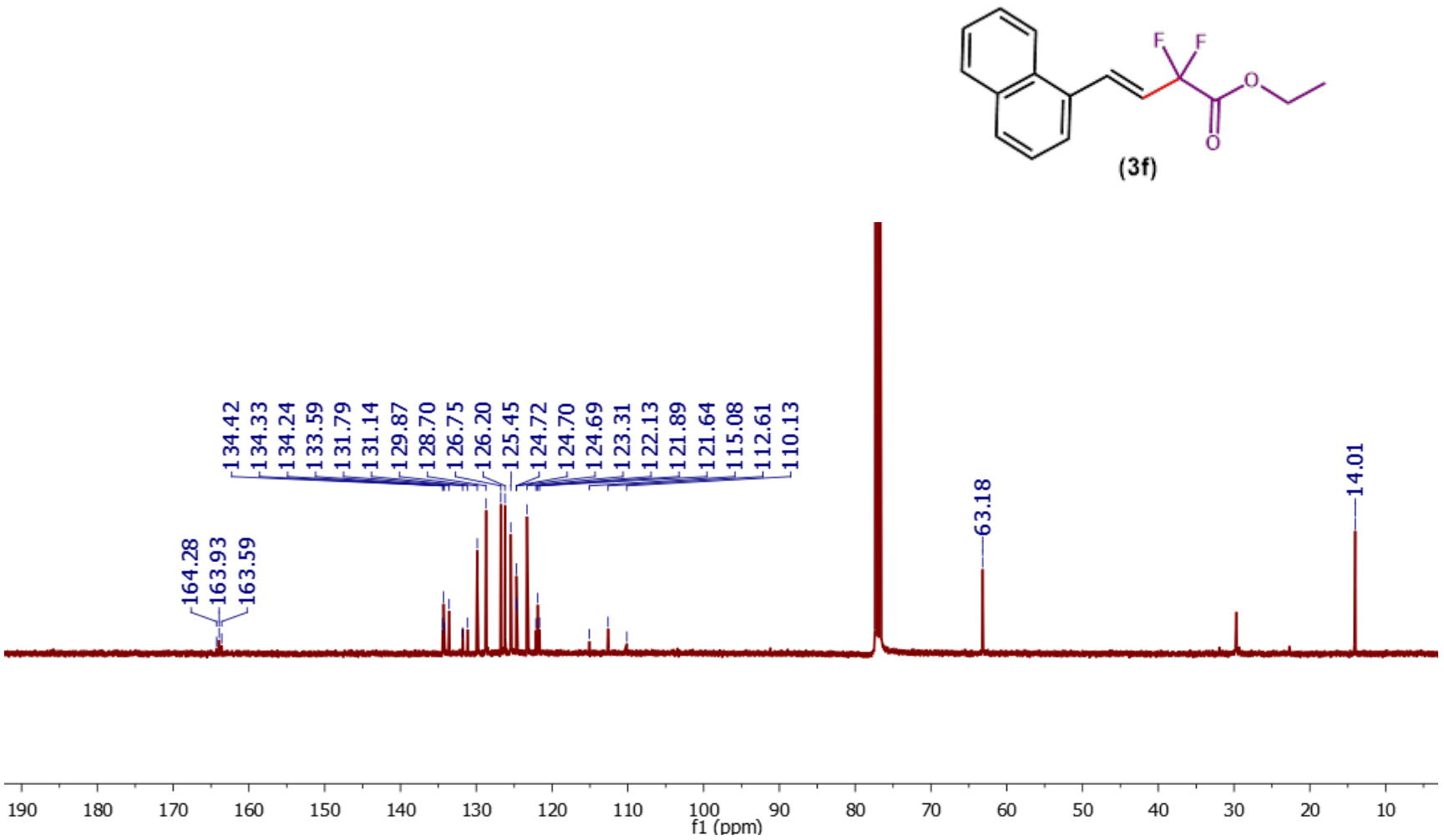

Figure S36. ^{13}C NMR (101 MHz) of **3f** in $CDCl_3$.

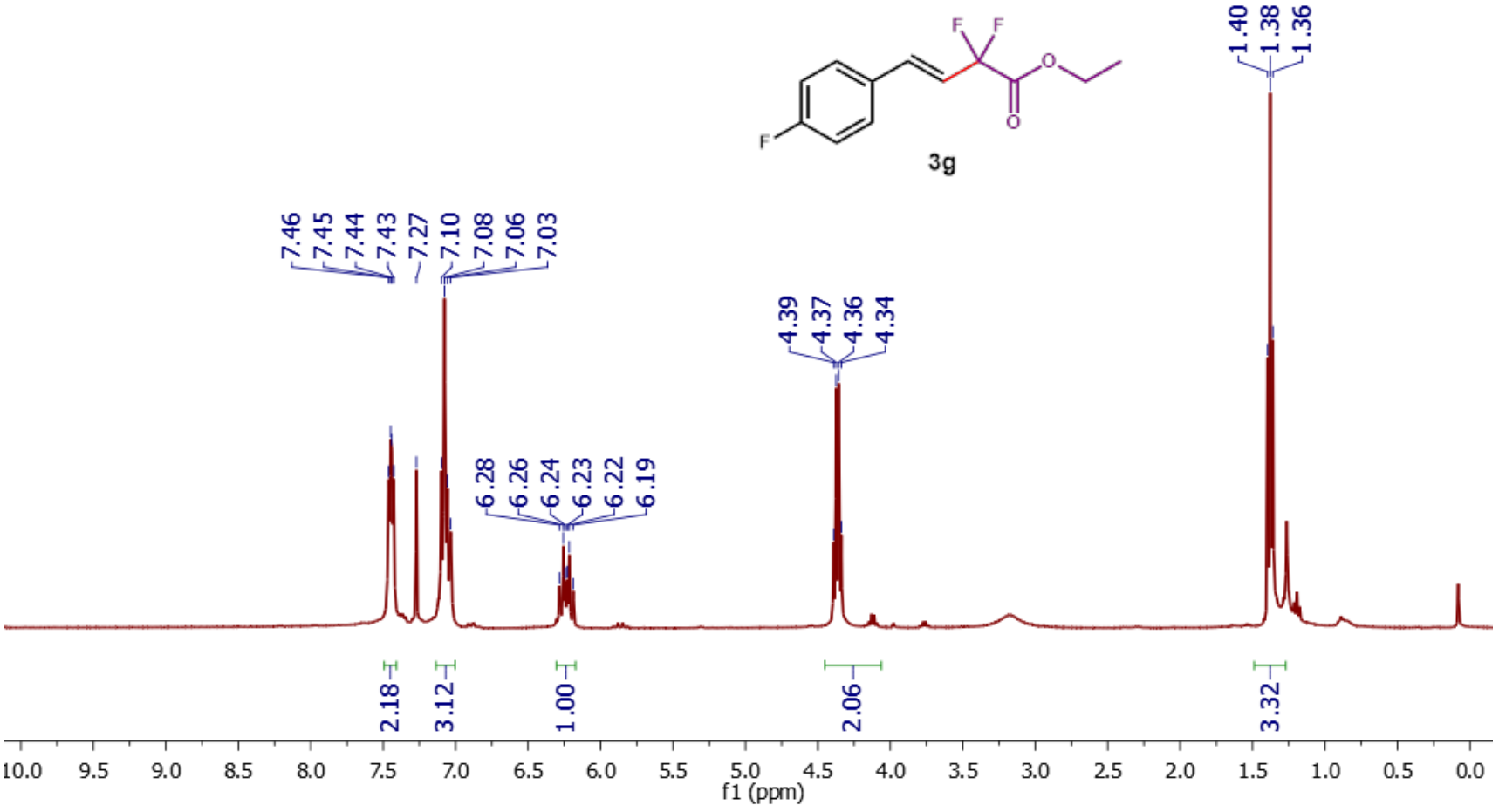

Figure S37. ^{1}H NMR (400 MHz) of **3g** in $CDCl_3$.

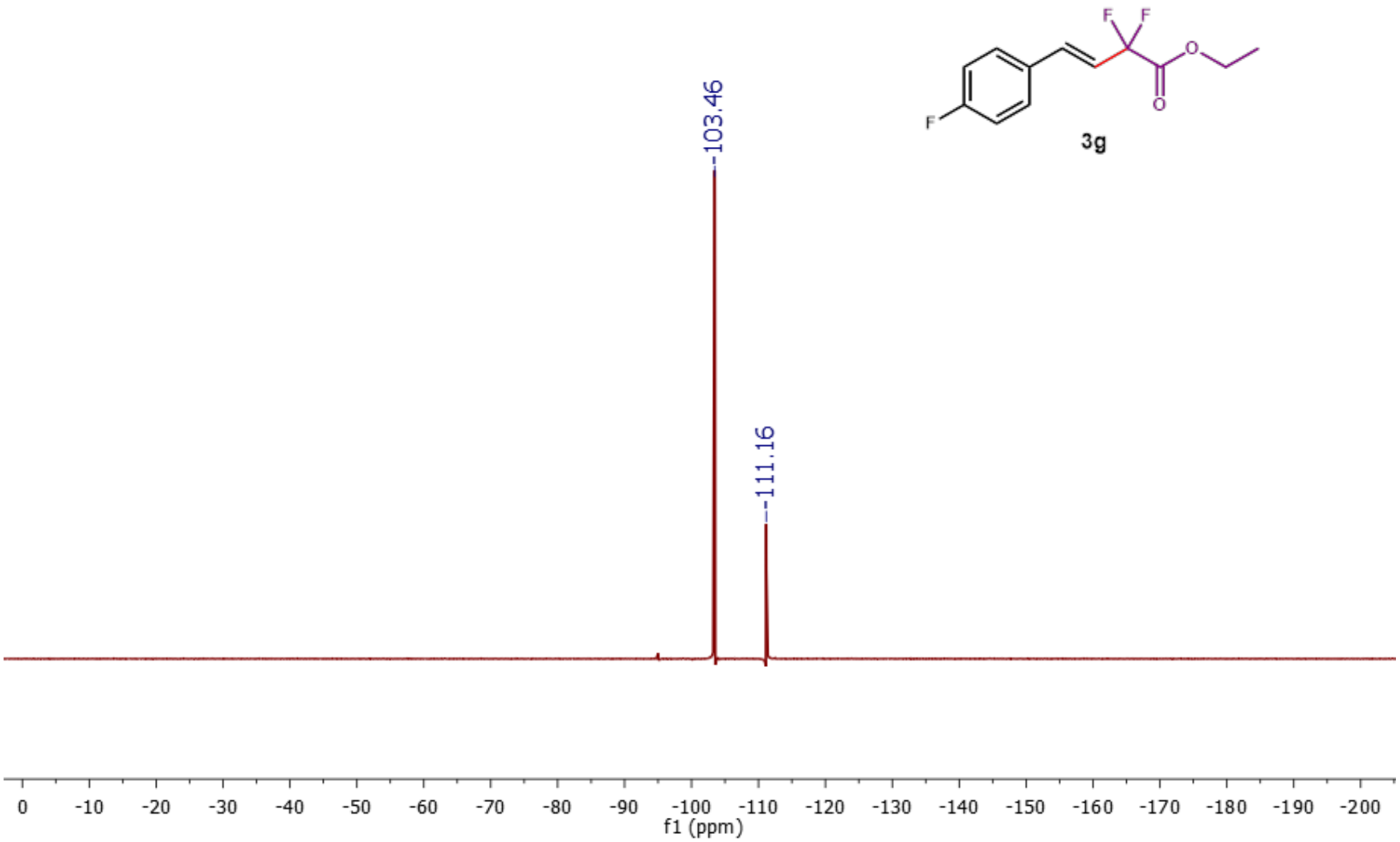

Figure S38. ^{19}F NMR (376 MHz) of **3g** in $CDCl_3$.

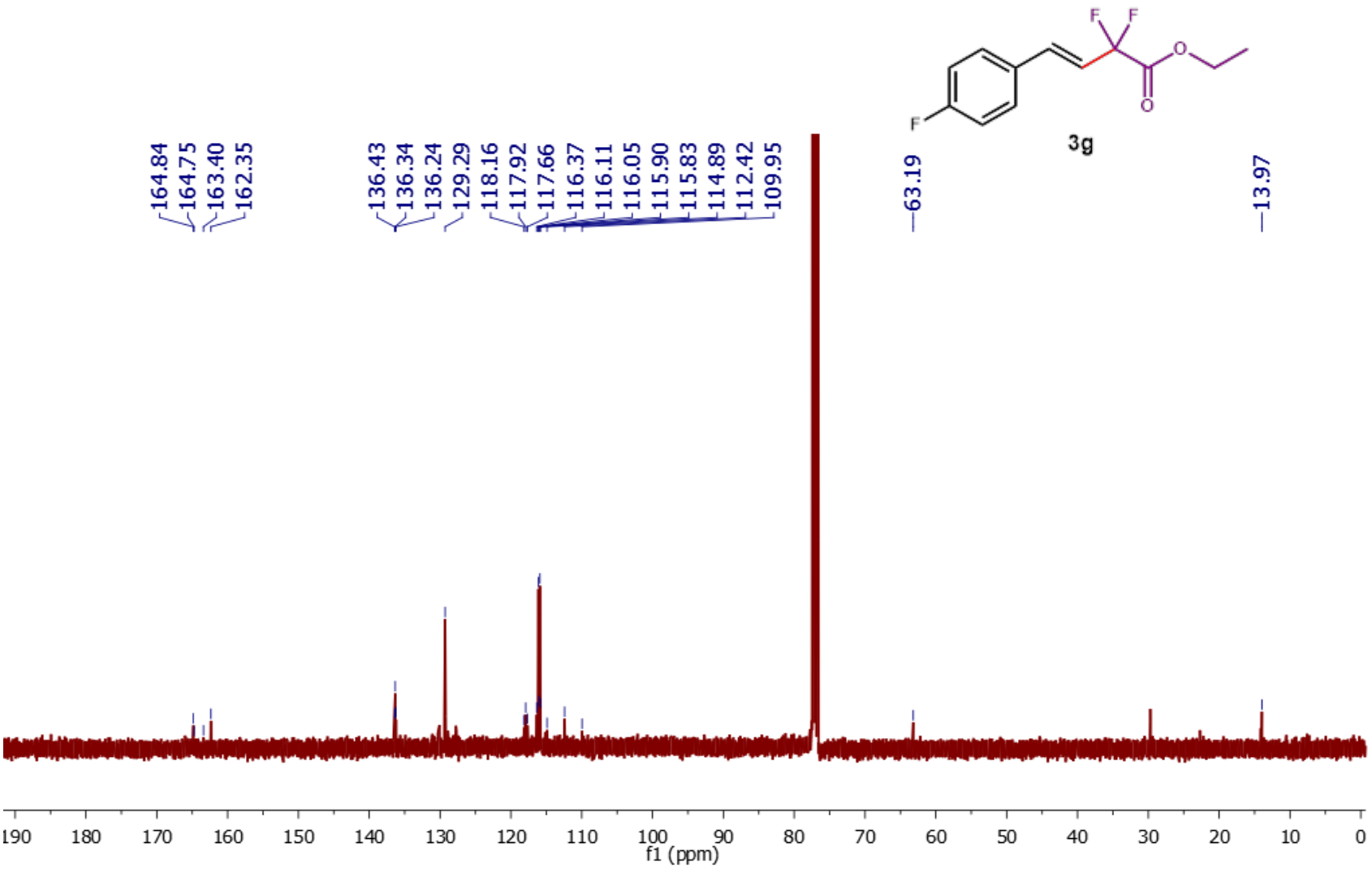

Figure S39. ^{13}C NMR (101 MHz) of **3g** in $CDCl_3$.

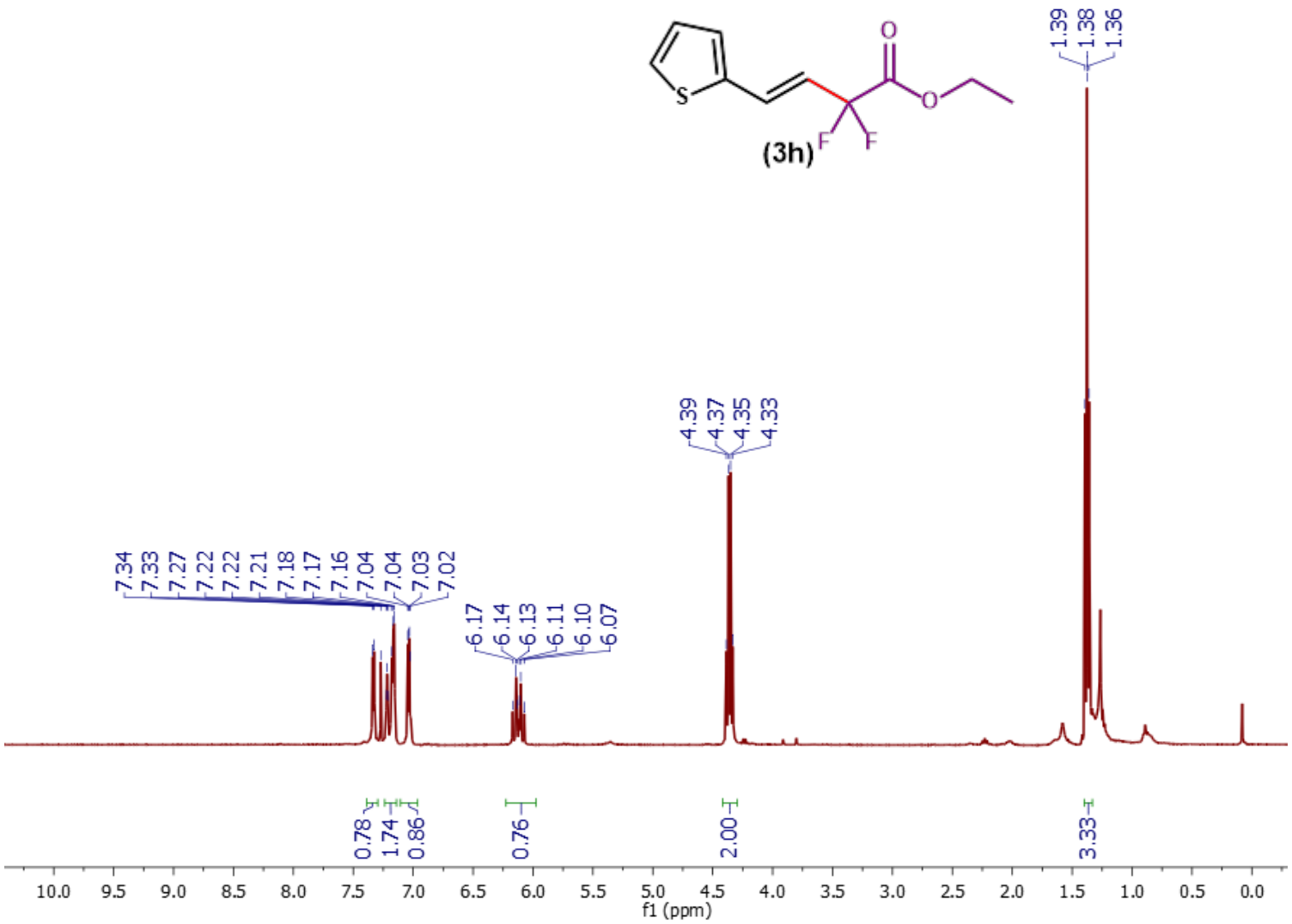

Figure S40. ^{1}H NMR (400 MHz) of **3h** in $CDCl_3$.

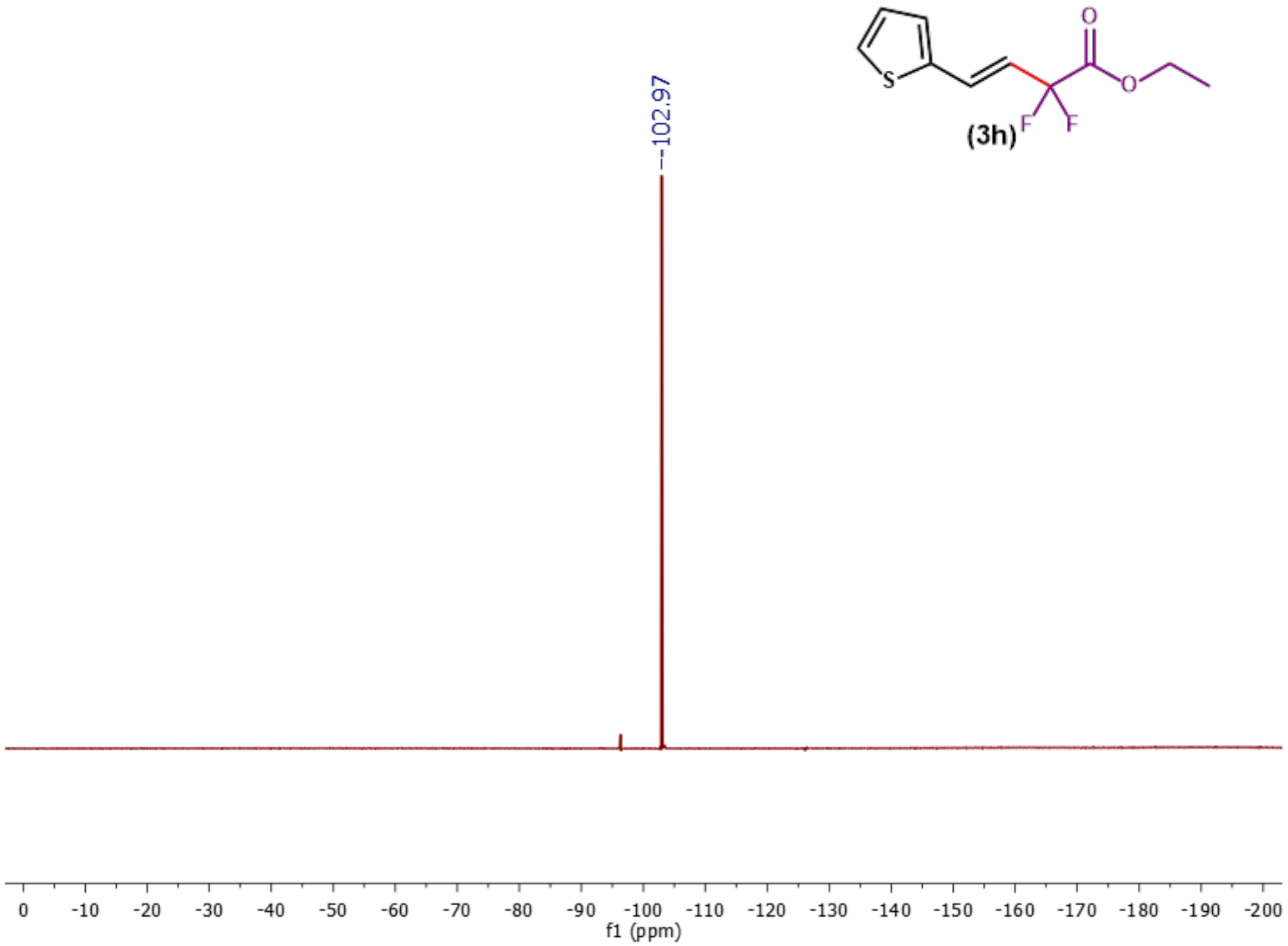

Figure S41. ^{19}F NMR (376 MHz) of **3h** in $CDCl_3$.

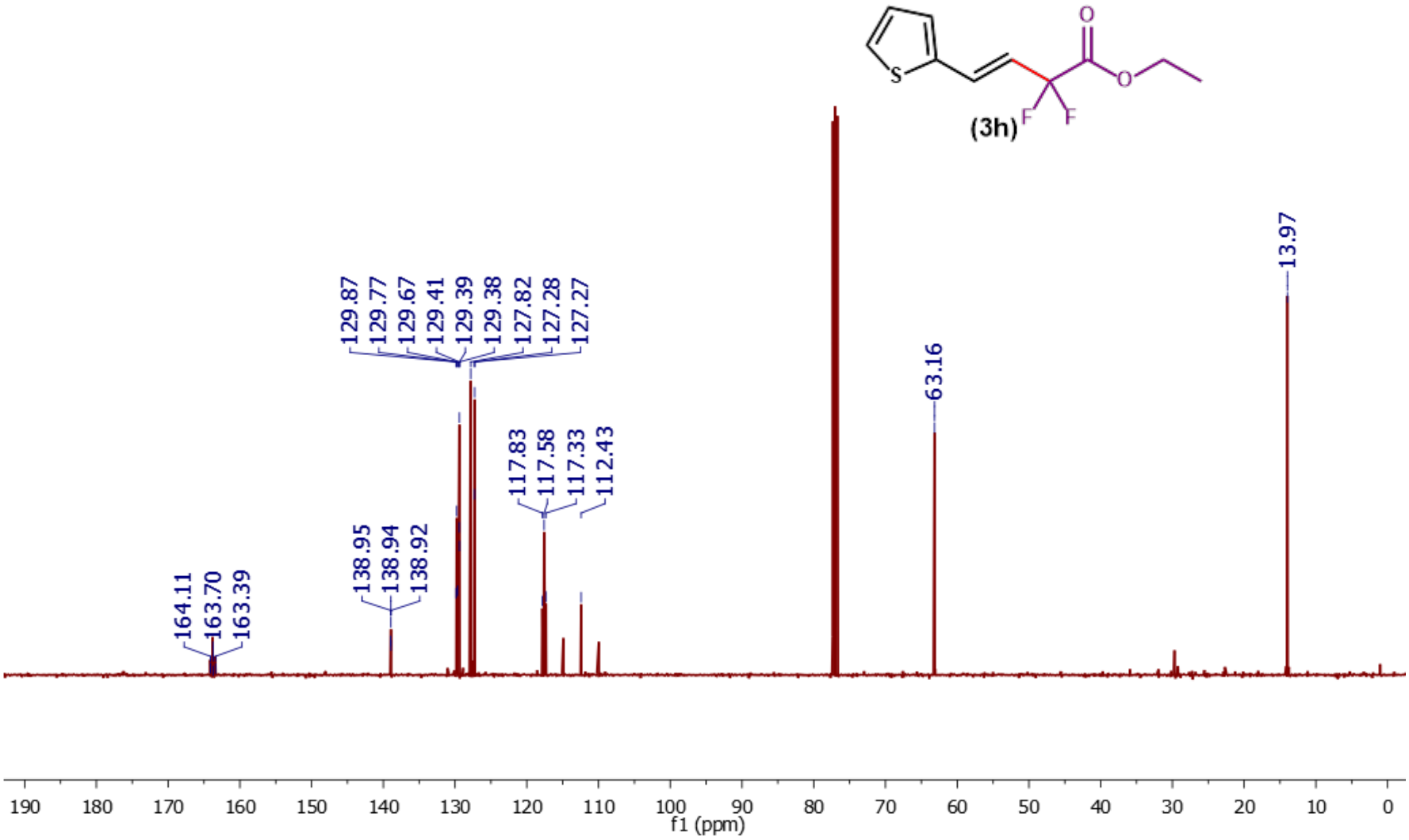

Figure S42. ^{13}C NMR (101 MHz) of **3h** in $CDCl_3$.

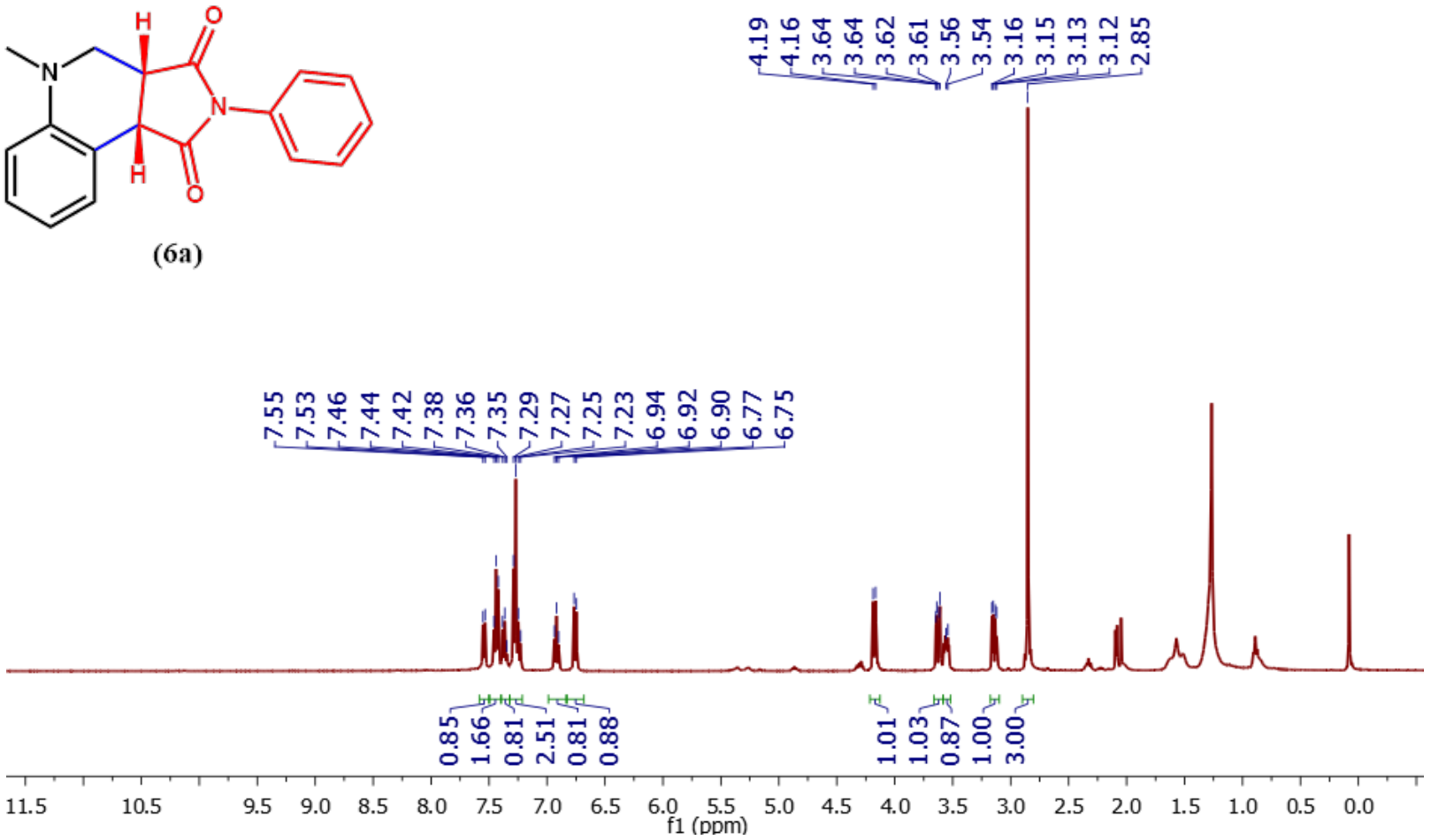

Figure S43. ^{1}H NMR (400 MHz) of 6**a** in $CDCl_3$.

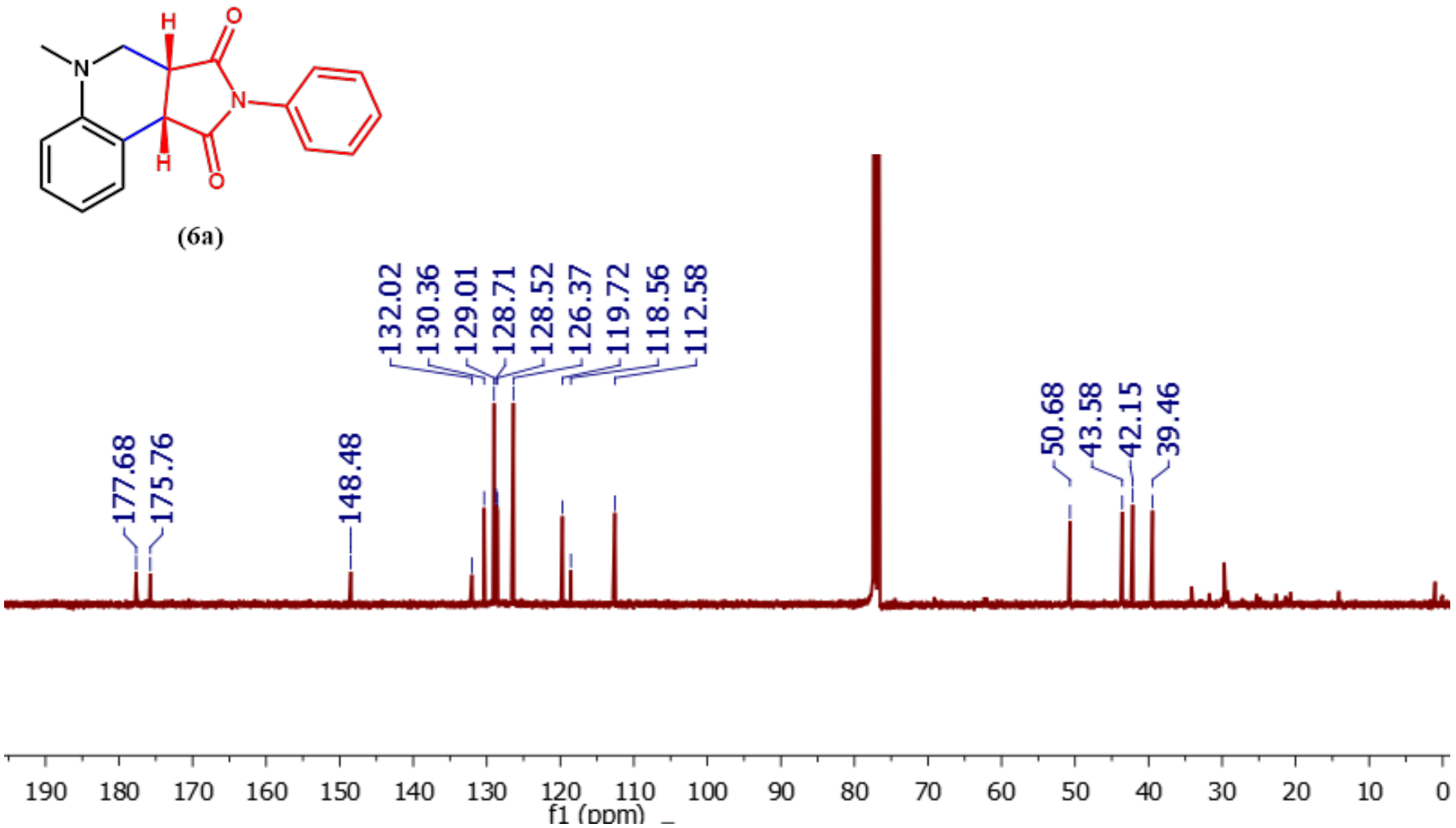

Figure S44. ^{13}C NMR (101 MHz) of **6a** in $CDCl_3$.

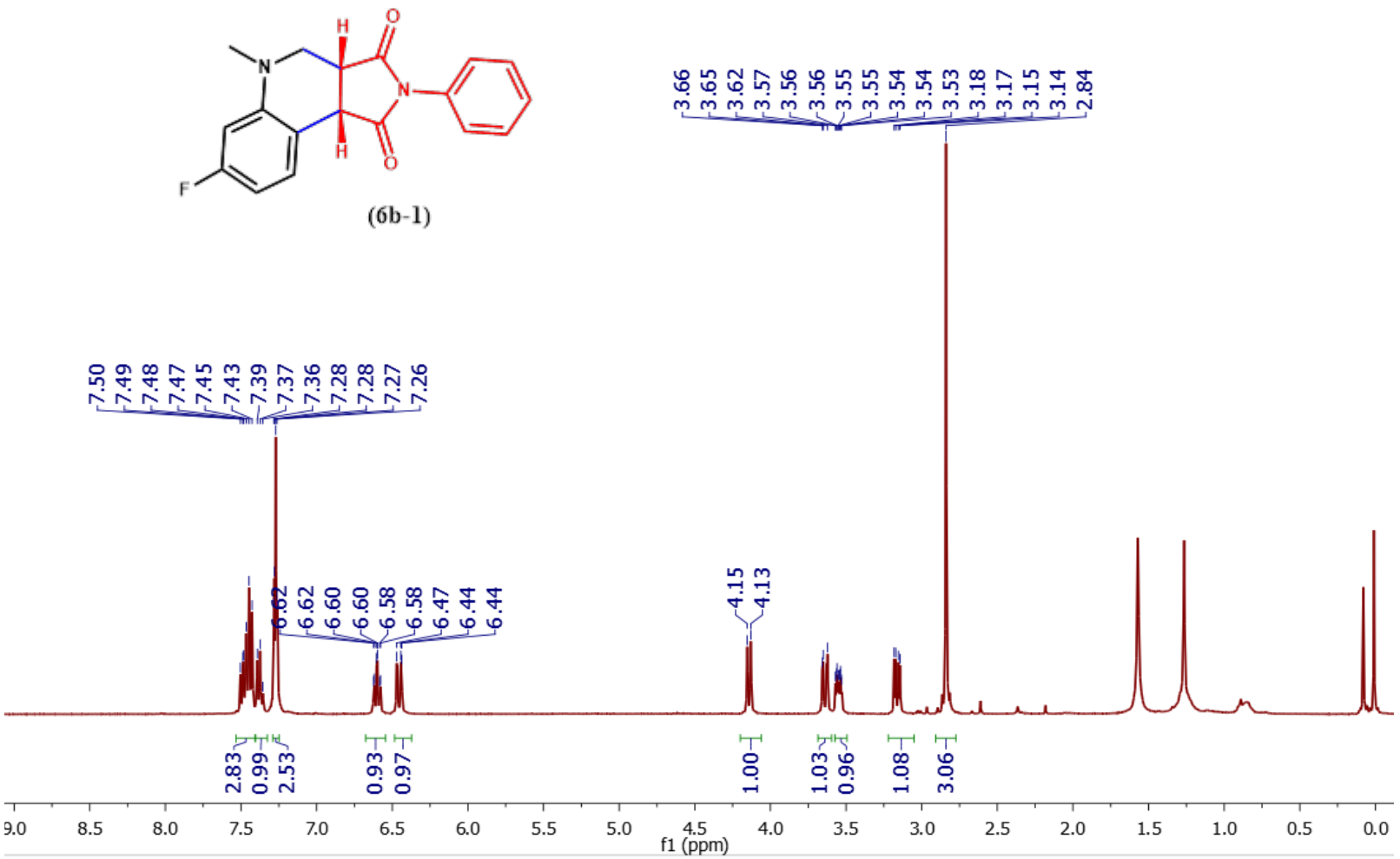

Figure S45. ^{1}H NMR (400 MHz) of **6b-1** in $CDCl_3$.

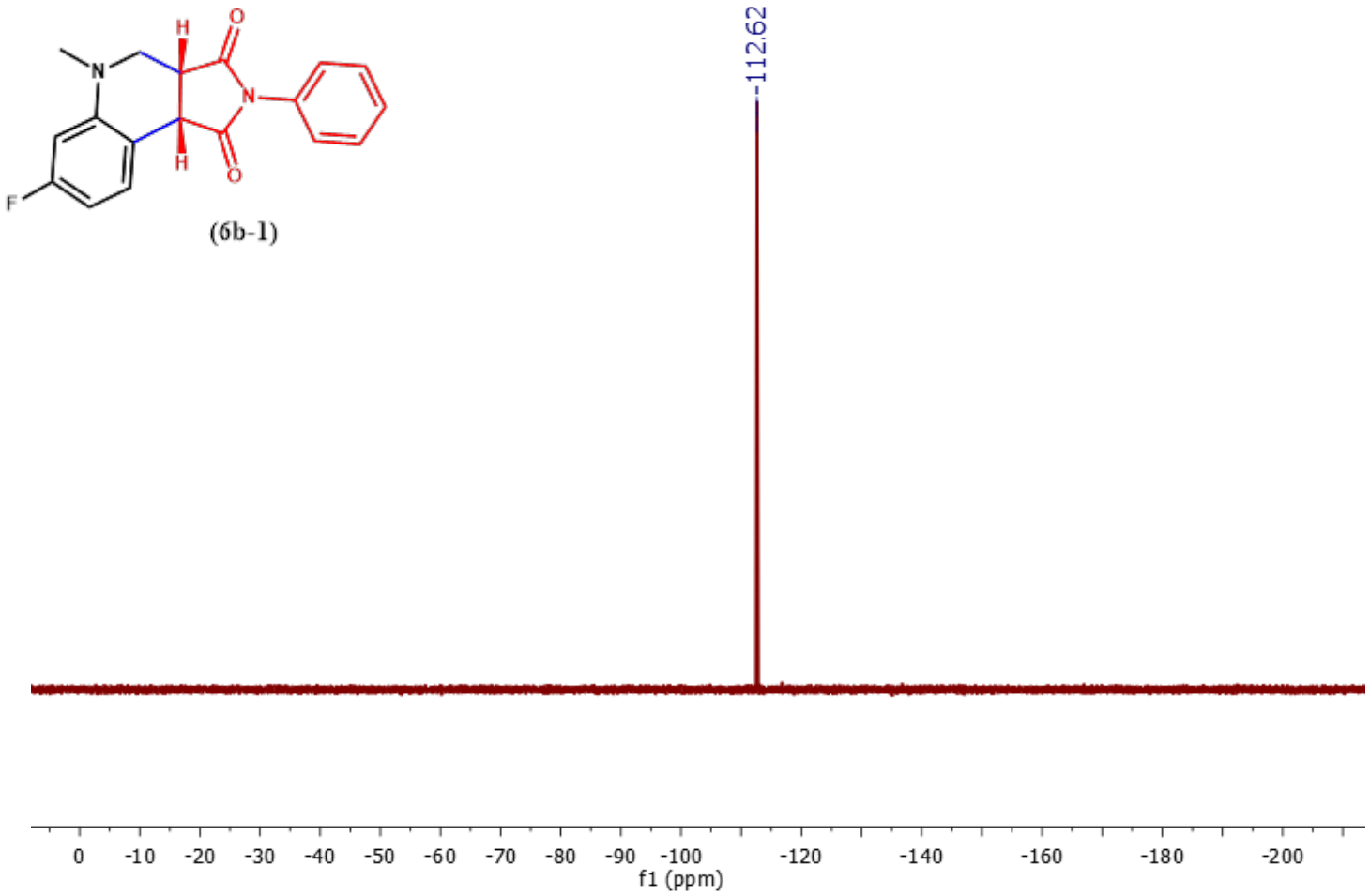

Figure S46. ^{19}F NMR (376 MHz) of **6b-1** in $CDCl_3$.

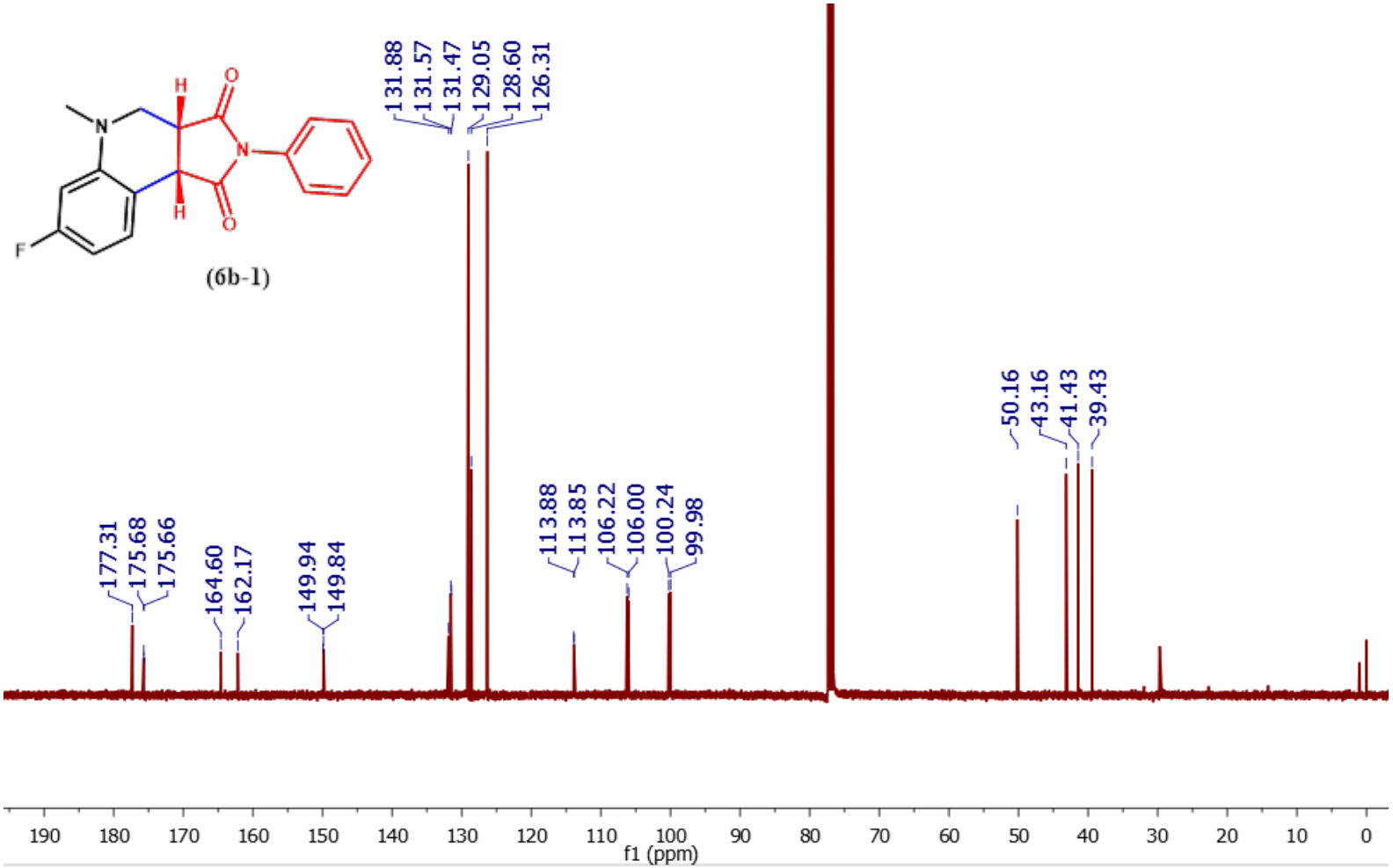

Figure S47. ^{13}C NMR (101 MHz) of **6b-1** in $CDCl_3$.

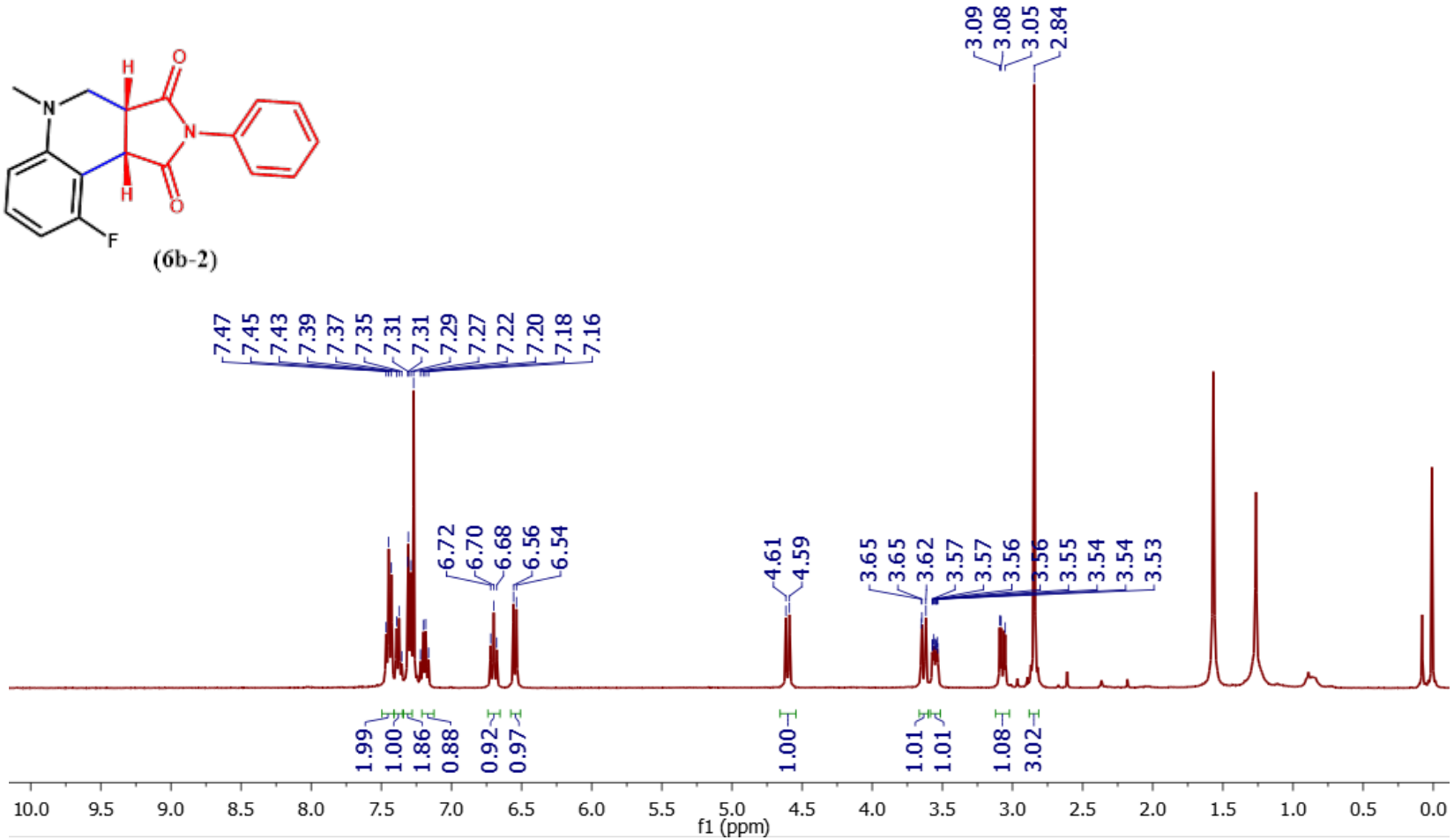

Figure S48. ^{1}H NMR (400 MHz) of **6b-2** in $CDCl_3$.

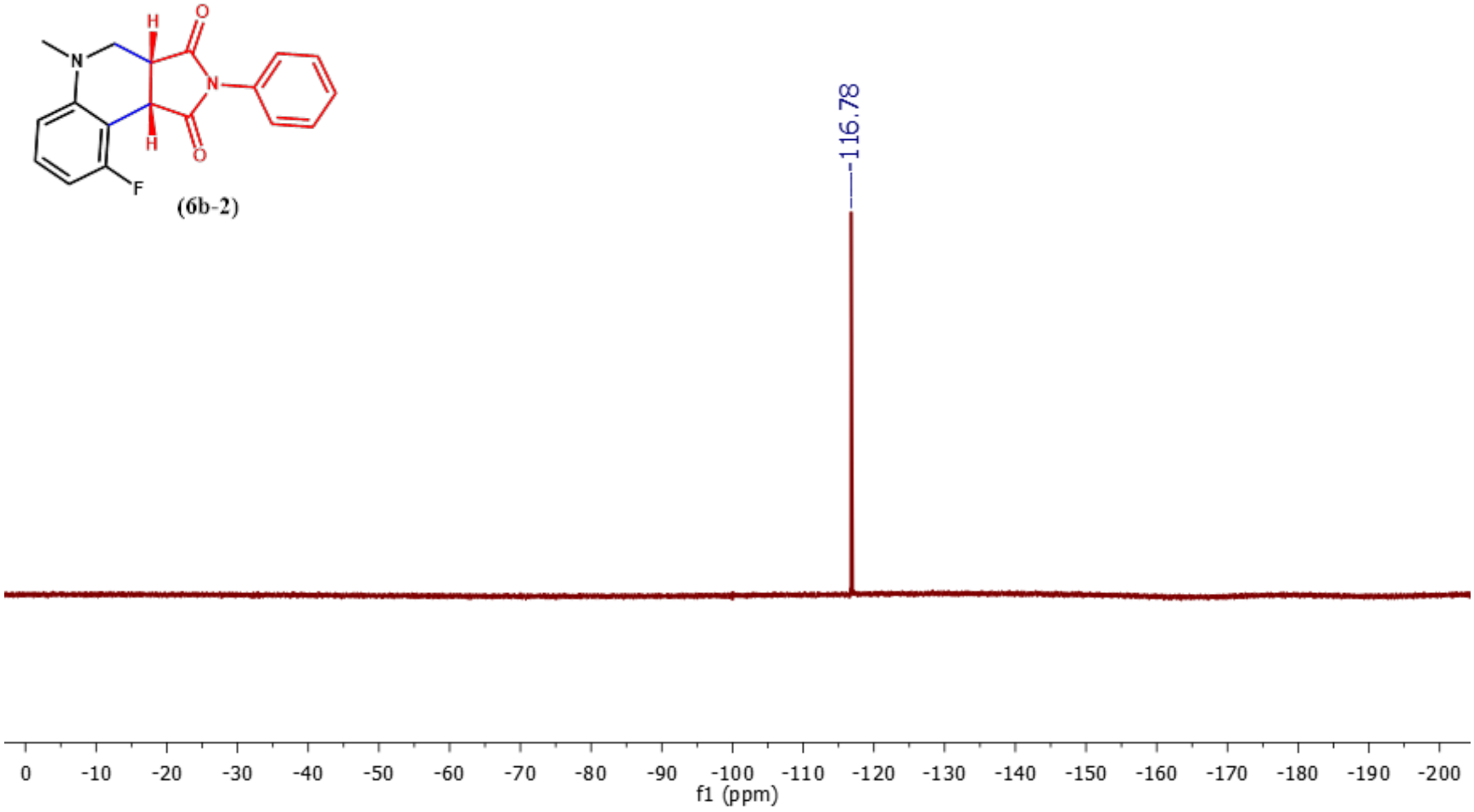

Figure S49. ^{19}F NMR (376 MHz) of **6b-2** in $CDCl_3$.

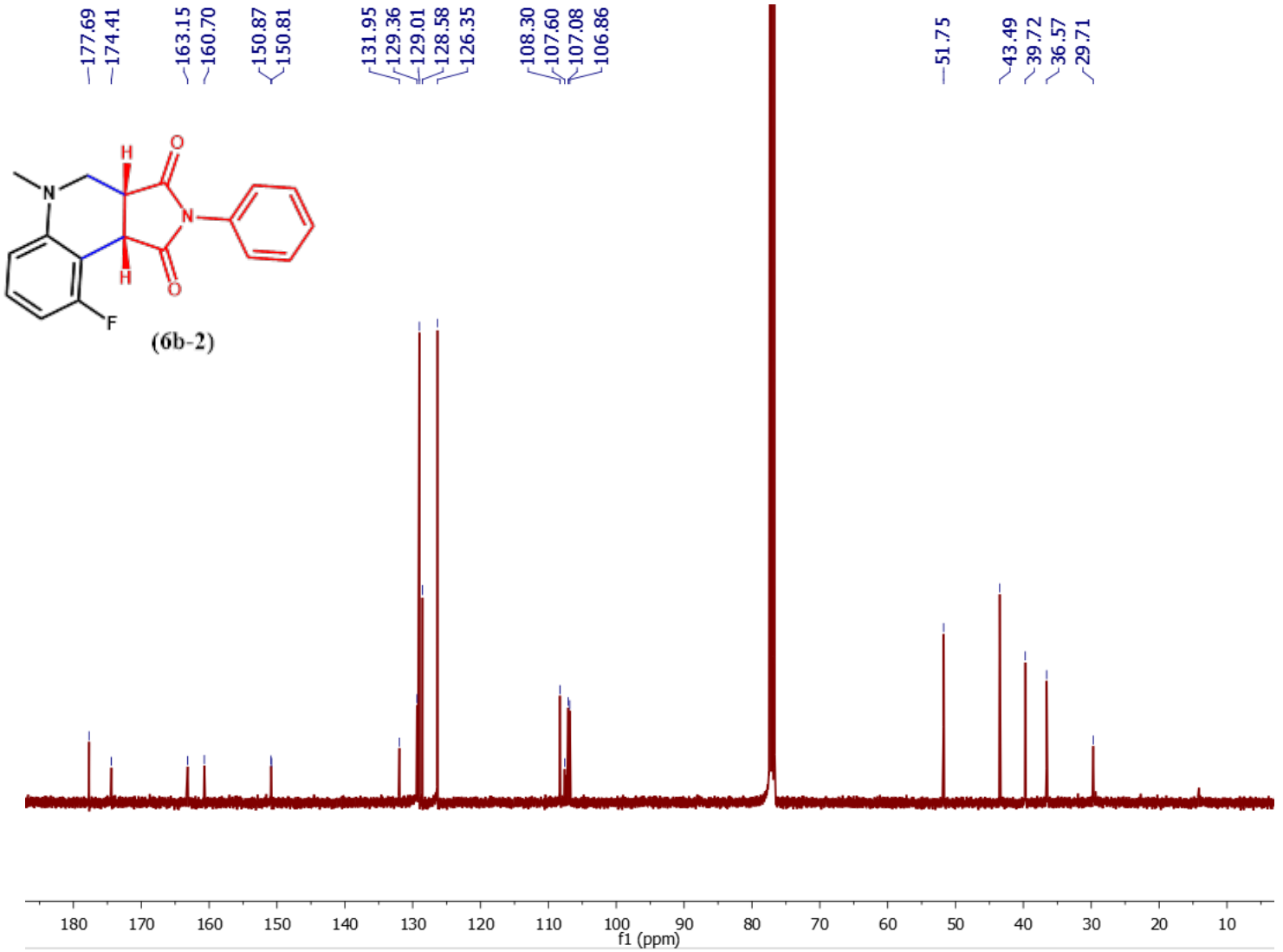

Figure S50. ^{13}C NMR (101 MHz) of **6b-2** in $CDCl_3$.

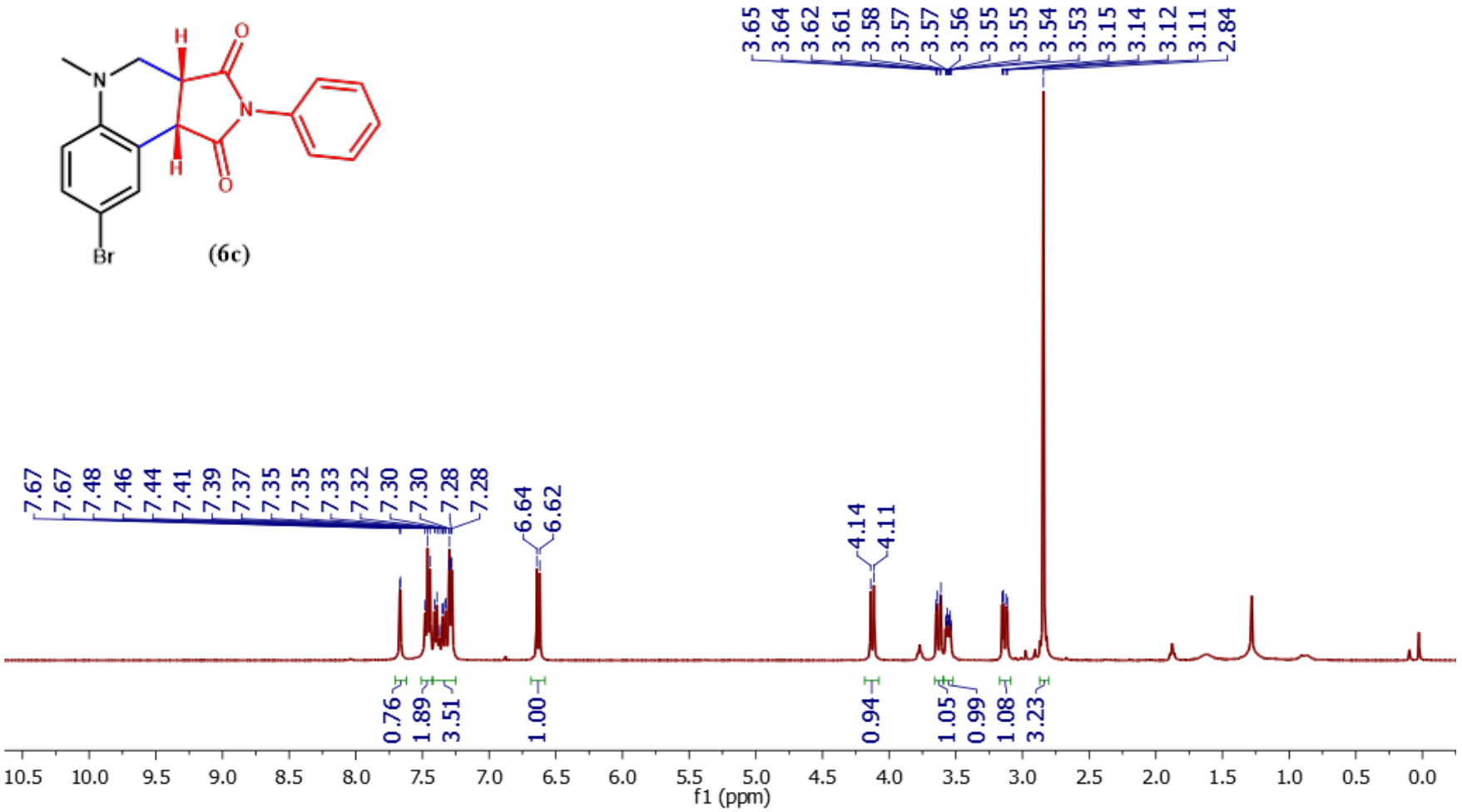

Figure S51. ^{1}H NMR (400 MHz) of **6c** in $CDCl_3$.

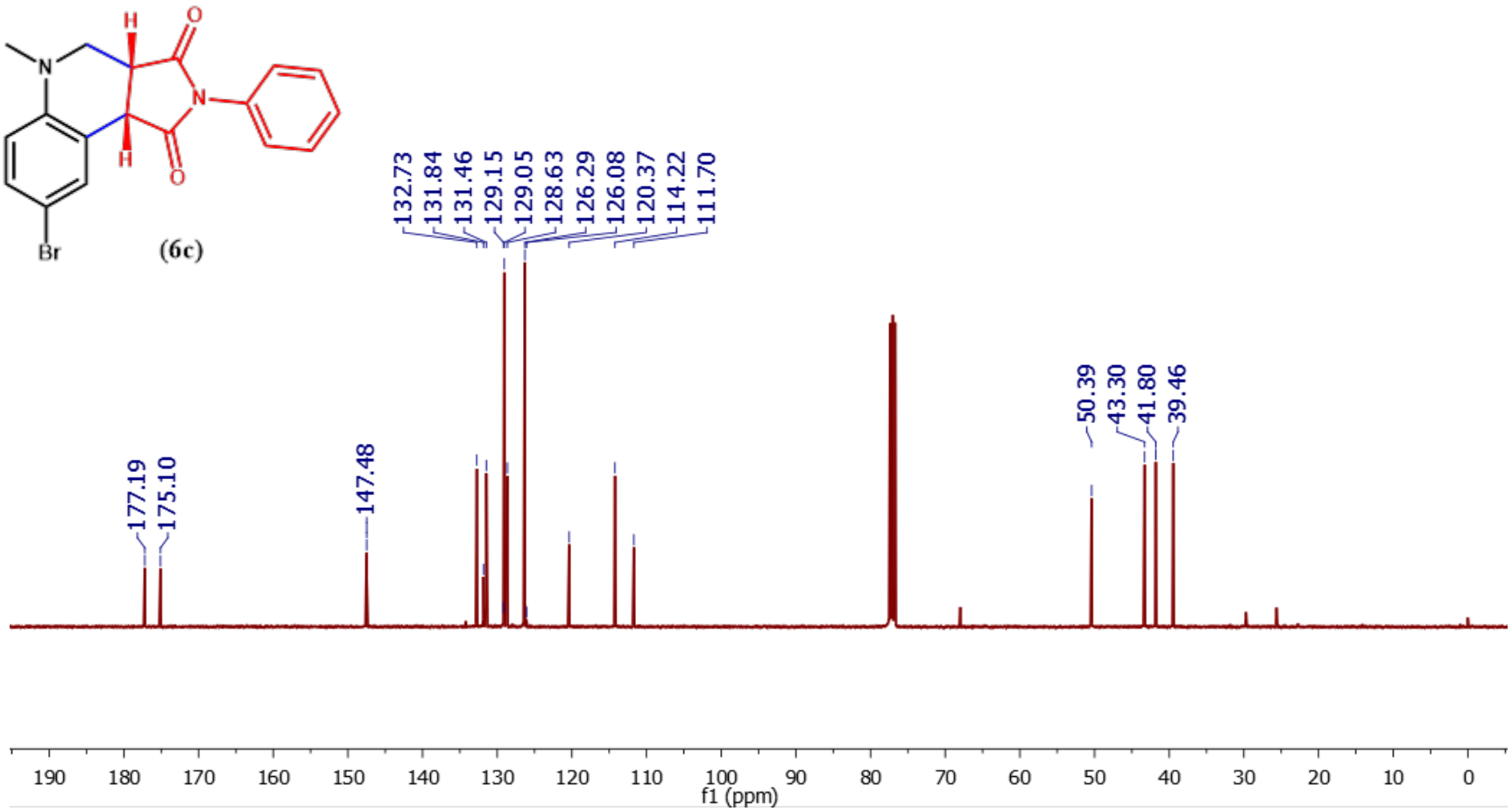

Figure S52. ^{13}C NMR (101 MHz) of **6c** in $CDCl_3$.

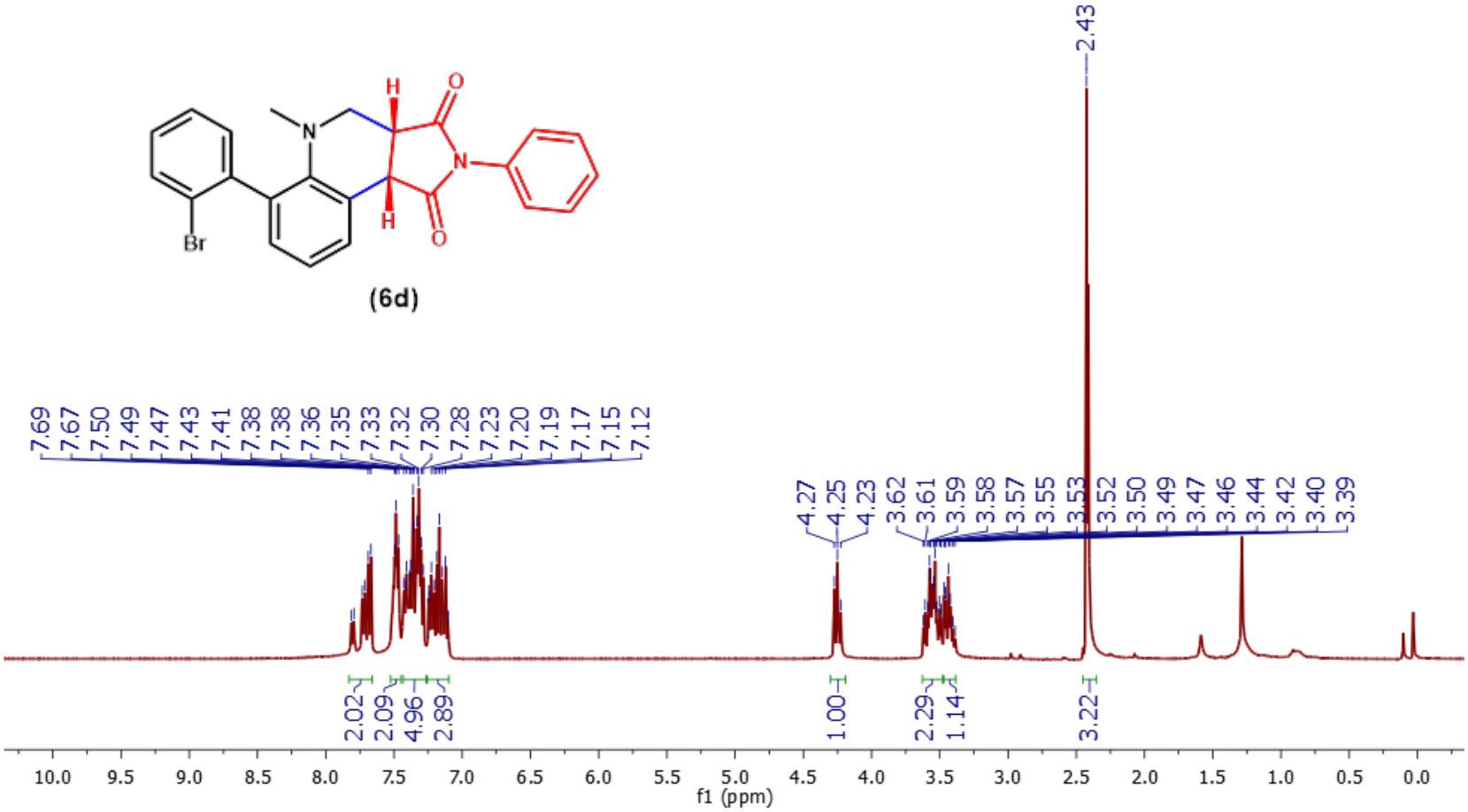

Figure S53. ^{1}H NMR (400 MHz) of **6d** in $CDCl_3$.

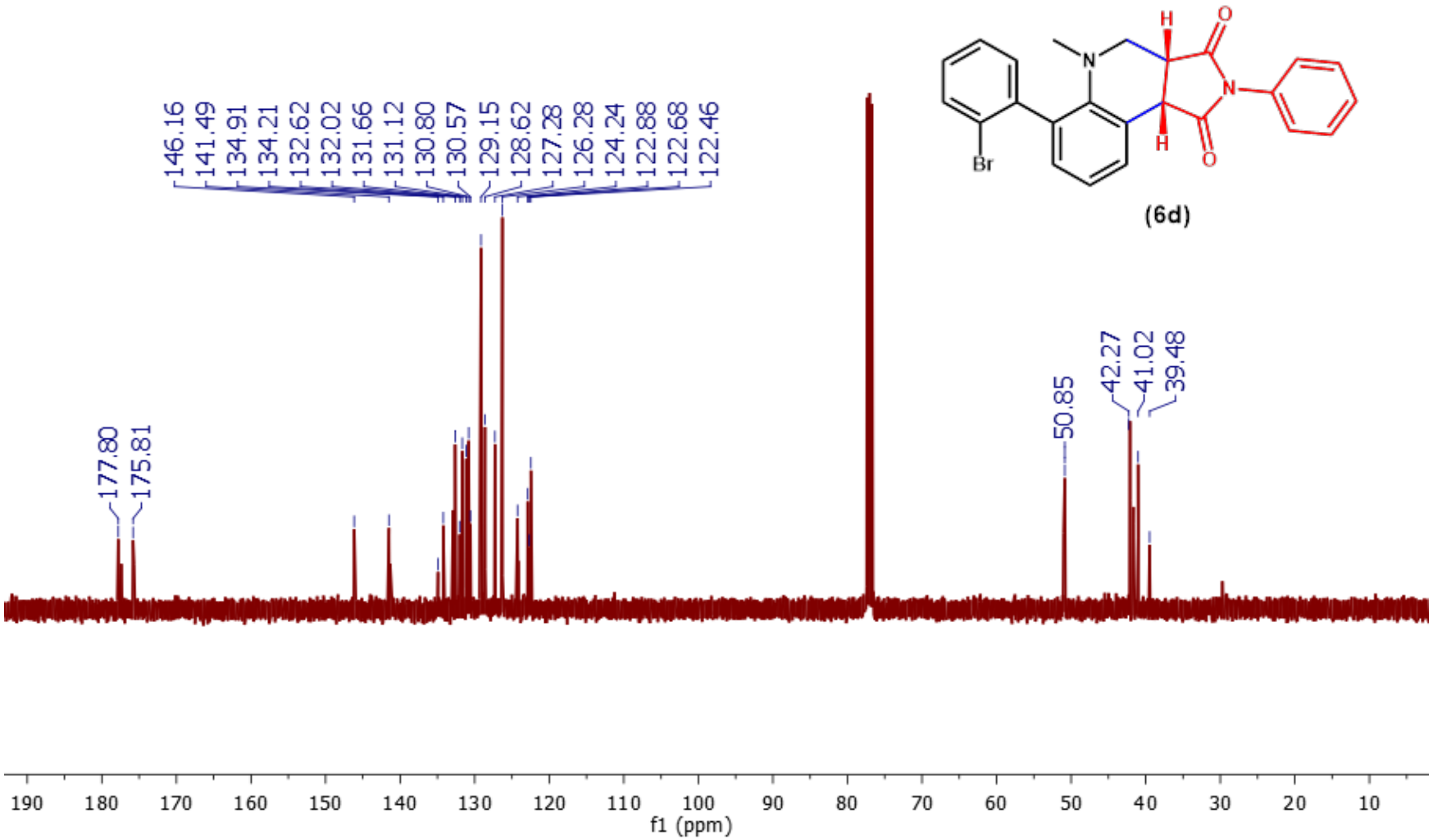

Figure S54. ^{13}C NMR (101 MHz) of **6d** in $CDCl_3$.

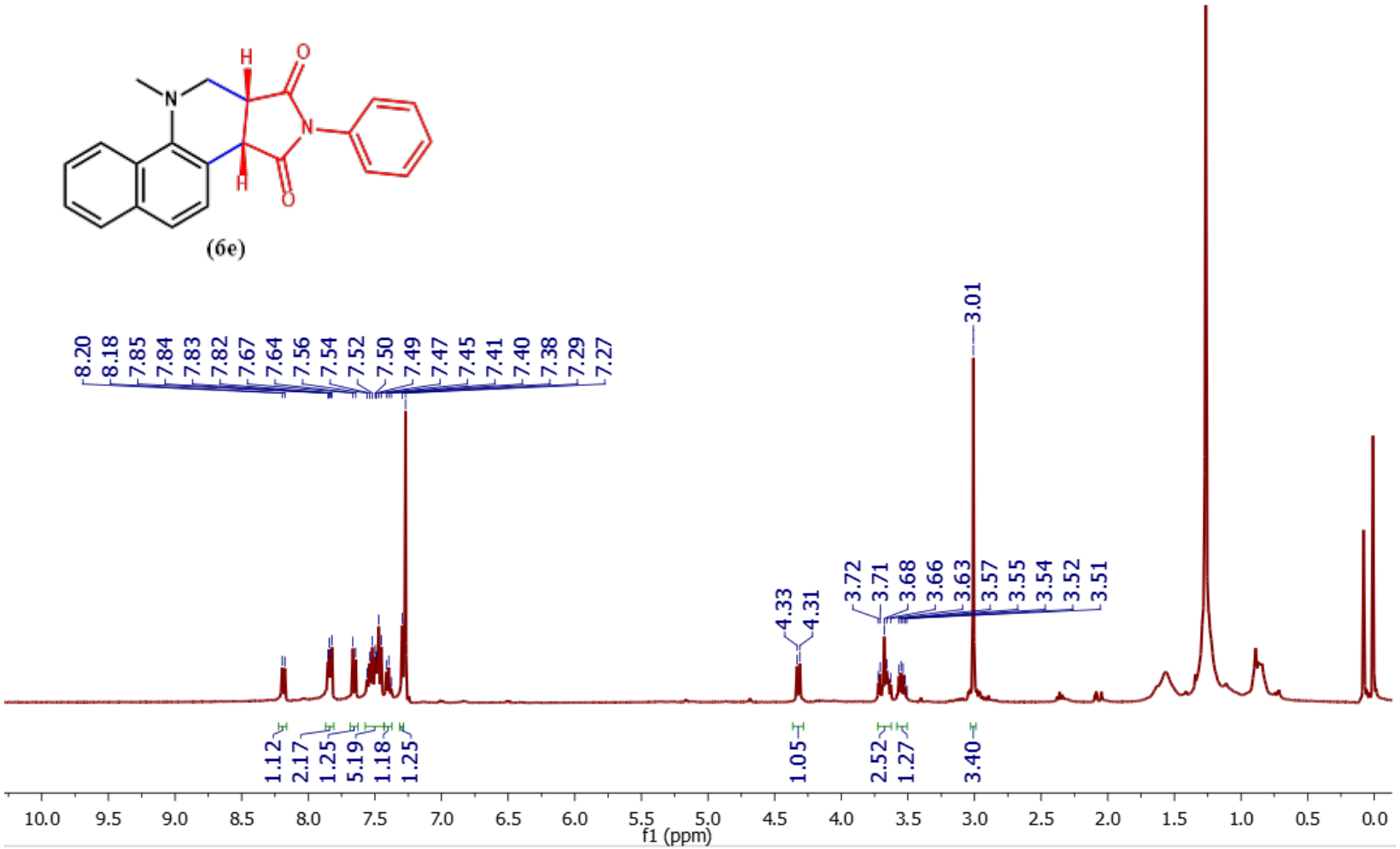

Figure S55. ^{1}H NMR (400 MHz) of **6e** in $CDCl_3$.

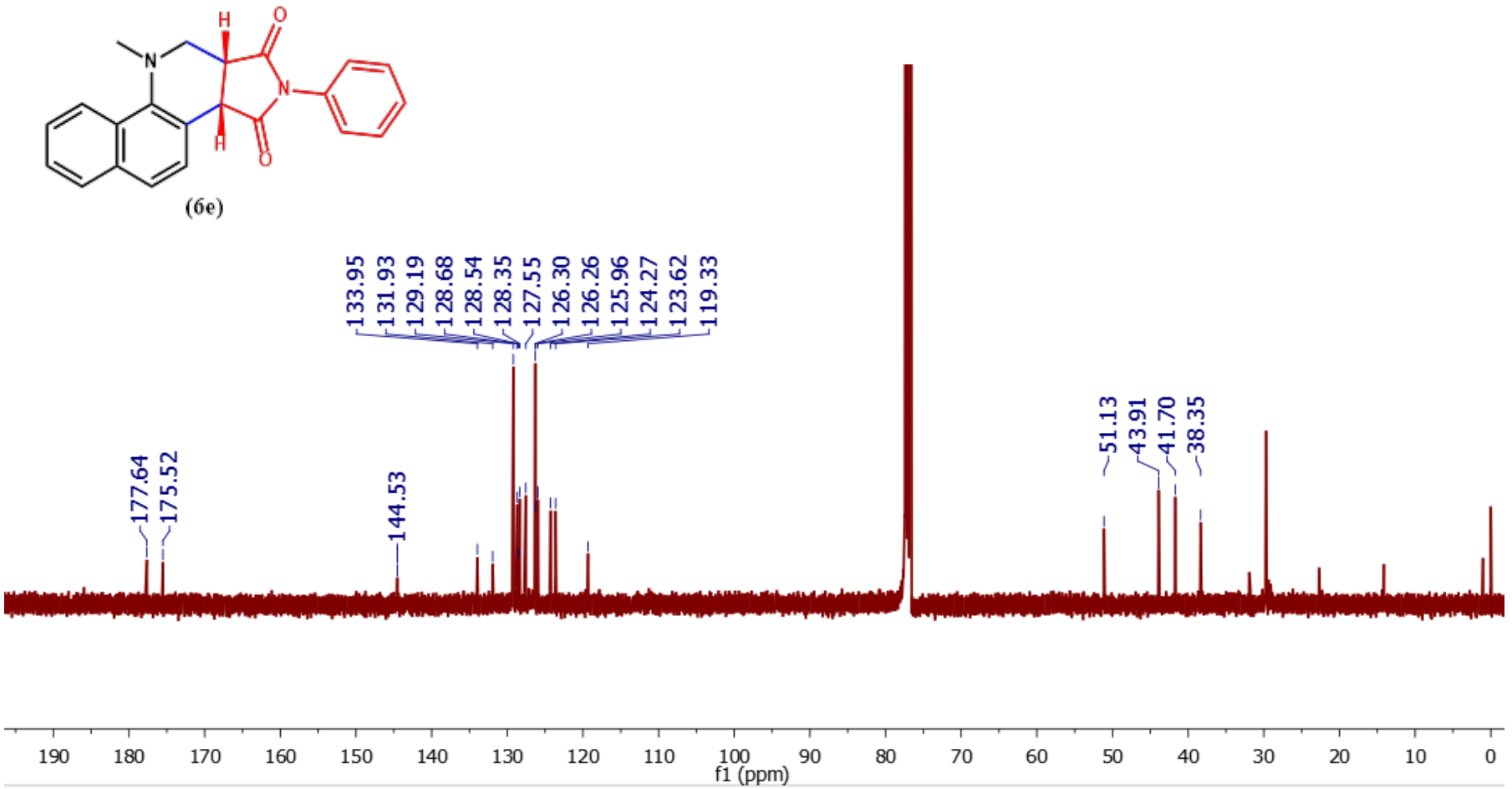

Figure S56. ^{13}C NMR (101 MHz) of **6e** in $CDCl_3$.

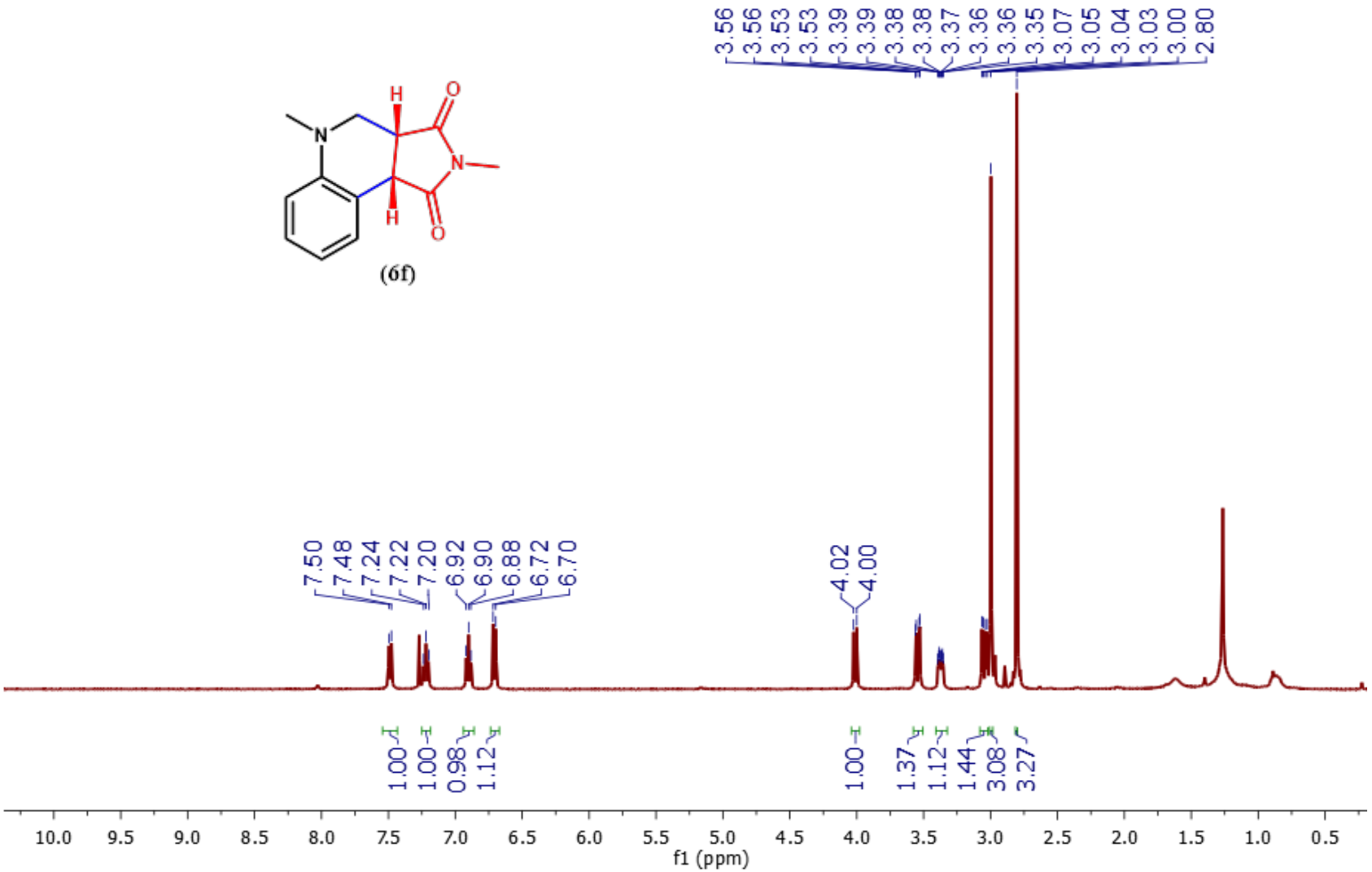

Figure S57. ^{1}H NMR (400 MHz) of **6f** in $CDCl_3$.

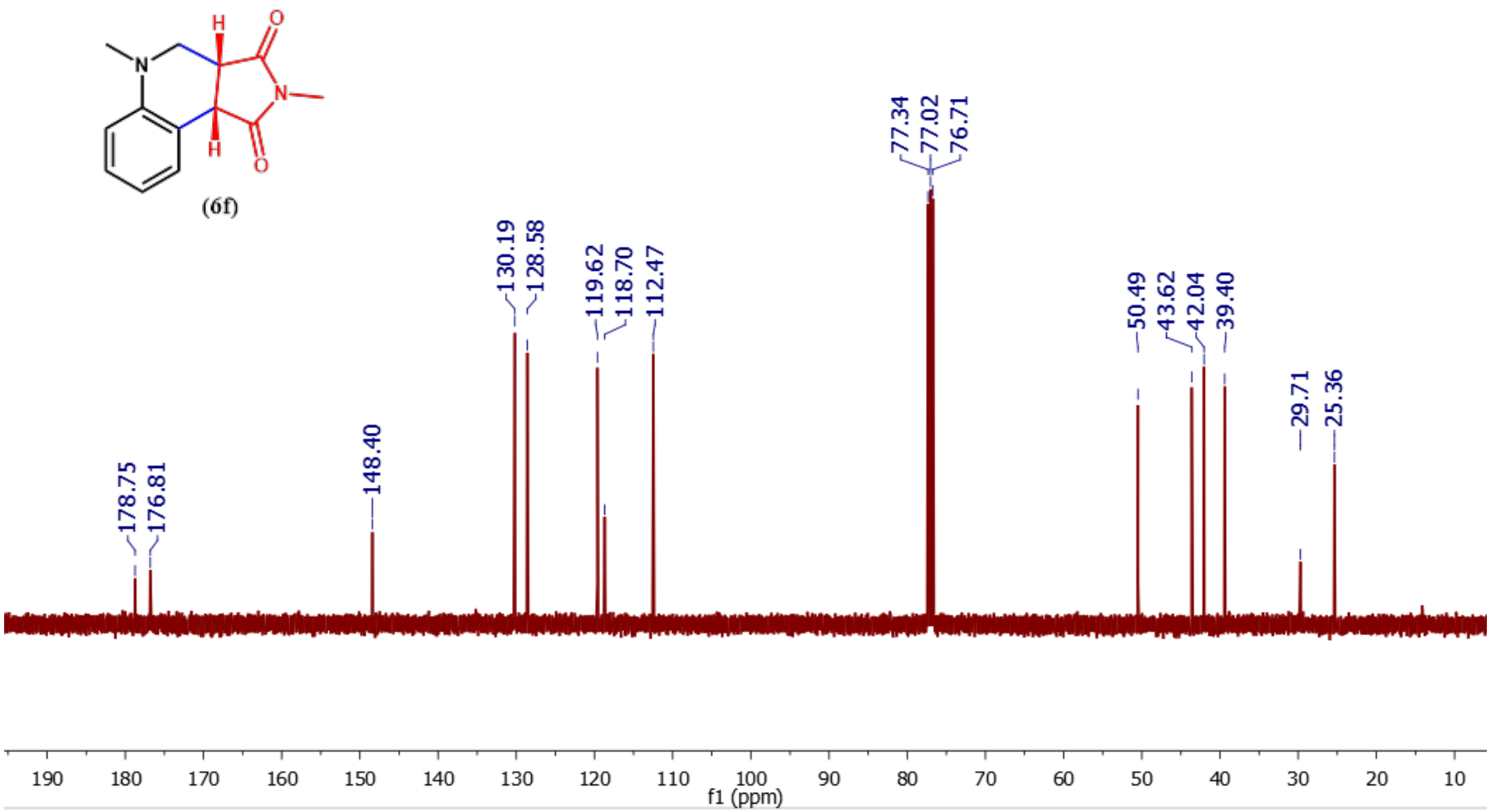

Figure S58. ^{13}C NMR (101 MHz) of **6f** in $CDCl_3$.

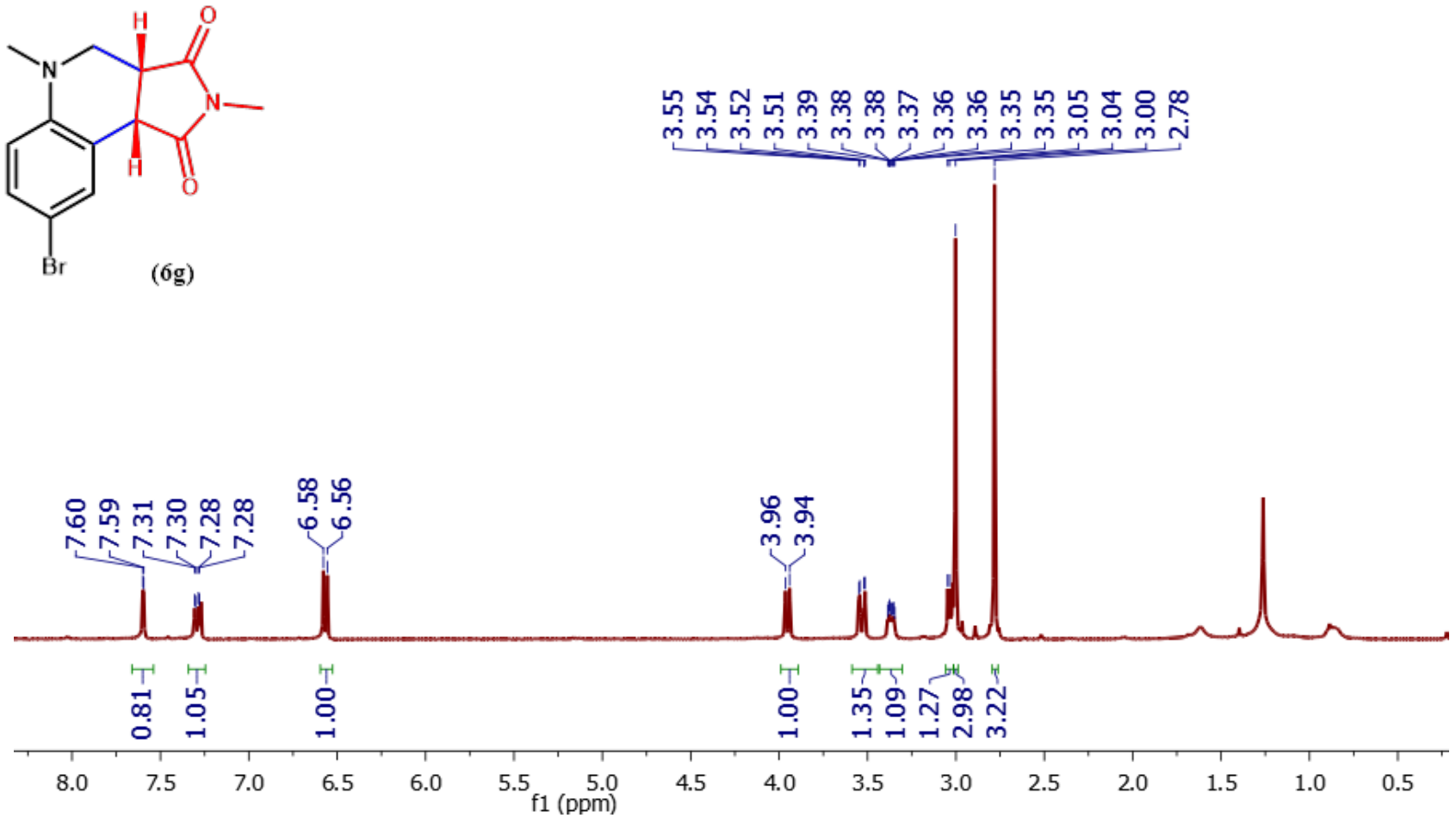

Figure S59. ^{1}H NMR (400 MHz) of **6g** in $CDCl_3$.

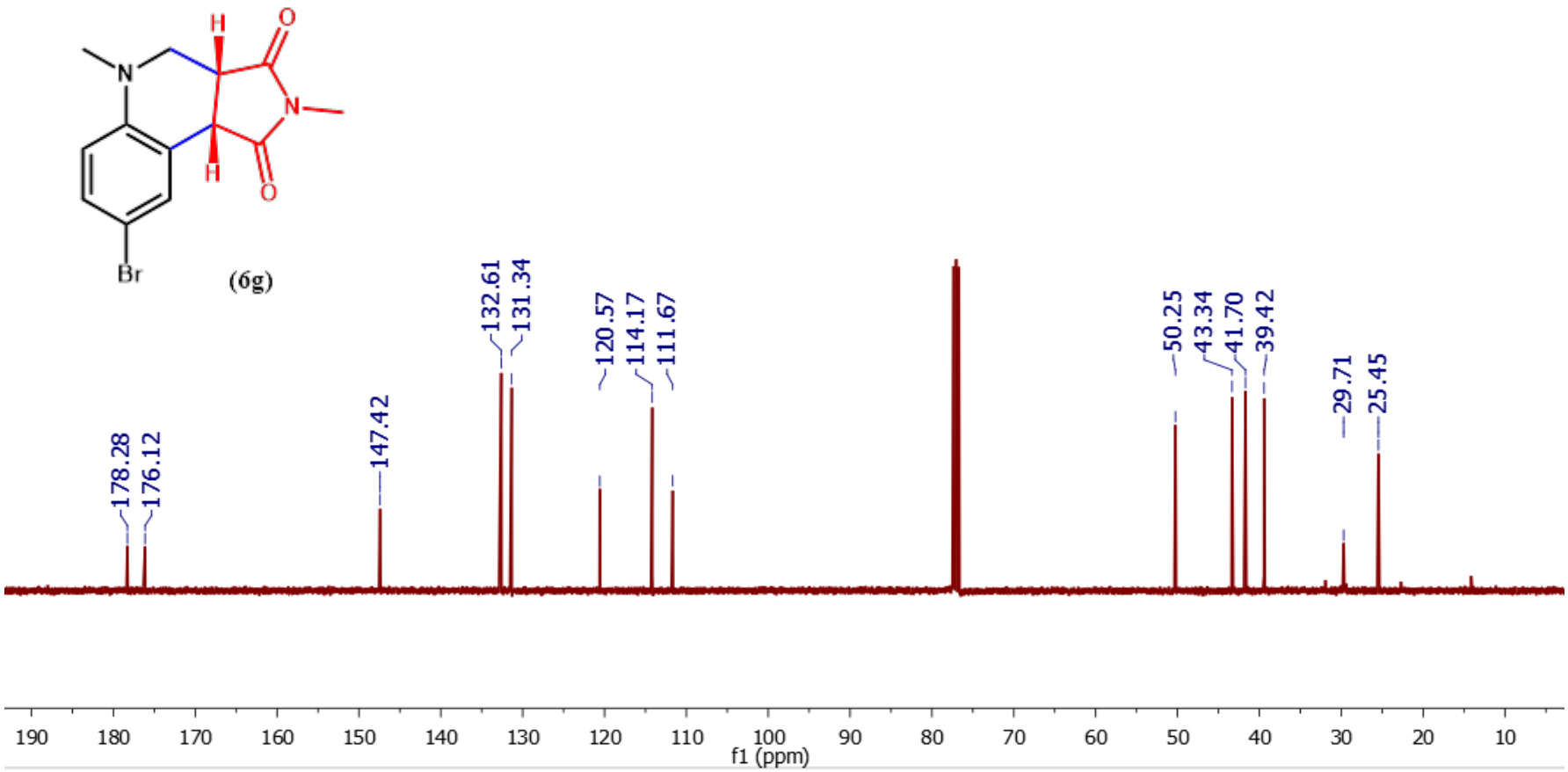

Figure S60. ^{13}C NMR (101 MHz) of **6g** in $CDCl_3$.

8. Reference

1. Jin, S.; Sakurai, T.; Kowalczyk, T.; Dalapati, S.; Xu, F.; Wei, H.; Chen, X.; Gao, J.; Seki, S.; Irle, S., Two-Dimensional Tetrathiafulvalene Covalent Organic Frameworks: Towards Latticed Conductive Organic Salts. *Chem. Eur. J.* **2014**, *20*, 14608-14613.

2. Wong, M. Y.; Xie, G.; Tourbillon, C.; Sandroni, M.; Cordes, D. B.; Slawin, A. M. Z.; Samuel, I. D. W.; Zysman-Colman, E., Formylated Chloro-Bridged Iridium(III) Dimers as OLED Materials: Opening up New Possibilities. *Dalton Trans.* **2015**, *44*, 8419-8432.

3. Dubbeldam, D.; Calero, S.; Ellis, D. E.; Snurr, R. Q., RASPA: Molecular Simulation Software for Adsorption and Diffusion in Flexible Nanoporous Materials. *Mol. Simulat.* **2016**, *42*, 81-101.

4. Mayo, S. L.; Olafson, B. D.; Goddard, W. A., DREIDING: A Generic Force Field for Molecular Simulations. *J. Phys. Chem.* **1990**, *94*, 8897-8909.

5. Zhang, L.; Siepmann, J. I., Direct Calculation of Henry's Law Constants from Gibbs Ensemble Monte Carlo Simulations: Nitrogen, Oxygen, Carbon Dioxide and Methane in Ethanol. *Theor. Chem. Acc.* **2006**, *115*, 391-397.

6. Zhong, J.-J.; Yang, C.; Chang, X.-Y.; Zou, C.; Lu, W.; Che, C.-M., Platinum(II) Photo-Catalysis for Highly Selective Difluoroalkylation Reactions. *Chem. Commun.* **2017**, *53*, 8948-8951.

7. Feng, X.; Wang, X.; Chen, H.; Tang, X.; Guo, M.; Zhao, W.; Wang, G., Copper-Mediated Regioselective Hydrodifluoroalkylation of Alkynes. *Org. Biomol. Chem.* **2018**, *16*, 2841-2845.

8. Liang, Z.; Xu, S.; Tian, W.; Zhang, R., Eosin Y-Catalyzed Visible-Light-Mediated Aerobic Oxidative Cyclization of N,N-Dimethylanilines with Maleimides. *Beilstein J. Org. Chem.* **2015**, *11*, 425-430.